PERCEPTION OF WHITE APPEARANCE AND DEGREE OF CHROMATIC ADAPTATION UNDER DIFFERENT VIEWING CONDITIONS

CHEN SIYUAN

PhD

The Hong Kong Polytechnic University

2020

The Hong Kong Polytechnic University

Department of Building Services Engineering

Perception of white appearance and degree of chromatic adaptation under different viewing conditions

CHEN Siyuan

A thesis submitted in partial fulfilment of the requirements for the degree of Doctor of Philosophy

July 2020

CERTIFICATE OF ORIGINALITY

I hereby declare that this thesis is my own work and that, to the best of my knowledge and belief, it reproduces no material previously published or written, nor material that has been accepted for the award of any other degree or diploma, except where due acknowledgement has been made in the text.

(Signed)

CHEN Siyuan (Name of student)

Abstract

The colour appearance of a stimulus is affected not only by its spectral composition but also by the viewing condition. When perceiving a stimulus under different viewing conditions, the chromatic adaptation mechanism in the human visual system can automatically remove the colour cast of the illumination, so that the colour appearance of the stimulus remains relatively constant. Colour appearance models (CAMs) embedding chromatic adaptation transforms (CATs) were developed to characterize the colour appearance of stimuli under a limited number of light sources simulating standard illuminants (e.g., Illuminant A, D65, and D50). In recent years, light-emitting diodes (LEDs) are becoming more and more popular for illumination. For luminous efficacy, most white-light LED products contain little amount of radiation in the short and long wavelength regions of the visible spectrum. This was found to affect the white appearance of surface colours. On the other hand, the easy adjustment of the light source chromaticities was also found to affect the degree of the chromatic adaptation, which is critically important to the colour appearance characterizations of a stimulus.

This dissertation starts with the investigation of whiteness appearance of surface colours under LED illumination through psychophysical experiments. The whiteness values calculated using the existing whiteness formulae failed to consider the effect of illuminant CCT that degree of chromatic adaptation decreased with the decrease of adapting CCT. An optimization was performed on the degree of chromatic adaptation factor *D* in CAT02, which significantly improved the performance of the CIE whiteness formula. Furthermore, the whiteness appearance of surface colours was also

investigated from a perspective of image appearance. A scene including three whiteness samples containing different amounts of FWAs and a Macbeth ColourChecker was captured by a digital still camera under two 6500 K illuminants with different levels of UV/violet radiation and white balanced using nine statistical algorithms. The lack of UV/violet radiation significantly affected the appearance of the whiteness samples, regardless of the white balance algorithms, which simultaneously affected the appearance of the ColourChecker.

The concept of white appearance was further employed to investigate the degrees of chromatic adaptation under different adapting conditions. A psychophysical experiment was conducted to investigate how the adapting CCT and luminance simultaneously affected the degree of chromatic adaptation. It was found that the adapting luminance and CCT jointly affected the degree of chromatic adaptation. Moreover, the experiment results suggested that the viewing mode, instead of the viewing medium, affected the degree of chromatic adaptation. Finally, since Augmented Reality (AR) is becoming more and more popular in recent years, psychophysical experiments were also carried out to investigate chromatic adaptation for viewing optical see-through and video see-through AR setups. Generally, a lower degree of chromatic adaptation was found when viewing virtual stimuli than viewing physical stimuli.

In general, this dissertation thoroughly investigated how viewing conditions affected chromatic adaptation through the perception of white appearance of various stimuli. The findings and models are beneficial to various communities related to colour reproduction and imaging through better characterizations of the colour appearance of stimuli.

Acknowledgement

Firstly, I would like to express my sincere appreciation to my supervisor Prof. Minchen Wei, for his continuous guidance. His intelligence and knowledge helped me to make a lot of progress over the past four years. I could not finish the research work presented in this dissertation without his kind support and thoughtful criticism.

I would like to thank my colleagues Wenyu Bao, Jun Wang, Yiqian Li, and Jialu Wu to make the working environment a most pleasant one. I also want to thank the visiting students Yuzhao Wang, Hsin-Po Huang, Yu Hu, Zheng Huang, Xiangzhen Kong, Yuechen Zhu, Mengmeng Wang, and Jie Yang. They brought their insights and perspectives with them and I learnt a lot.

I would also like to thank Dr. Michael Murdoch, Dr. Mark Fairchild, Dr. Susan Farnand, and Miss Val Hemink for their generous instructions when I was a visiting student at the Rochester Institute of Technology. The fellow students Hao Xie, Che Shen, Luke Helwig, Yue Yuan, Anku Manderna, Tucker Downs, Yongmin Park, Lily Zhang, and Jenibel Paray in the lab offered me all the help I needed.

Special thanks to my wife Shuyi Wang for coming to Hong Kong and always being by my side. She is the most cheerful person on this planet and every day with her was a blessing.

Table of Contents

List of Figures

List of Tables

Chapter 1 Introduction

1.1 Light and Human Vision

Light is a type of electromagnetic radiation that the human visual system can perceive. The wavelengths of visible light range between 380 and 780 nm to a colour-normal human. Spectral power distribution (SPD) is used to describe the radiant power at each wavelength between 380 and 780 nm, with the vertical axis describing the radiant power and the horizontal axis describing the wavelength. Figure 1.1 shows the SPD of the D65 illuminant. Light leaving from a light source interacts with objects that may reflect, transmit, or absorb the radiation. Spectral reflectance radiation (SRD) is typically used to characterize the ability of a surface to reflect the radiation at different wavelengths, in terms of the percentage of the reflected power at each wavelength. Figure 1.2 shows the SRDs of some colour samples in the IES TM-30-15 colour sample set [David et al. 2015]. The light leaving from a light source, or being reflected from a surface, goes into our eyes, excites the photoreceptors in the retina, and provokes perception of colours. Figure 1.3 shows the structure of the human eye including the eye, the retina, and the layers of neural cells.

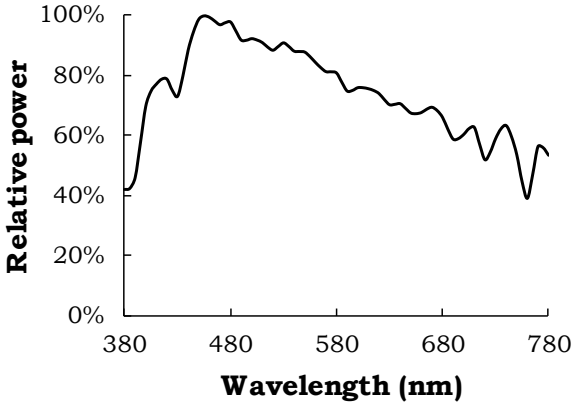

Fig. 1.1. Spectral power distribution of the D65 illuminant.

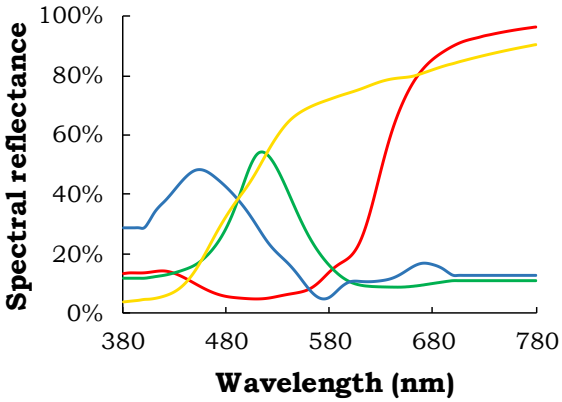

Fig. 1.2. Spectral reflectance distributions (SRDs) of some colour samples in the IES TM-30-15 colour sample set [David et al. 2015].

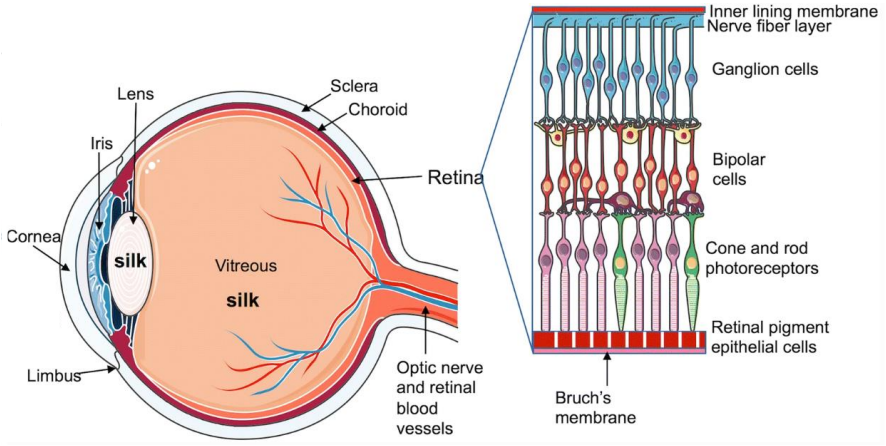

Fig. 1.3. Structure of the eye, including the eye, the retina, and the layers of neural cells [Tran et al. 2018].

There are three types of photoreceptors in the retina—rods, cones, and intrinsically photosensitive retinal ganglion cells (ipRGCs), with the cones and rods being responsible for the visual responses and the ipRGCs being responsible for the non-visual responses. The three types of cones (i.e., L-, M-, and S-cones), which are active under high light levels (i.e., photopic vision), help us to see various colours; the one type of rods, which are active under low light levels (i.e., scotopic vision), do not contribute to our colour perception. The existence of the three types of cones, however, cannot explain certain phenomena. For example, the human visual system never perceives a colour as a mixture of red and green. The opponent-process theory proposed by Hering [1964] is believed to better explain these phenomena. The three

opponent channels—red/green, blue/yellow, and a luminance channel—receive input from the three types of cones and produce the signals to our brain. Figure 1.4 illustrates the process of signals in the human visual system.

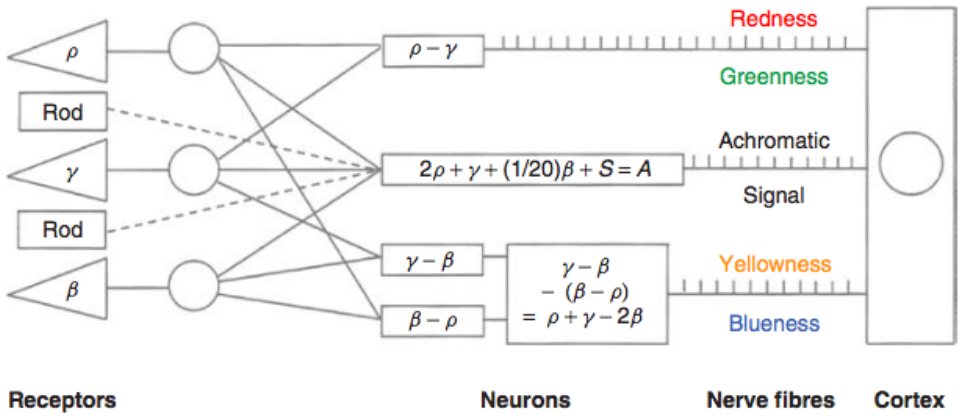

Fig. 1.4. Illustration of the opponent-process theory [Hunt and Pointer 2011].

1.2 Photometry and Colorimetry

Photometry is used to characterize the amount of light perceived by the human visual system. A weighting formula, the luminous efficiency function, is used to describe the relative sensitivity of the human visual system in terms of brightness, to the radiation at different wavelengths from 380 to 780 nm. The luminous efficiency functions were derived through psychophysical experiments using the equality-of-brightness method or flicker photometry method [Osborne 1917]. In an equality-of-brightness experiment, the observers viewed a reference beam and a test beam simultaneously and adjusted the intensity of the test beam to match the brightness of the reference beam. The wavelengths of the test and the reference beams were always close to each other and were changed throughout the visible spectrum. In a flicker photometry experiment, the visual task was the same but the test and reference beams were presented alternatively under a certain rate, which was fast enough to prevent colour difference detection but slow enough for

brightness difference perception. Figure 1.5 shows the International Commission on Illumination (CIE) luminous efficiency function—V(λ)—which is the basis for all the photometric quantities.

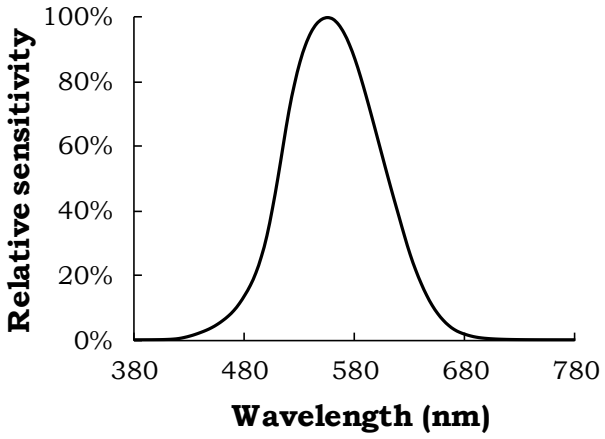

Fig. 1.5. The CIE luminous efficiency function for photopic vision.

Colorimetry characterizes whether two stimuli with different spectral contents have matched colour appearance under a same viewing condition, which is characterized based on the colour matching functions (CMFs). In the experiments deriving CMFs, the observers observed a 2° luminous disk that was divided into a test field and a reference field with a dark surround. The reference field was illuminated by a monochromatic light, while the test field was illuminated by three chromatic lights (i.e., a set of primaries), as shown in Fig. 1.6. The observers adjusted the intensities of the three chromatic lights in the test field until the colour appearance of the test field matched that of the reference field. The experiment was repeated by changing the wavelength of the monochromatic light from 380 to 780 nm for the reference field. The observer was also allowed to move one chromatic light in the test field to the reference field when he/she could not create a colour match. Figure 1.7 shows the intensities of the three monochromatic lights in the test field that were used to match the colour appearance of the monochromatic light in the

reference field from 380 to 780 nm, with the negative values indicating that the chromatic light was moved to the reference field. The three curves are called the CMFs for this primary set.

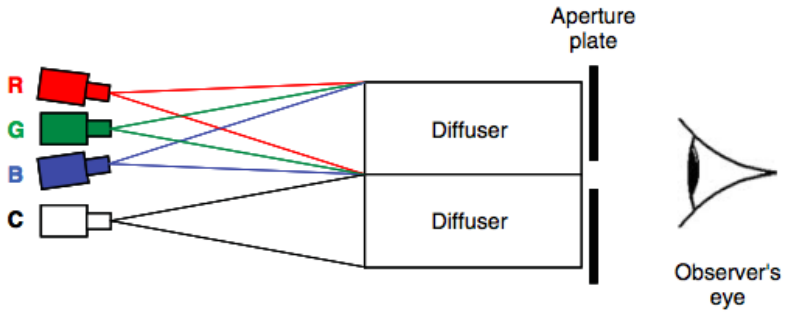

Fig. 1.6. An illustration for the colour matching experiment [Judd and Wyszecki 1975].

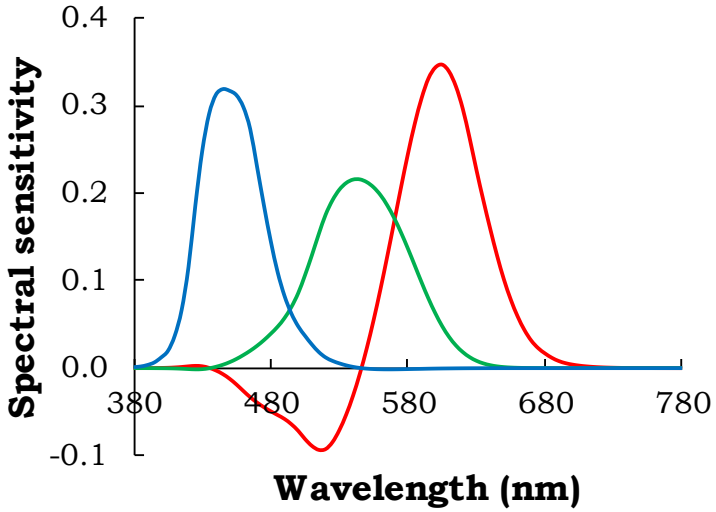

Fig. 1.7. The RGB CMFs derived from the colour matching experiments.

In order to avoid the negative values for calculations, CIE implemented a mathematic transformation using an imaginary set of primaries (X, Y, and Z) to transform the RGB CMFs to the XYZ CMFs. Two sets of XYZ CMFs were proposed by CIE, as shown in Fig. 1.8, with the CIE 1931 2° CMFs for stimuli with a field of view (FOV) of 2° and the CIE 1964 10° CMFs for stimuli with an FOV of 10°. The metrics specifying the colour of a stimulus, such as tristimulus values and correlated colour temperature (CCT), are all calculated using the CIE 1931 2° CMFs.

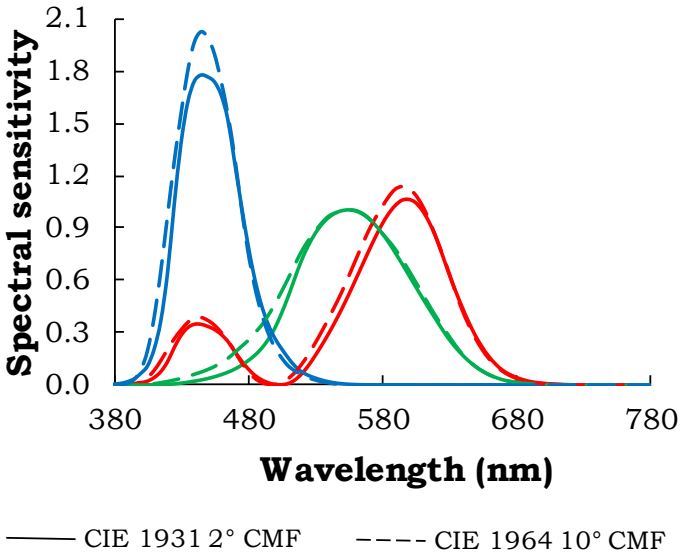

Fig. 1.8. The CIE 1931 2° CMFs and the CIE 1964 10° CMFs.

1.3 Colour Spaces and Colour Appearance Models

To better characterize the colour match and colour differences of colours under different adapting conditions, two three-dimensional colour spaces, CIELAB and CIELUV, were developed by CIE in 1976. The two colour spaces, however, were developed mainly for characterizing the colour differences between surface colours with the same size and shape under the illumination similar to D65 with a neutral background [CIE 1986]. They were not designed to characterize the various perceived colour attributes under various viewing conditions. In contrast, colour appearance models (CAMs) were developed to characterize the perceived colour attributes of stimuli under different viewing conditions. The colour attributes include absolute (i.e., brightness, colourfulness, and hue) and relative attributes (i.e., lightness, chroma, hue, and saturation). When characterizing the effect of adapting field on perceived colour attributes of a stimulus, the chromatic adaptation transform (CAT) is embedded in CAMs to characterize the chromatic adaptation mechanism of the human visual system. Currently, CIECAM02, CAM02-UCS, and CAT02 are the most widely used CAM, uniform colour

space, and CAT in the community [Fairchild 2013]. In recent years, other CAMs and uniform colour spaces have been developed to overcome some weaknesses. For example, Ja_zb_z colour space [Safdar et al. 2017] and IC_TC_P colour space [DOLBY 2016] were developed to characterize the colour differences of the stimuli in high dynamic range viewing conditions. In addition, several recent studies suggested that the existing models underestimate the effect of adapting field on the colour appearance of physical stimuli (e.g., [Smet et al. 2017a; Smet et al. 2017b; Zhai and Luo 2018]).

1.4 Chromatic Adaptation and White Balance

1.4.1 Chromatic Adaptation

Chromatic adaptation is the ability of the human visual system for discounting the colour of illumination to some extent and maintaining the colour appearance of illuminated objects relatively constant. For example, the colour appearance of a white paper remains similar under the illumination of daylight and an incandescent lamp, though the daylight has lower radiation in the long wavelengths of the visible spectrum and the incandescent lamp has much lower radiation in the short wavelengths of the visible spectrum.

The chromatic adaptation mechanisms can be classified into low and high levels of encoding of a stimulus (a.k.a., the sensory and cognitive mechanisms [Fairchild 2013]). The former refers to the adaptation that responds automatically upon the appearance of the stimulus and relates to the sensitivities of the L-, M-, and S-cones in the first few stages of the human visual system [Sharma and Bala 2002]. The latter refers to the subjective cognition of an observer, which relates to the understanding of the stimulus

content and the scene. Though it is hard to quantify the effects of the low and high levels of encoding respectively, it is believed that when viewing a stimulus under a prevailing illumination, both types of encoding are active, with the low levels of encoding responding to the spectral content of the stimulus and the high levels of encoding responding to the illumination to discount its colour. When viewing a stimulus produced by a display, on the other hand, the stimulus is unlikely to be perceived as an illuminated colour and only the low levels of encoding are active, causing a lower degree of chromatic adaptation [Fairchild 2013]. In short, the chromatic adaptation is critically important to the colour appearance.

1.4.2 White Balance

The chromatic adaptation mechanism allows the human visual system to automatically remove the colour cast of the illumination, which does not exist in cameras. In order to reproduce the colours perceived by the human visual system, cameras simulate the chromatic adaptation mechanism through white balance.

In a common digital still camera, a Colour Filter Array (CFA) is placed on top of the camera sensor so that each pixel of the sensor is covered by one of three coloured filters (i.e., red, green, and blue). Therefore, each pixel of a RAW image only carries one colour value, either red (R), green (G), or blue (B). The raw sensor data are recorded in a non-linear colour space, so an optoelectronic conversion function (OECF) is used to linearize the values. White balance is then applied to the linearized data to balance the red, green, and blue values in the camera colour space, after which demosaicing is performed to decode and estimate the missing RGB values for each pixel. The balanced RGB values of each pixel are finally transformed from the

camera colour space to a device independent colour space (e.g., sRGB colour space) by applying a 3 × 3 transformation matrix, which allows an accurate rendering on different calibrated output devices (e.g., display). The entire process is illustrated in Fig. 1.9.

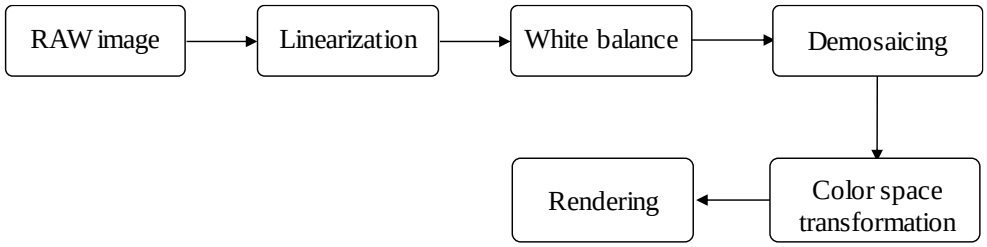

Fig. 1.9. A workflow for processing RAW images.

Different white balance algorithms have been developed. These algorithms can be classified by three categories—statistical methods, gamut-based methods, and learning-based methods. Statistical methods estimate the colour of the illumination in a scene by examining the statistical properties of the RGB values in the image. Gamut- and learning-based methods require more computational power, with the former considering the finite gamut of sensors and scene appearance under different illumination and the latter determining the colour and spatial-statistic information based on the training images to estimate the colour of the illumination [Cheng et al. 2014].

1.5 Research Goals

This dissertation aimed to comprehensively investigate the white appearance produced by surface colors, self-luminous displays, and two types of Augmented Reality (AR) technology. The investigation of the white appearance was used to understand the degrees of chromatic adaptation under different viewing conditions and to further our understanding about chromatic adaptation.

1.6 Structure

The structure of this dissertation is organized as follows. Chapter 2 reviews the past studies that are relevant to the dissertation. Chapter 3 goes through the research investigating the whiteness appearance of surface colours under light-emitting diode (LED) illumination. The performance of the existing whiteness formulae was evaluated and the degrees of chromatic adaptation under the viewing conditions of different CCT levels were discussed. Successively, Chapter 4 reports the investigation on the whiteness appearance of surface colours from the perspective of image appearance. Various white balance algorithms were used to process the images captured under two illumination conditions with one simulating a high quality D65 illuminant and the other simulating a typical blue-pumped white LED. The effect of the lack of UV/violet radiation in an illumination, which happens to typical white-light LED sources, on the colour appearance of the white samples and colour samples in the images was investigated using different white balance algorithms. Chapter 5 reports the experiments that investigated the degrees of chromatic adaptation under different adapting conditions through the investigation of the white appearance of a stimulus. The effect of viewing mode and the joint effect of adapting CCT and luminance on the white appearance of a stimulus were discussed. Chapter 6 goes over the experiments related to the white appearance of virtual stimuli produced by two types of Augmented Reality (AR) setups—optical see-through and video see-through setups—and discusses the chromatic adaptation for viewing a virtual stimulus. Chapter 7 summarizes the findings and contributions.

Chapter 2 Literature Review

2.1 Chromatic Adaptation

2.1.1 Chromatic Adaptation Transforms and Degree of Adaptation

In order to investigate how chromatic adaptation affects the colour appearance of stimuli, psychophysical experiments using different colour matching methods (e.g., haploscopic matching [McCann et al. 1976; Breneman 1987], local-adaptation matching [MacAdam 1956], magnitude estimation [Kuo et al. 1995], and memory colour matching [Smet at al. 2017a]) were conducted to obtain data of corresponding colours. Corresponding colours is a pair of colour stimuli under the two adapting conditions that have the same colour appearance to an observer [Luo 1995]. Based on the datasets of corresponding colours, various CATs have been developed. These CATs can be classified into three groups: those occur as a part of colour spaces (e.g., CIELUV and CIELAB), those depend on the scaling of cone responses (e.g., the von Kries transformation), and those included in colour appearance models (e.g. CAT97 and CAT02) [Hunt and Pointer 2011]. Most CATs apply the von Kries coefficient law (a.k.a., the Young-Helmholtz theory), which assumes that the relative spectral sensitivity of each of the three types of cones remains unchanged under different adapting conditions, as shown in Eq. 2.1,

$$R_C = \alpha R, G_C = \alpha G, B_C = \alpha B \tag{2.1}$$

where R_c, R, G_c, G, B_c, and B are the cone responses under the two adapting conditions.

The degree of chromatic adaptation plays an important role in the CATs that are based on the von Kries coefficient law. In practice, a degree of chromatic

adaptation factor D between 0 and 1 is usually included in a one-step von Kries transform, which can be described using Eq. 2.2 [Smet et al. 2017a],

$$X'_B = (D_{A,B}\Lambda_{A,B} + (1 - D_{A,B}))X_A \quad (2.2)$$

where X_A and X_B are the responses under different adapting conditions A and B and $\Lambda_{A,B}$ is the diagonal matrix of the gain controls. Smet et al. [2017a] proposed the two-step von Kries transform in order to interpret the process of chromatic adaptation more clearly. The two-step von Kries transform transforms the colour under one adapting condition A to a baseline condition, and then transforms it further to the other condition B, as shown in Eq. 2.3,

$$X'_B = (D_{B,0}\Lambda_{B,0} + \left(1 - D_{B,0}\right))^{-1} \cdot (D_{A,0}\Lambda_{A,0} + \left(1 - D_{A,0}\right)) X_A \quad (2.3)$$

where $D_{A,0}$ and $D_{B,0}$ are the degrees of chromatic adaptation for the first and second step of the transform respectively. It was suggested that the two-step transform could be more accurate when the degrees of two steps of transform are significantly different. When one of the two illuminants is close to the baseline state, the one-step and two-step transforms perform similarly [Smet et al. 2017a]. The degree of chromatic adaptation has been modelled differently in previous studies. For example, the widely used CAT02, which is embodied in the CIECAM02, calculates the degree of chromatic adaptation factor D as shown in Eq. 2.4.

$$D = F\ (1\ -\ \frac{1}{3.6}\ e^{-(L_A+42)/92}) \quad (2.4)$$

where F is a parameter characterizing the surround condition (i.e., dark, dim, and average) and L_A is the adapting luminance. Various studies have shown that the chromaticities of the adapting condition also affected the degree of chromatic adaptation and should be considered in the calculation of the degree of chromatic adaptation factor [Smet et al. 2017a; Smet et al.

2017b; Zhai and Luo 2018; Wei et al. 2017b; Zhai and Luo 2018]. Smet et al. [2017a; 2017b] conducted experiments using the method of long-term memory colour matching and investigated the effect of the chromaticities of the adapting condition on the degree of chromatic adaptation. It was found that the degree of chromatic adaptation was significantly lower than that predicted by CATs, especially when the adapting condition was highly chromatic. Wei et al. [2017a] investigated the white appearance of white samples with and without fluorescent whitening agents (FWAs) under the adapting conditions with different levels of CCT and UV/violet radiation. The samples under the 3000 K conditions were rated to be less white than those under the 4000 and 6500 K conditions, which indicated a lower degree of chromatic adaptation under the 3000 K conditions. Huang et al. [2018] investigated the white appearance of a tablet display under various adapting conditions and discovered the effect of the chromaticities of the adapting condition on the degree of chromatic adaptation. The degree of chromatic adaptation increased with the adapting CCT and it was higher under the condition with a D_{uv} of 0.02 than that under the condition with a D_{uv} of -0.04 or +0.02. Zhai and Luo [2018] conducted colour matching experiments using surface and display colours, under the adapting conditions with various CCT levels and D_{uv}. The chromatic adaptation was found to be more complete when viewing the surface colours than viewing the display colours. Such a difference was attributed to the different viewing media and two models were developed for characterizing the degree of chromatic adaptation. A trend was found that the degrees of chromatic adaptation

when viewing display colours increased with the CCT levels of the adapting conditions.

2.1.2 White Balance Algorithms

Various white balance algorithms, including the statistical methods, gamut-based methods, and learning-based methods have been developed by the researchers. The gamut- and learning-based methods require significantly more computational power and are not suited for real-time use [Cheng et al. 2014]. Statistical methods, with their high efficiency, are widely used in imaging systems. Most statistical methods are based on either the Grey World assumption [Buchsbaum 1980] or the Retinex theory [McCann et al. 1976] (a.k.a., Perfect Reflector [Zapryanov et al. 2012] or White Patch assumption [Lukac 2008]). The Grey World assumption assumes that any captured image should be achromatic on average (i.e., the average RGB values of an image should be equal), which is more likely to hold when a scene is not dominated by one or two colours [Lam et al. 2004]. The Retinex theory, on the other hand, assumes that the colour of the pixel(s) with the maximal RGB values in an image is the colour of the illumination.

The GW algorithm and maxRGB algorithms, the two simplest algorithms based on the Grey World assumption and the Retinex theory respectively, can be described using Eq. 2.5, with a Minkowski norm (i.e., p) value of 1 and $+\infty$ respectively [Finlayson and Trezzi 2004]. The calculated Minkowski means t_C (C = R, G, and B), which are the average and the maximal RGB values of an image respectively, are used to calculate the gain factors for R and B values (i.e., *corrR* and *corrB*) using Eq. 2.6. The balanced R and B values (i.e., R' and B') can be derived using Eq. 2.7 (Note the G values are typically kept unchanged). Instead of using an extreme value for p, Finlayson

and Trezzi [2004] proposed the Shades-of-Grey (SoG) algorithm, with a p value between 1 and +∞. They also found that a p value between 2 and 29 can lead to a higher accuracy.

$$t_C = \left(\frac{\sum I_C(x)^p}{N}\right)^{\frac{1}{p}} \tag{2.5}$$

$$corrR = \frac{t_G}{t_R},\ corrB = \frac{t_G}{t_B} \tag{2.6}$$

$$R' = corrR \times R, G' = G, B' = corrB \times B \tag{2.7}$$

where C denotes R, G, or B, $I(x)$ is the R, G, or B value of each pixel, p is the Minkowski norm, and N is the number of pixels in an image.

Efforts have been made on modifying the GW and maxRGB algorithms to further improve their performance and robustness. The MWG algorithm allows a variation for the average RGB values of an image, as shown in Eqs. 2.8-2.10, when deriving the gain factors for R and B values. The three parameters—a, b, and c—are used to adjust the range of variation.

$$-a < \bar{B} - \bar{G} < a \tag{2.8}$$

$$-b < \bar{R} - \bar{G} < b \tag{2.9}$$

$$-c < (\bar{R} - \bar{G}) + (\bar{B} - \bar{G}) < c \tag{2.10}$$

The Standard Deviation Weighted Grey World (SDWGW) algorithm [Lam et al. 2004] divides the captured image into n blocks and puts higher weights to the blocks with larger variations of the RGB values. Specifically, the standard deviation weighted average (*SDWA*) is calculated for the RGB values as Eqs. 2.11-2.13 and the RGB values of each pixel are then adjusted using the three *SDWA* values, as shown in Eqs. 2.14-2.16.

$$SDWA_R = \sum_{k=1}^{n} \frac{SD_R(k)}{\sum_{i=1}^{n} SD_R(i)} \times \overline{R(k)} \tag{2.11}$$

$$SDWA_G = \sum_{k=1}^{n} \frac{SD_G(k)}{\sum_{i=1}^{n} SD_G(i)} \times \overline{G(k)} \tag{2.12}$$

$$SDWA_B = \sum_{k=1}^{n} \frac{SD_B(k)}{\sum_{i=1}^{n} SD_B(i)} \times \overline{B(k)} \tag{2.13}$$

$$R' = R \times \frac{SDWA_R + SDWA_G + SDWA_B}{3 \times SDWA_R} \tag{2.14}$$

$$G' = G \times \frac{SDWA_R + SDWA_G + SDWA_B}{3 \times SDWA_G} \tag{2.15}$$

$$B' = B \times \frac{SDWA_R + SDWA_G + SDWA_B}{3 \times SDWA_B} \tag{2.16}$$

The Auto Level algorithm [Limare et al. 2011], named after a function in Adobe Photoshop, extends the concept by scaling the *RGB* values of each pixel linearly using the maximum and minimum RGB values in an image, as shown in Eqs. 2.17-2.19. To improve the robustness of the algorithm, a saturation factor *p* is used to exclude the possible outliers, with only the RGB values between 0.5*p*% and 1-0.5*p*% being included.

$$R' = 255 \times \frac{R - R_{min,0.5p\%}}{R_{max,1-0.5p\%} - R_{min,0.5p\%}} \tag{2.17}$$

$$G' = 255 \times \frac{G - G_{min,0.5p\%}}{G_{max,1-0.5p\%} - G_{min,0.5p\%}} \tag{2.18}$$

$$B' = 255 \times \frac{B - B_{min,0.5p\%}}{B_{max,1-0.5p\%} - B_{min,0.5p\%}} \tag{2.19}$$

Unlike the above algorithms, Lam [2005] proposed a GWR (i.e., Grey World + Retinex) algorithm to consider both assumptions simultaneously. The *R*' and *B*' values are calculated using a quadratic function, as shown in Eqs. 2.20 and 2.22, with the coefficients—*a*, *b*, *c*, and *d*—being calculated using Eqs. 2.23 and 2.24.

$$R' = aR^2 + bR \tag{2.20}$$

$$G' = G \tag{2.21}$$

$$B' = cB^2 + dB \tag{2.22}$$

$$\begin{pmatrix} \sum R^2 & \sum R \\ \max R^2 & \max R \end{pmatrix} = \begin{pmatrix} a \\ b \end{pmatrix} \begin{pmatrix} \sum G \\ \max G \end{pmatrix} \tag{2.23}$$

$$\begin{pmatrix} \sum B^2 & \sum B \\ \max B^2 & \max B \end{pmatrix} = \begin{pmatrix} c \\ d \end{pmatrix} \begin{pmatrix} \sum G \\ \max G \end{pmatrix} \tag{2.24}$$

The performance of the white balance algorithms was typically evaluated by comparing the colour difference between the chromaticities of the estimated and actual light sources or the colour difference between the colours in balanced and reference images. In earlier days, images were typically captured under conventional light sources or standard illuminant simulators (e.g., TL84, CIE Illuminant A, D50, D65, and D75) [Liu et al. 1995; Chikane and Fuh 2006; Huo et al. 2006; Zapryanov et al. 2012]. In recent years, the evaluations and comparisons were made using different datasets including a large number of images [Finlayson and Trezzi 2004; Gehler et al. 2008; Cheng et al. 2014], such as the SFU Lab dataset [Barnard et al. 2002], the Grey-ball dataset [Ciurea and Funt 2003], the Shi-Funt-Gehler dataset [Gehler et al. 2008], and the NUS dataset [Cheng et al. 2014]. These datasets include both natural outdoor scenes under daylight and indoor scenes under common indoor light sources. A Macbeth ColourChecker or a grey object is typically included in these scenes for measuring the chromaticities of the actual illumination.

2.2 Perception of White Appearance

2.2.1 White Appearance of Surface Colours

White is one of the most common colours in our daily life. White appearance relates to how natural and pleasant objects appear [David et al. 2013] and white is associated with high quality, freedom of contaminants, and cleanness [Wei et al. 2017b]. Since 5000 BC, human beings have made great efforts to

understand the human perception to white and used numerous approaches to enhance the whiteness appearance. In addition, white is one of the most unambiguous colours to human beings and specifying white under different viewing conditions is critically important to understand colour perception.

In colorimetry, white is defined as a colour devoid of hues and is bright enough to avoid an appearance of grey. For surface colours, however, it has been found that adding a certain amount of blue tint can make objects appear whiter. The fluorescent whitening agents (FWAs), which absorb violet or ultraviolet radiation from the illumination and re-emit blue radiation, can simultaneously increase the lightness and introduce a blue tint for white objects and are widely used in textile, paper, and detergent products. Manufacturers modulate the amount of FWAs to produce white appearance at different levels. In order to characterize the whiteness appearance of FWA-enhanced whites, whiteness metrics have been proposed for the industry. In 1986, CIE proposed the CIE whiteness metric (i.e., W_{CIE}) [CIE 2004], which was based on the analysis of the published formulae and applied the equation of the Ganz-Griesser whiteness formula. The whiteness metric W_{CIE} and a tint value T_{CIE} of a sample are calculated using Eqs. 2.25 and 2.26 respectively.

$$W_{CIE} = Y + 800(\mathrm{x_n} - x) + 1700(y_{\mathrm{n}} - y) \tag{2.25}$$

$$T_{CIE} = 900(x_{\mathrm{n}} - x) - 650(y_{\mathrm{n}} - y) \tag{2.26}$$

Where Y is the luminance factor; (x, y) and (x_{n}, y_{n}) are the chromaticities of the sample under a D65 simulator and those of the simulator. The chromaticities were calculated using the CIE 1964 10° CMFs. The formulae are applicable when W_{CIE} is between 40 and 5Y-280 and T_{CIE} is between -4 and +2.

The limitations of the CIE whiteness formula have been documented in previous studies. The range for the whiteness specification was found to be too small [Uchida and Fukuda 1987] and it was only developed under D65. It failed when characterizing whiteness under other illuminants, especially for typical phosphor-converted white-light LEDs [Houser et al. 2014; Wei et al. 2014; Wei et al. 2017a]. In 1998, Uchida extended the CIE whiteness formula by using 5*Y*-275 as a base point, as described in Eqs. 2.27-2.29 [Uchida 1998].

When $40 < W_{\mathrm{CIE}} < 5Y\text{-}275$ (i.e., in-base point):

$$W_{\mathrm{Uchida}} = W_{\mathrm{CIE}} - 2(T_{\mathrm{CIE}})^2 \tag{2.27}$$

When $W_{\mathrm{CIE}} > 5Y\text{-}275$ (i.e., out-base point):

$$W_{\mathrm{Uchida}} = P_{\mathrm{W}} - 2(T_{\mathrm{CIE}})^2 \tag{2.28}$$

$$P_{\mathrm{W}} = (5Y - 275) - 800[0.2742 + 0.00127(100 - Y) - x]^{0.82} - 1700[0.2762 + 0.00176(100 - Y) - y]^{0.82} \tag{2.29}$$

As spectrally tunable LED lighting is becoming more and more popular, extending the application of the metrics for characterizing samples under an arbitrary light source is of great importance and interest. David et al. [2013] proposed an adaptation of the CIE whiteness formula, as shown in Eq. 2.30, which adapted W_{CIE} to light sources of any CCT.

$$W_{\mathrm{CIE,adapted}} = Y - \omega \cdot \cos(\eta + \varphi)/\cos\varphi \cdot (x - x_0) - \omega \cdot \sin(\eta + \varphi)/cos\varphi \cdot (y - y_0) \tag{2.30}$$

Where Y and (x, y) are the luminance factor and the chromaticities of a sample under a light source, (x_0,y_0) are the chromaticities of the light source, ω = 1800 is the sensitivity of whiteness to saturation, η is the angle between the x-axis and the direction from (x_0,y_0) to (0.1152, 0.1090) (i.e., the chromaticities of a monochromatic light at 470 nm), φ = 16.6° is a small angle

between the direction of enhanced white appearance and the direction towards the chromaticities of the 470 nm monochromatic light. Later, Ma et al. [2016] proposed an optimized formula, as shown in Eqs. 2.31-2.33, which used the parameters that were calculated by the CCT of the light source.

$$W_{\mathrm{CIE,optimized}} = Y + a(x_0 - x) + b(y_0 - y) \tag{2.31}$$

$$a = -0.1891\ CCT + 2267.2 \tag{2.32}$$

$$b = 0.3203\ CCT - 493.36 \tag{2.33}$$

Chromatic adaptation transforms are also considered to be embedded in the whiteness formula [Wei et al. 2017a], so that he chromaticities of the samples and light sources can be transformed to the corresponding values under the CIE standard D65 illuminant. Based on a series of psychophysical experiments carried out by Ma et al. [2016] and Wei et al. [2017a], it was found that the CIE whiteness formula with CAT02 (i.e., $W_{\mathrm{CIE,CAT02}}$) outperformed the other formulae in terms of the correlation between the calculated whiteness values and the perceived whiteness appearance of the samples under the sources at different CCT levels.

2.2.2 White Appearance of Self-luminous Stimuli

The white appearance is not only important to surface colours, but also to self-luminous colours, such as displays and spectral lights. Helson and Michels [1948] investigated the chromaticities for producing a white appearance with different surrounds and found the stimulus with a CCT of 15000 K and chromaticities on the blackbody locus appeared the whitest. Hurvich and Jameson [1951] investigated the white appearance of the stimuli with different FOVs and a dark surround and found that the stimuli at 5500 and 7500 K required the lowest luminance level to be perceived as white.

Valberg [1971] investigated the colour appearance of unique hues and specified the chromaticities for producing a white appearance to be close to the chromaticities of 5600, 7050, 7750, and 11000 K daylight illuminants. Choi and Suk [2016] investigated the white appearance of displays under the illuminants between 2500 and 20000 K. A chromaticity region with the CCT between 6200 and 7500 K and D_{uv} between +0.004 and +0.014 was identified. Huang et al. [2018] investigated the white appearance of a tablet display under different adapting conditions. The chromaticity region for producing a white appearance was identified for each adapting CCT level and it was revealed that the white appearance under each adapting condition was notably different.

By comparing the studies investigating surface stimuli and self-luminous stimuli, the chromaticities for producing a white appearance were obviously different [Fairchild 1993; Oicherman et al. 2008; Luo et al. 2008; Huang et al. 2011; High et al. 2017; Zhai and Luo 2018]. Some studies specifically compared the differences caused by surface colour and self-luminous colours [Fairchild 1993; Zhai and Luo 2018]. Fairchild [1993] investigated the chromaticities for producing white with printed images and a display and found obvious chromaticity differences. It concluded that the two types of chromatic adaptation mechanisms, sensory and cognitive, were both active when viewing surface colours, while only the sensory chromatic adaptation was active when viewing display colours. Zhai and Luo [2018] investigated the white appearance of surface colours using Natural Colour System (NCS) colour samples and self-luminous colours produced by a mobile phone display and found a significant difference between the chromaticities for producing a white appearance. It was found that the chromaticities for

producing a white appearance on a display generally shifted away from the chromaticities of the adapting conditions towards a higher CCT level and were close to the blackbody locus. In comparison, the chromaticities for producing a white appearance to surface colours were much closer to the adapting chromaticities.

In short, the chromaticities for producing a white appearance on self-luminous displays were found to be shifted from the adapting chromaticities towards a higher CCT and the chromaticities for producing a white appearance to surface colour samples were much closer to the chromaticities of the adapting conditions [Hunt and Winter 1975; Breneman 1987; Fairchild 1991; Berns and Gorzynski 1991; Choi and Suk 2016; High et al. 2017; Huang et al. 2018; Zhai and Luo 2018; Zhu et al. 2018]. The difference was commonly attributed to the different degrees of chromatic adaptation caused by the two different viewing media, with a lower degree of chromatic adaptation when viewing self-luminous stimuli.

Chapter 3 Whiteness Appearance of Surface Colours

3.1 Motivation

Whiteness appearance is critically important to surface colour industry and numerous efforts have been made to enhance the whiteness appearance of surface colours. The invention of FWAs allows the manufacturers to modulate the amount of FWAs in white objects to produce different degrees of whiteness appearance. Under a conventional light source that contains a certain amount of UV/violet radiations, a surface containing a greater amount of FWAs appear whiter. White-light LEDs that are becoming more and more popular for general illumination, however, contain little amount of radiation in the short wavelength regions of the spectrum for high luminous efficacy and cannot excite the FWAs contained in white objects. The CIE whiteness formula, the most widely used whiteness formula, only characterizes the whiteness appearance under the CIE standard D65 and does not consider the effect of the spectral content of a light source. In past studies, the adoption of CAT02 was found to be able to improve the performance of the CIE whiteness formula, but it could not characterize the whiteness appearance of surface colours under arbitrary light sources across different CCT levels.

The study in this chapter aimed to develop a whiteness formula that allows the characterization of the whiteness appearance of surface colours under light sources at different CCT levels.

3.2 Method

3.2.1 Apparatus and Illuminants

Two viewing booths with dimensions of 60 cm (depth) × 60 cm (width) × 60 cm (height) were placed side-by-side. The interiors of the booths were painted with Munsell N7 neutral grey paint. A 14-channel spectrally tunable LED device was placed above each booth to provide a horizontal illuminance of 1000 ± 20 lx at the booth floor. The experiment setup is shown in Fig. 3.1. A chin-rest was mounted in front of the two booths to align the observer's sagittal plane with the dividing panel between the booths, so that a haploscopic viewing condition and a 0°:45° viewing geometry was created. The intensities of the channels in the LED devices were carefully designed to produce seven illuminants. A CIE D65 simulator of high quality was always used in the left booth as the reference illuminant, which had CIE metamerism indices M_v of 0.84 and M_u of 0.69. Six illuminants were used in the right booth, comprising three CCT levels (i.e., 3000, 4000, and 5000 K) and two violet radiation levels (i.e., low and high). The two violet radiation levels were used to produce different whiteness appearance to the samples placed in the booth, and the samples were maintained to appear white. The SPDs of the illuminants were measured using a calibrated JETI specbos 1811UV spectroradiometer with a reflectance standard, with the SPDs shown in Fig. 3.2. Table 3.1 summarizes the colourimetric characteristics of the seven illuminants. Four and eight diffuse acrylic whiteness samples with different amounts of FWAs were placed in the left and right booths respectively.

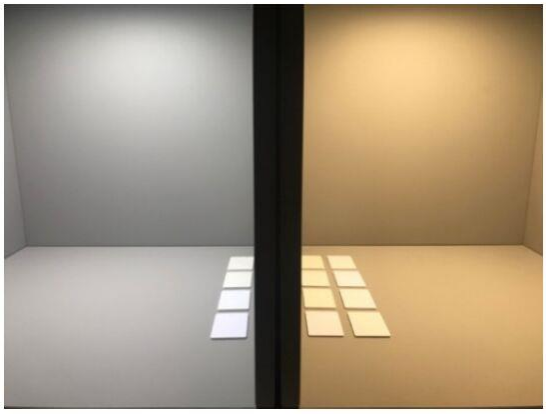

Fig. 3.1. Photograph of the experiment setup taken from the observer's eyes position.

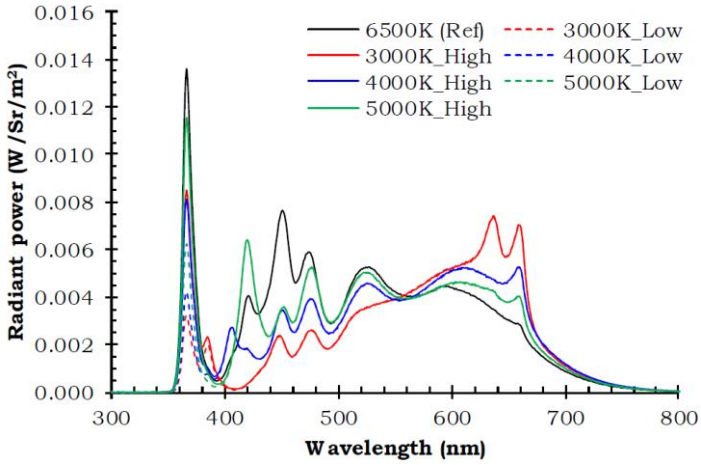

Fig. 3.2. SPDs of the illuminants measured using a calibrated JETI specbos 1811UV spectroradiometer with a reflectance standard.

Table 3.1. Colourimetric characteristics of the illuminants

Illuminants	CIE 1964 (x,y)	CCT	D_{uv}	CRI R_a
6500K (Ref)	(0.316,0.323)	6484	-0.0012	96.6
3000K Low	(0.437,0.403)	3081	+0.0008	98.1
3000K High	(0.436,0.403)	3098	+0.0007	98.4
4000K Low	(0.387,0.380)	3948	+0.0013	98.0
4000K High	(0.387,0.380)	3950	+0.0014	97.8
5000K Low	(0.347,0.354)	4982	+0.0020	98.4
5000K High	(0.347,0.354)	4968	+0.0018	98.4

3.2.2 Whiteness Samples and Evaluation

Under each pair of illuminants, the observers were asked to evaluate the whiteness appearance of the eight samples in the right booth and scale the whiteness values in comparison to the four reference samples under the D65 simulator in the left booth. The four samples in the left booth were reference samples, which had CIE whiteness values (i.e., W_{CIE}) of 84.3, 90.7, 122.1,

and 142.9. These samples were carefully selected, so that the whiteness values allowed observers to understand the whiteness difference of 10, 30, and 20 points. The eight samples in the right booth under the six illuminants had similar lightness values *Y* between 88.5 and 93.9, so the whiteness differences between the samples were introduced by the chromaticity differences. The rating was not limited between 84 and 143. Figure 3.3 shows the chromaticities of the whiteness samples calculated using the CIE 1964 10° CMFs under each illuminant.

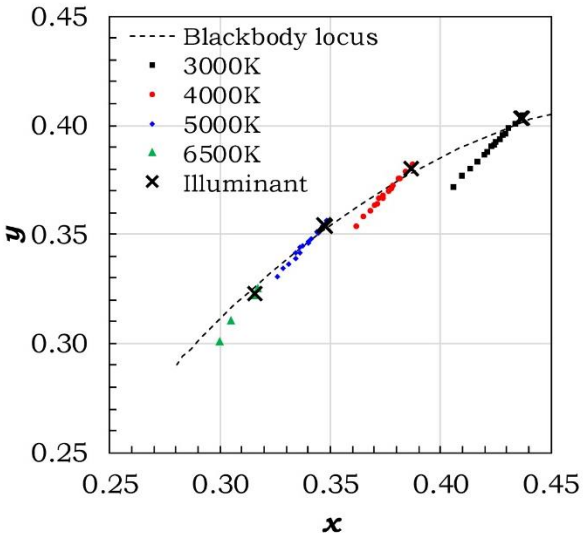

Fig. 3.3. Chromaticities of the whiteness samples under each illuminant, calculated using CIE 1964 10° CMFs.

3.2.3 Observers

Fifteen observers (four females and 11 males) with an age between 20 and 25 (mean = 21.4, std. dev. = 1.40) participated in the experiments. All the observers had a normal colour vision, as tested by the Ishihara Colour Vision Test [Dain 2004].

3.2.4 Experimental Procedure

Upon arrival, the observer completed a general information survey and the Ishihara Colour Vision Test. Then the observer was escorted to the viewing booths and was seated in front of the booths with his/her chin being rested on

the chin rest, so that a similar haploscopic viewing geometry was formed for all the observers. Under each pair of the illuminants, the observer viewed the samples in the two booths for two minutes for chromatic adaptation. The illuminant in the left booth was the 6500 K reference illuminant (i.e., CIE D65 simulator) and the illuminant in the right booth was one of the other six illuminants. A rating sheet was placed in the right booth, with the whiteness values of the four reference samples in the left booth being labelled as 84, 91, 122, and 143. The observer was asked to rate the whiteness of the samples in the right booth by comparing their whiteness appearance with that of the samples in the left booth. The experimenter reminded the observer that the four samples in the left booth had a 10-, 30-, and 20-point differences in the whiteness values and the rating could be below 84 or above 143. Among the six pairs of illuminants, two pairs were selected randomly for each observer to repeat the evaluations, which was used to evaluate the intra-observer variations. A new rating sheet was used for each pair of illuminants. The order of the eight pairs of illuminants was randomized for each observer.

3.3 Results

3.3.1 Inter- and Intra-observer Variations

The intra- and inter-observer variations were characterized using the Standardized Residual Sum of Squares (STRESS) [García et al. 2007], which was commonly used in colour appearance evaluations [Wei et al. 2017b; Huang et al. 2018]. The intra-observer variation was characterized by comparing the perceived whiteness values of the samples that were rated by each observer twice under the two illuminants. The STRESS values of the 15 observers ranged between 5.1 and 16.0 with an average of 10.4. The inter-

observer variations were characterized by comparing the perceived whiteness values of the eight samples rated by each observer and the average perceived whiteness rated by the observers (i.e., an average observer) under each CCT. The mean STRESS values for the 3000, 4000, and 5000 K illuminants were 13.0, 11.3, and 9.6 respectively. Both the STRESS values for the inter- and intra-observer variations were much smaller than those in previous studies [Shamey et al. 2010; Xu et al. 2016; Wei et al. 2017a; Wei et al. 2017b; Hunag et al. 2018], indicating a high reliability of this experiment.

3.3.2 Performance of Whiteness Formulae

The performance of six whiteness formulae (i.e., W_{CIE}, $W_{CIE,(xn,yn)}$, $W_{CIE,CAT02}$, $W_{CIE,adapted}$, $W_{Uchida,CAT02}$, and $W_{CIE,optimized}$) were evaluated by comparing the calculated whiteness values and the perceived whiteness values, as shown in Fig. 3.4. All the calculated whiteness values were well correlated to the perceived whiteness values under each individual CCT level regardless of the whiteness formulae, with a Pearson correlation coefficient (r) between 0.92 and 0.97. The formulae, however, failed to characterize the whiteness levels under the illuminants across different CCT levels. As shown in Fig. 3.3, the calculated whiteness values using each formula were higher than the perceived whiteness (except W_{CIE}), especially under low CCT levels. The errors of each formula under the illuminants of each CCT level was characterized by the root-mean-square error (RMSE), as summarized in Table 3.2. Overall, the performance of $W_{CIE,optimized}$ was the best and that of W_{CIE} was the worst. Furthermore, the RMSE values were always higher for the illuminants of lower CCT levels, regardless of the formulae.

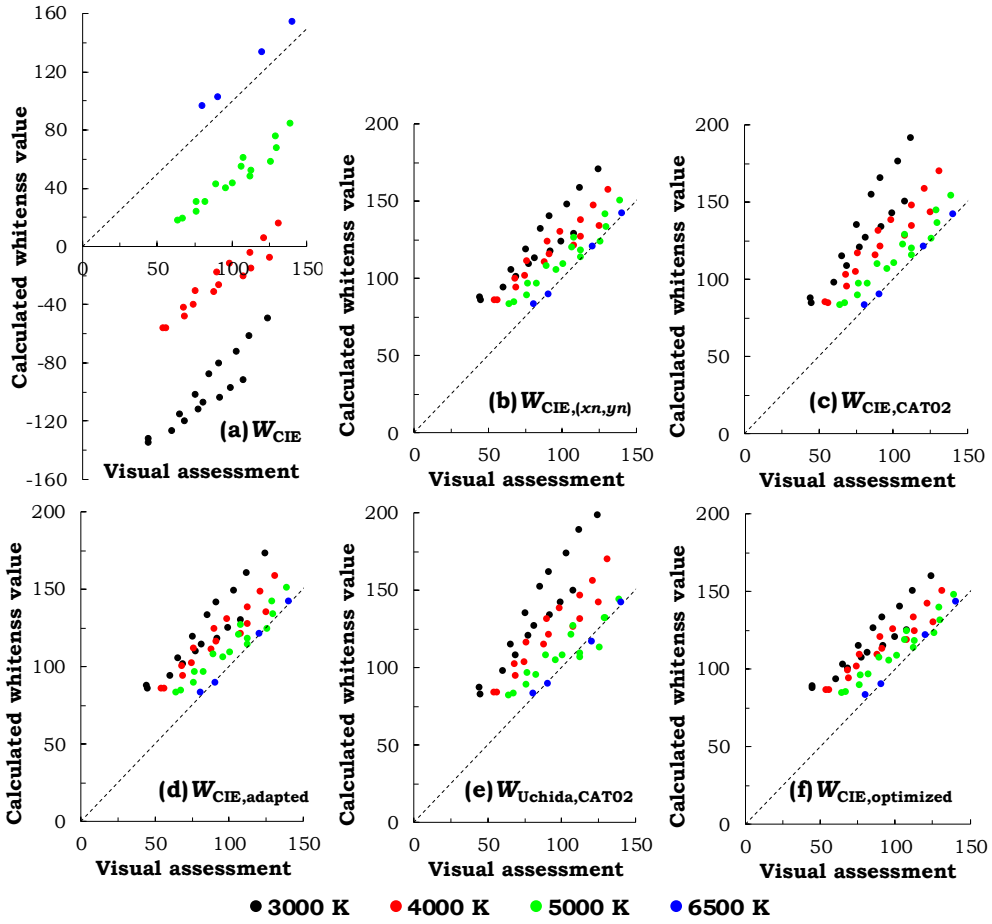

Fig. 3.4. Scatter plots of the perceived whiteness values rated by the observers versus the calculated whiteness values using different formulae. (a)W_{CIE}; (b) $W_{CIE,(xn,yn)}$; (c) $W_{CIE,CAT02}$; (d) $W_{CIE,adapted}$; (e) $W_{Uchida,CAT02}$; (f) $W_{CIE,optimized}$.

Table 3.2. RMSE between the perceived whiteness values and the calculated whiteness values using the six whiteness formulae

RMSE	W_{CIE}	$W_{CIE,(xn,yn)}$	$W_{CIE,CAT02}$	$W_{CIE,adapted}$	$W_{Uchida,CAT02}$	$W_{CIE,optimized}$
3000 K	182.4	39.7	57.4	40.7	55.5	36.0
4000 K	115.9	27.5	33.2	28.0	32.4	25.4
5000 K	53.8	14.3	15.5	14.4	13.6	13.8
Overall	128.6	29.1	39.3	29.7	38.0	26.7

3.4 Discussion

The effect of CCT on whiteness appearance, as revealed in Fig. 3.4, corroborated the findings in Wei et al [2017a]. The whiteness appearance of the samples significantly depended on the chromaticity shifts, as the lightness values *Y* of the samples were similar (i.e., between 88.5 and 93.9). A same magnitude of chromaticity shift under an illuminant at a lower CCT, however,

produced a lower perceived whiteness, as shown in Fig. 3.5. Though CAT02 was applied in $W_{CIE,CAT02}$ and $W_{Uchida,CAT02}$ to take the effect of illuminant chromaticity into consideration, the chromaticity shifts under the 3000K illuminants after applying the CAT02 were even larger and led to higher calculated whiteness values, as shown in Fig. 3.6. This was inconsistent with the visual assessments that the perceived whiteness under the illuminants of lower CCT level was lower. This was likely due to a lower degree of chromatic adaptation under an illuminant at a lower CCT level, as described in Wei et al. [2017a] and Zhai et al [2016].

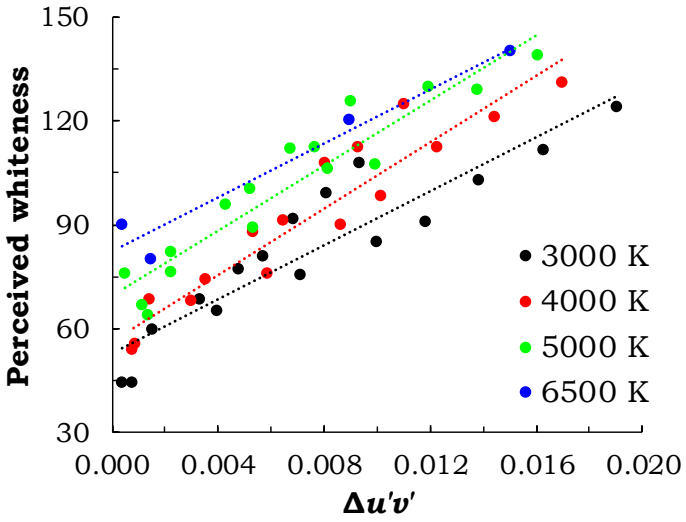

Fig. 3.5. Scatter plot of the perceived whiteness versus the magnitude of chromaticity shifts in CIE 1976 UCS from the chromaticities of the illuminants to those of the samples under the corresponding illumination.

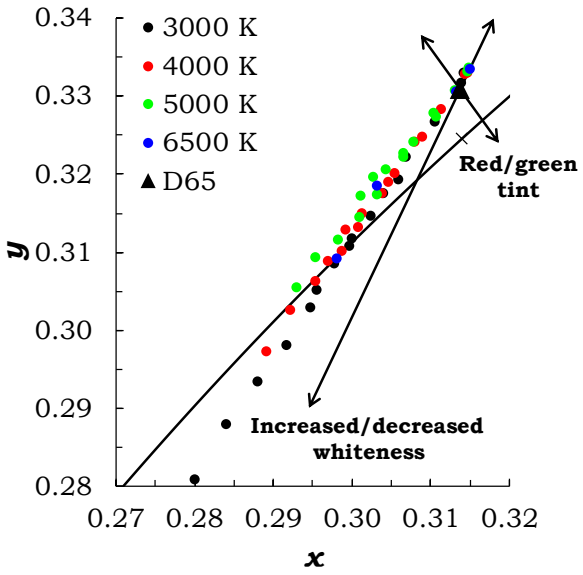

Fig. 3.6. Chromaticities of the samples under different illuminants, calculated using the CIE 1964 CMFs, after being transformed to those under D65 using CAT02 with *D* = 1. Two lines with arrows illustrated the directions of increased and decreased whiteness and red and green tint, which were obtained by the CIE whiteness formula.

In CAT02, the calculation of the degree of chromatic adaptation factor *D* is only affected by the surround conditions and the luminance level of the adapting field, and the chromaticities of the adapting field are not considered. Thus, a same *D* value of 1 was used for the illuminants at different CCT levels, as the high luminance level used in the experiment was assumed to introduce a complete chromatic adaptation. The degree of chromatic adaptation factor *D* was optimized for each CCT level, with a goal to minimize the RMSE value between the calculated and the perceived whiteness values. As summarized in Table 3.3, these optimized factors not only reduced the RMSE for each CCT level, but also the overall RMSE value. It can also be observed in Fig. 3.7 that the calculated whiteness values using the optimized *D* values were able to characterize the perceived whiteness appearance of the samples under the illuminants across 3000, 4000, and 5000 K with higher accuracies. Figure 3.7 shows the chromaticities of the samples using the optimized *D* values, which are more consistent with the perceived whiteness than using *D* values of 1.

Table 3.3. RMSE between perceived whiteness values and calculated whiteness values with $W_{CIE,CAT02}$, using D values of 1 and the optimized D values respectively

	Optimized D	RMSE (D=1)	RMSE (Optimized D)
3000 K	0.72	57.4	14.7
4000 K	0.75	33.2	7.1
5000 K	0.78	15.5	6.2
Overall RMSE	/	39.3	10.1

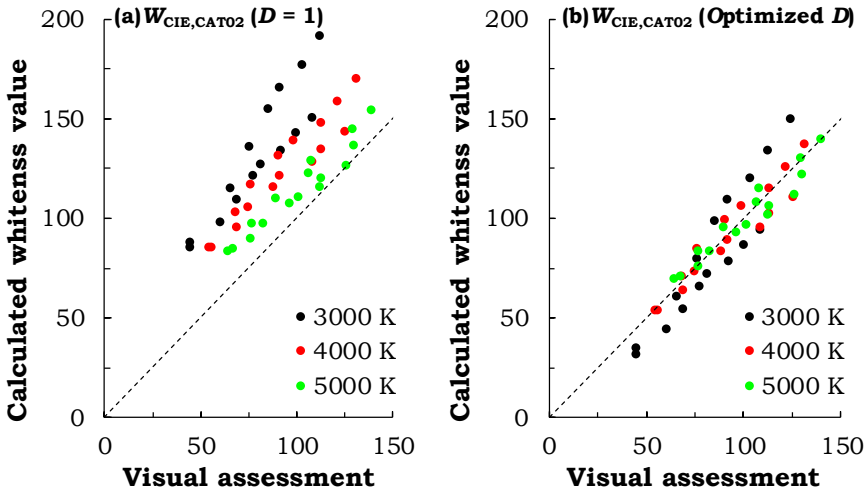

Fig. 3.7. Scatter plot of the perceived whiteness versus whiteness values calculated with $W_{CIE,CAT02}$ for 3000, 4000, and 5000 K illuminants. (a) Using D values of 1; (b) Using optimized D values.

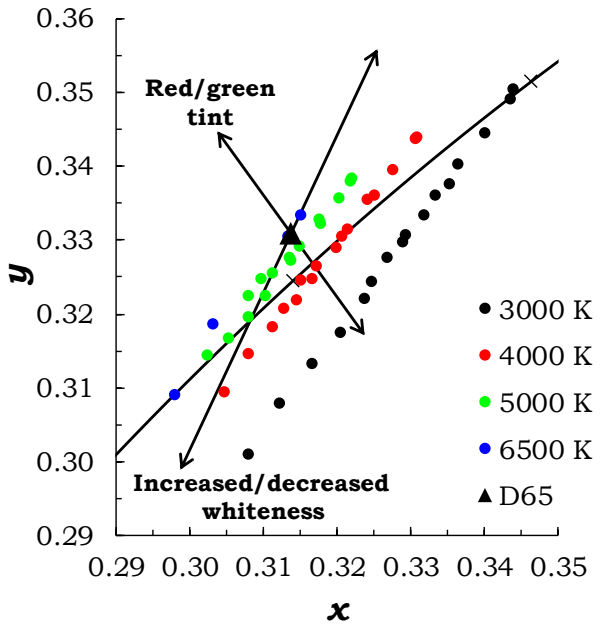

Fig. 3.8. Chromaticities of the samples under different illuminants, calculated using CIE 1964 CMFs, after being transformed to those under D65 using CAT02 with the optimized D values.

3.5 Summary

In this study, a psychophysical experiment was conducted to investigate the whiteness appearance of surface colours under arbitrary light sources, in which the observers rated the whiteness appearance of eight whiteness samples containing different amounts of FWAs under six illuminants in comparison to the whiteness of four reference samples under a CIE D65 simulator in a haploscopic viewing condition. The six illuminants were organized as a 3 × 2 factorial design, including three levels of CCT and two levels of UV/violet radiation. The perceived whiteness values rated by the observers were compared to the whiteness values calculated using six whiteness formulae. Though all the formulae produced a high correlation between the perceived and calculated whiteness values under each CCT level, they failed to characterize the whiteness appearance of surface colours across different CCT levels. This was due to the fact that they were only designed to characterize the whiteness of surface colours under a D65 simulator. Specifically, the whiteness sample under an illuminant at a lower CCT was evaluated to be less white than a sample having a similar magnitude of the chromaticity shift from the illuminant chromaticities under a higher CCT. This was considered to be caused by the lower degree of chromatic adaptation, since CAT02 does not consider the chromaticities of the adapting field in calculating the degree of chromatic adaptation. The degree of chromatic adaptation factor *D* in CAT02 was optimized for each CCT level, which was 0.72, 0.75, and 0.78 for the 3000, 4000, and 5000 K illuminants respectively. Using CAT02 and the optimized *D* values, the performance of the CIE

whiteness formula was significantly improved and the whiteness appearance of surface colours under an arbitrary light source could be better characterized.

Chapter 4 White Appearance and Image Colour Reproduction

4.1 Motivation

White objects widely exist in our daily life, and thus are commonly captured by imaging systems. Though the white appearance of surface colours containing FWAs has been investigated, it was never investigated from the perspective of imaging systems. Given the fact that imaging systems use white balance algorithms to estimate the colour of illumination and adjust the various colours in images, the appearance of white objects is likely to affect the performance of white balance algorithms and the appearance of other colours.

The purpose of the study in this chapter was to investigate how the white appearance of surface colours containing FWAs affected the image colour reproduction. A scene including three whiteness samples containing different amounts of FWAs and a Macbeth ColourChecker was captured by a digital still camera under two 6500 K illuminants, with one containing a normal level of UV/violet radiation to simulate a high quality D65 illuminant and the other containing a similar amount of UV/violet radiation as a typical blue-pumped white LED. Nine statistical white balance algorithms were used to process the RAW images taken under the two illuminants and the colour appearance of the whiteness samples and ColourChecker was investigated.

4.2 Method

4.2.1 Apparatus, Experiment Setup, and Whiteness and Colour Samples

The study was conducted using a viewing booth and a 14-channel spectrally tunable LED device. The viewing booth had dimensions of 50 cm (width) × 50 cm (depth) × 60 cm (height) and the interiors were painted with Munsell N7 neutral paint. The LED device placed above the viewing booth provided a uniform illumination to the booth floor. The peak wavelengths of the 14 channels covered a range from 350 to 680 nm. A 45° viewing table was placed at the booth centre, on which a Macbeth ColourChecker and three calibrated diffuse whiteness samples containing different amounts of FWAs were placed, as shown in Fig. 4.1. The setup was designed to include colours in various hues and a neutral grey background, so that the scene did not have a dominant hue and both the Grey World assumption and the Retinex theory should be applicable. The setup was considered to repeat a typical interior scene, as it contained colours in different hues and different whiteness levels. Similar setups that included a ColourChecker was commonly used in previous studies to investigate the performance of white balance algorithms (e.g., [Cheng et al. 2014, Chikane and Fuh 2006, Zapryanov et al. 2012]).

Fig. 4.1. Photograph of the experiment setup, which was captured under the illuminant containing a normal level of UV/violet radiation.

The intensities of the 14 channels were carefully adjusted to create two 6500 K illuminants with different levels of UV/violet radiation (i.e., designated normal and low). The UV/violet radiation levels, defined as the percentage of the radiant power below 430 nm to the total radiant power, of the two illuminants were 2.7% and 16.1% respectively. The illuminant with a normal UV/violet radiation was designed to simulate CIE standard D65, with a UV/violet emission level of 17.4%. The illuminant with a low UV/violet radiation was designed to simulate a typical blue-pumped 6500 K white LED, which has an average violet emission level of 3.6% [Wei and Houser 2012]. The illuminants were calibrated to provide an illuminance of 1000 ± 10 lx at the centre of the viewing table using a calibrated Minolta T-10 illuminance meter. The SPDs of the two illuminants, measured with a calibrated JETI 1411UV specbo spectroradiometer and a diffuse reflectance standard, are shown in Fig. 4.2, and the corresponding colourimetric characteristics are summarized in Table 4.1. The three whiteness samples, labelled as $W_{84.4}$, $W_{121.6}$, and $W_{138.9}$, contained different amounts of FWAs and had CIE whiteness values W of 84.4, 121.6, and 138.9 respectively. The whiteness sample with a higher W contained a greater amount of FWAs; $W_{84.4}$ did not contain FWAs at all. These whiteness samples represented a range of whiteness appearance that commonly appears in daily life. The SRDs of the 24 colour patches on the ColourChecker were measured using a calibrated Xrite i1-Pro spectrophotometer.

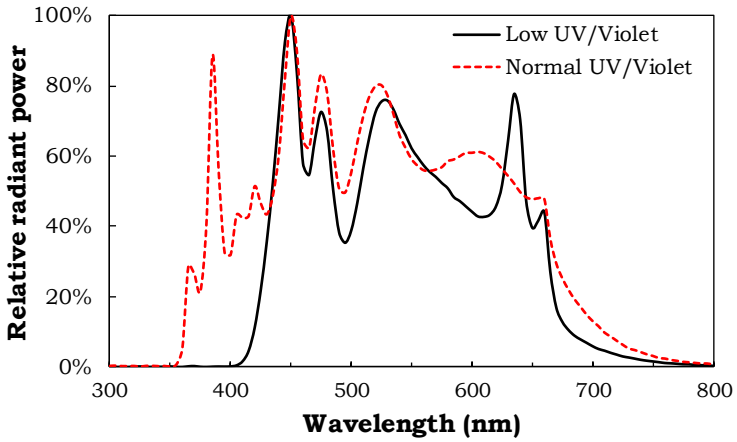

Fig. 4.2. Relative spectral power distributions of the two illuminants.

Table 4.1. Colourimetric characteristics of the two illuminants

UV/violet level	CCT (K)	D_{uv}	CIE 1964 (x,y)	CRI-R_a	M_v	M_u
Low	6588	+0.008	(0.310,0.335)	94	1.49	6.07
Normal	6461	+0.004	(0.313,0.330)	98	0.62	1.52

4.2.2 Image Processing

Two RAW images with a resolution of 6000 × 4000 were captured using a Canon EOS 80D camera, with one under each illuminant. They were processed according to the workflow described in [Sumner 2014]. Linearization was performed to obtain a linearized Bayer array $Bayer_{lin}$ using Eq. 4.1.

$$Bayer_{lin} = \frac{Bayer_{raw} - blk}{sat - blk} \tag{4.1}$$

where $Bayer_{raw}$ was the original Bayer array; *blk* and *sat* were the black and saturation levels respectively. The values that were beyond one or below zero due to the sensor noise were clipped to one and zero. Demosaicing was then performed on the linearized Bayer array (i.e., $Bayer_{lin}$) with a MATLAB built-in demosaic function using a gradient-corrected linear interpolation [Malver et al. 2004]. After demosaicing, the image was characterized by a 6000 × 4000 × 3 matrix RGB_{lin} that contained RGB values for each of the 6000 × 4000 pixels.

White balance algorithm was then applied to RGB_{lin} using nine statistical algorithms introduced in Chapter 2 (i.e., the GW, MGW, SDWGW, maxRGB, Auto Level, GWR algorithms, and three SoG algorithms with different Minkowski norm values) with the relevant parameters being listed in Table 4.2, followed by a series of colour space transformations to derive the chromaticities of each pixel in the CIELAB colour space. The 3 × 3 transformation matrix of the camera used in Eq. 4.2 was derived from the DNG metadata. Figure 4.3 illustrates the entire workflow for processing the images.

$$RGB_{sRGB} = \begin{pmatrix} 0.540 & 0.385 & 0.075 \\ 0.066 & 0.698 & 0.236 \\ 0.015 & 0.265 & 0.720 \end{pmatrix} \times RGB_{lin\_WB} \qquad (4.2)$$

For each of the balanced images, the average (L^*, a^*, b^*) values of the 100 × 100 pixels at the centre of each colour patch and whiteness sample was used for the following analyses.

Table 4.2. Relevant parameters set for the algorithms

Algorithm	Parameter(s)	Value(s)
MGW	a, b, and c in Eq. 1.14	15
SDWGW	Size of each block	150 x 200
Auto level	Saturation factor p in Eq. 1.19	1

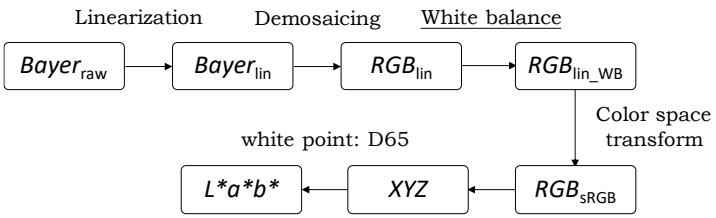

Fig. 4.3. Workflow of processing the images from the RAW format to the chromaticity coordinates in the CIELAB colour space.

4.3 Result

4.3.1 Colour Differences of ColourChecker Caused by the Low UV/violet Radiation in Physical Measurement and Unbalanced Images

The low UV/violet radiation contained in one illuminant did not produce a large colour difference to the ColourChecker. As shown in Fig. 4.4, the two illuminants produced small colour differences to the physical measurements and to the unbalanced images. Specifically, the physical measurement of the 24 patches under the two illuminants had colour differences between 0.01 and 3.37, with an average of 1.44; the 24 patches in the unbalanced images captured under the two illuminants had colour differences between 0.58 and 5.28, with an average of 2.53.

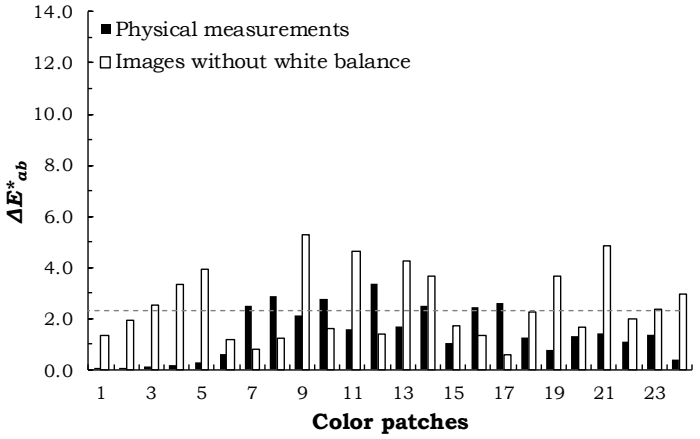

Fig. 4.4. Colour difference of the 24 colour patches on the MacBeth ColourChecker in the CIELAB colour space caused by the low UV/violet radiation level, which were derived from the physical measurements and the images without white balance. The dotted line represents a just-noticeable colour difference (i.e., ΔE^*_{ab} = 2.3 [Sharma and Wang 2001]). (Note: the 24 patches were ordered from right to left and bottom to top, with the black patch as Patch 1.)

4.3.2 Colour Differences of Whiteness Samples and ColourChecker Caused by the Low UV/violet Radiation in Balanced Images

As the illuminants produced little colour differences to the ColourChecker in both physical measurements and the unbalanced images, the colour differences between the images that were balanced using a same algorithm

could be attributed to the FWA excitation. The colour differences of the 24 patches and three whiteness samples between the images that were captured under the two illuminants and balanced using the same algorithm are listed in Table 4.3, with the average colour differences being shown in Fig. 4.5. Figure 4.6 shows the colour difference of the whiteness samples individually.

Table 4.3. Colour difference of each colour patch and whiteness sample caused by the low UV/violet radiation level and processed with each white balance algorithm

Patch/ standard	GW	MGW	SDWGW	SoG (p=4)	SoG (p=8)	SoG (p=20)	maxRGB	Auto Level	GWR
1	5.0	4.5	0.6	2.6	3.3	3.8	4.2	0.8	0.5
2	0.8	1.0	5.6	3.0	3.9	4.8	5.2	4.5	1.2
3	1.3	1.1	4.0	4.0	5.3	6.3	7.0	6.9	1.1
4	1.4	1.4	4.5	5.0	6.6	8.0	8.8	9.1	1.3
5	1.6	1.6	4.8	5.9	7.8	9.5	10.4	10.9	3.5
6	1.8	1.8	5.9	6.8	9.0	10.9	11.9	12.4	7.5
7	3.5	3.1	6.6	7.5	9.3	10.7	11.3	11.8	2.2
8	3.3	3.6	6.0	6.4	7.7	8.8	9.6	9.6	2.6
9	4.5	3.9	4.0	4.4	5.2	5.9	4.9	4.2	5.3
10	1.9	2.3	3.4	3.4	4.0	4.6	5.1	4.5	2.0
11	2.8	2.4	2.4	2.7	3.7	4.8	5.1	5.3	3.7
12	7.2	6.6	10.4	12.9	15.1	16.9	17.8	20.2	6.1
13	3.7	2.9	2.8	3.5	4.2	5.1	4.9	3.5	4.2
14	4.3	4.1	3.1	3.7	4.5	5.5	5.6	6.2	5.1
15	2.5	2.1	1.8	4.6	5.8	6.8	7.5	7.2	1.3
16	1.9	2.2	4.0	4.7	5.8	6.9	7.5	7.5	1.3
17	5.4	5.1	8.3	10.8	13.0	14.9	15.9	16.9	6.1
18	1.6	1.0	2.8	3.5	4.7	5.7	5.9	6.4	1.8
19	1.4	1.5	4.8	4.9	6.6	8.0	8.9	9.2	1.3
20	3.0	3.3	6.6	7.4	9.1	10.6	11.6	12.0	2.9
21	2.9	2.2	1.5	2.4	3.2	3.9	4.1	4.1	3.5
22	2.8	2.6	6.8	7.4	9.2	10.8	11.8	12.3	3.2
23	1.8	2.2	5.1	5.6	7.2	8.5	9.3	9.7	2.0
24	1.0	1.1	3.5	3.8	5.1	6.2	6.8	6.8	1.1
$W_{84.4}$	1.4	1.5	4.9	5.7	7.6	9.3	10.3	10.8	3.8
$W_{121.6}$	6.4	6.3	1.0	0.9	1.4	3.3	4.6	4.6	1.2
$W_{138.9}$	10.9	10.5	4.6	5.0	2.6	0.7	1.7	1.4	2.9

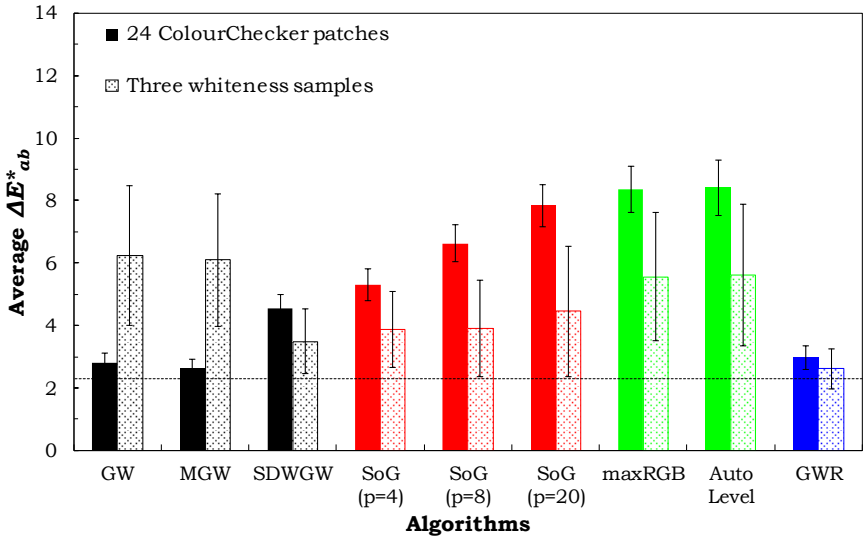

Fig. 4.5. Average colour difference of the 24 ColourChecker patches and the three whiteness samples in the CIELAB colour space, together with the error bars, caused by the low level of UV/violet radiation when using different algorithms. (Note: the algorithms based on the Grey World assumption are in black; those based on the Retinex theory are in red; the SoG and GWR algorithms are in green and blue respectively.)

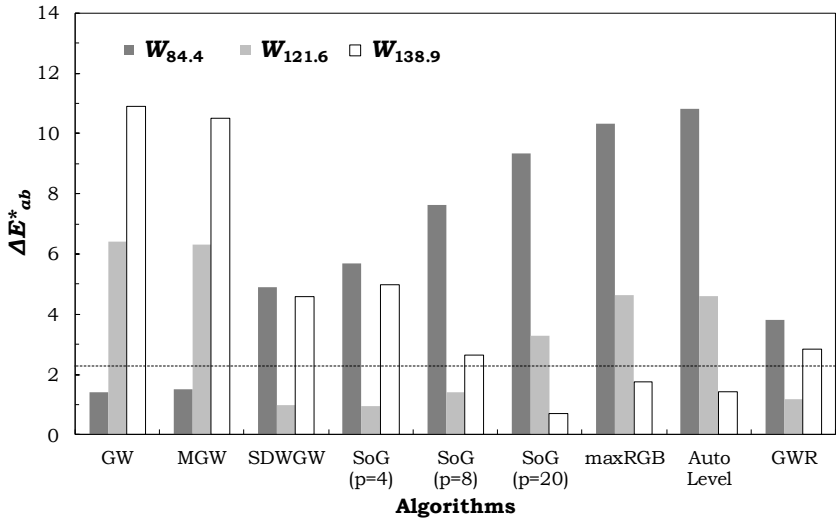

Fig. 4.6. Colour difference of individual whiteness samples in the CIELAB colour space caused by the low UV/violet radiation level, when using different algorithms. The dotted line represents a just noticeable colour difference (i.e., ΔE^*_{ab} = 2.3).

It can be observed in Fig. 4.5 that the low UV/violet radiation level introduced noticeable colour differences to the whiteness samples and ColourChecker in the balanced images, no matter which algorithm was used. For the whiteness samples, the low UV/violet radiation level caused a larger difference to a whiteness sample containing a greater amount of FWAs in the images that were balanced using the two algorithms based on the Grey World assumption

(i.e., the GW and MGW algorithms), but a larger difference to a whiteness sample containing less amount of FWAs in the images that were balanced using the algorithms based on the Retinex theory (i.e., the maxRGB and Auto Level algorithms). When the images were balanced using the SoG algorithms, $W_{84.4}$ always had the largest differences, while the differences of $W_{121.6}$ and $W_{138.9}$ depended on the Minkowski norm value. For the ColourChecker, the colour differences caused by the low UV/violet radiation level were generally smaller in the images that were balanced using the algorithms based on the Grey World assumption (i.e., the GW, MGW, and SDWGW algorithms) than those based on the Retinex theory (i.e., the maxRGB and Auto Level algorithms). The effect of the low UV/violet radiation level was medium to the SoG algorithms, with a larger Minkowski norm value (i.e., *p*) producing a larger colour difference. In addition, the effect on the images that were balanced using the GWR algorithm was similar to those that were balanced using the GW algorithm, though the GWR algorithm combines both the GW and maxRGB algorithms.

4.3.3 Colour Differences Among Three Whiteness Samples Caused by Low UV/violet Radiation in Balanced Images

In addition to the colour difference of each whiteness sample, the colour differences among the three whiteness samples in an image are also critically important, as the different amounts of FWAs were added to produce different degrees of whiteness appearance. As summarized in Table 4.4, the low UV/violet radiation level obviously reduced the colour differences among the three samples regardless of the white balance algorithms, making the samples appear similar to each other.

Table 4.4. Colour differences among the three whiteness samples in each white-balanced image, which was captured under each illuminant and processed using each algorithm.

Illuminant	Algorithm	$W_{121.6}$ - $W_{84.4}$				$W_{138.9}$ - $W_{84.4}$			
		ΔE	ΔL	Δa	Δb	ΔE	ΔL	Δa	Δb
Low UV/violet radiation level	GW	6.2	6.2	-0.6	0.3	10.6	10.5	-0.6	0.6
	MGW	6.4	6.2	-1.6	0.7	10.8	10.5	-2.1	1.2
	SDWGW	5.5	5.5	-0.5	0.2	9.4	9.4	-0.3	0.5
	SoG (p=4)	6.2	6.2	-0.7	0.3	10.6	10.5	-0.5	0.5
	SoG (p=8)	6.2	6.2	-0.6	0.3	10.6	10.5	-0.4	0.5
	SoG (p=20)	6.2	6.2	-0.6	0.3	10.6	10.6	-0.4	0.5
	maxRGB	6.2	6.2	-0.7	0.3	10.6	10.5	-0.6	0.6
	Auto Level	6.7	6.6	-0.6	0.2	11.3	11.3	-0.4	0.4
	GWR	6.2	6.2	-0.6	0.3	10.6	10.6	-0.4	0.6
		$W_{121.6}$ - $W_{84.4}$				$W_{138.9}$ - $W_{84.4}$			
	Algorithms	ΔE	ΔL	Δa	Δb	ΔE	ΔL	Δa	Δb
Normal UV/violet radiation level	GW	9.1	6.5	1.2	-6.3	15.2	10.9	3.3	-10.1
	MGW	8.7	6.6	0.3	-5.7	14.3	10.9	1.4	-9.1
	SDWGW	8.0	5.9	1.1	-5.2	13.3	9.9	2.8	-8.5
	SoG (p=4)	9.0	6.6	1.2	-6.0	14.8	11.0	3.0	-9.5
	SoG (p=8)	8.9	6.6	1.1	-5.8	14.7	11.0	2.9	-9.2
	SoG (p=20)	8.8	6.6	1.0	-5.6	14.5	11.1	2.7	-9.0
	maxRGB	8.7	6.6	0.7	-5.5	14.3	11.1	2.2	-8.7
	Auto Level	9.4	7.2	1.0	-6.1	15.6	11.9	2.7	-9.6
	GWR	7.8	6.8	0.1	-3.9	12.7	11.4	0.8	-5.6

4.4 Discussion

The large colour differences introduced by the low UV/violet radiation level to the images that were balanced using the two simplest algorithms based on the Grey World assumption and the Retinex theory—the GW and the maxRGB algorithms—were due to the calculation of the gain factors (i.e., *corrR* and *corrB*), as listed in Table 4.5. The GW algorithm used the average RGB values of the images, while the maxRGB algorithm used the maximal RGB values. As the three whiteness samples only covered 4.5% pixels of the image, the failure of the low UV/violet radiation level in exciting the FWAs did not introduce large changes to the average RGB values of the image, causing little changes to both *corrR* and *corrB* in the GW algorithm. In contrast, the failure of the low UV/violet radiation level in exciting the FWAs reduced the maximal B value of the image, which happened to the pixel in

$W_{138.9}$ as shown in Fig. 4.7, increasing the value of *corrB* of the maxRGB algorithm. Thus, the low UV/violet radiation level shifted the chromaticities of the patches with a greater B value—the neutral patches with a high lightness (i.e., Patches 5 and 6) and the bluish patches (i.e., Patches 7, 12, 17, 20, and 22)—towards the blue direction as shown in Fig. 4.8, which changed both the hue and chroma of the patches as shown in Table 4.6. The effect of the low UV/violet radiation level on the gain factors of the SoG algorithms were between those on the GW and the maxRGB algorithms, with a similar *corrR* but different *corrB* values. As shown in Fig. 4.9, the increase of *corrB* caused by the low UV/violet radiation level was obvious for a greater Minkowski norm (i.e. *p*) value, making the effect on the SoG algorithm more similar to that on the maxRGB algorithm.

Table 4.5. Gain factors (i.e., *corrR* and *corrB*) in the GW and maxRGB algorithms and the change due to the low level of UV/violet radiation. The GW algorithm uses the average RGB values in the entire image; the maxRGB algorithm uses the maximal RGB values in the entire image.

Algorithm		UV/violet radiation level		Change due to the low UV/violet radiation
		Normal	Low	
GW	*corrR*	1.97	1.98	-0.01
	corrB	1.47	1.53	-0.06
	Avg *R*	25.10	26.07	-0.97
	Avg *G*	49.44	51.50	-2.06
	Avg *B*	33.61	33.58	0.03
maxRGB	*corrR*	2.01	1.99	0.02
	corrB	1.34	1.54	-0.20
	Max *R*	127.00	128.00	-1.00
	Max *G*	255.00	255.00	0.00
	Max *B*	191.00	166.00	25.00

Table 4.6. Colour shift, lightness shift, chroma shift, and hue angle shift in the CIELAB colour space caused by the low UV/violet radiation for the image balanced using the GW and maxRGB algorithms. (Note: a positive hue angle shift represents a counterclockwise hue angle shift.)

	GW				maxRGB			
Color patch	**Color shift**	**Lightness shift**	**Chroma shift**	**Hue angle shift (deg)**	**Color shift**	**Lightness shift**	**Chroma shift**	**Hue angle shift (deg)**
1	5.0	0.0	-130%	129.2	4.2	0.1	-89%	63.7
2	0.8	0.6	108%	20.6	5.2	0.2	-109%	115.3
3	1.3	0.9	-63%	34.1	7.0	0.3	-105%	118.1
4	1.4	1.0	1%	27.7	8.8	0.3	-99%	85.8
5	1.6	1.1	-13%	31.5	10.4	0.3	-98%	79.9
6	1.8	1.3	-16%	17.6	11.9	0.4	-82%	29.6
7	3.5	0.1	1%	7.3	11.3	-0.7	-7%	24.0
8	3.3	0.4	8%	-0.7	9.6	-0.3	19%	-7.0
9	4.5	2.1	3%	2.6	4.9	1.7	-5%	2.2
10	1.9	0.7	3%	-0.7	5.1	0.4	1%	-5.9
11	2.8	1.5	5%	0.2	5.1	1.1	-7%	3.9
12	7.2	-0.6	12%	3.3	17.8	-1.9	35%	9.2
13	3.7	1.7	2%	3.0	4.9	1.4	-7%	0.8
14	4.3	2.1	6%	1.7	5.6	1.7	-6%	3.3
15	2.5	0.4	8%	1.1	7.5	-0.1	32%	-1.3
16	1.9	0.6	3%	-1.6	7.5	0.1	1%	-9.9
17	5.4	0.1	10%	3.8	15.9	-1.1	39%	10.6
18	1.6	0.8	-2%	0.0	5.9	0.6	-8%	-2.6
19	1.4	1.2	-1%	1.3	8.9	0.5	-19%	12.9
20	3.0	0.5	12%	2.4	11.6	-0.3	67%	9.2
21	2.9	1.5	10%	1.7	4.1	1.1	-11%	4.5
22	2.8	0.6	9%	5.0	11.8	-0.2	32%	29.5
23	1.8	0.7	-1%	-4.5	9.3	0.2	-24%	-20.1
24	1.0	0.9	-3%	-0.7	6.8	0.4	-30%	-24.8

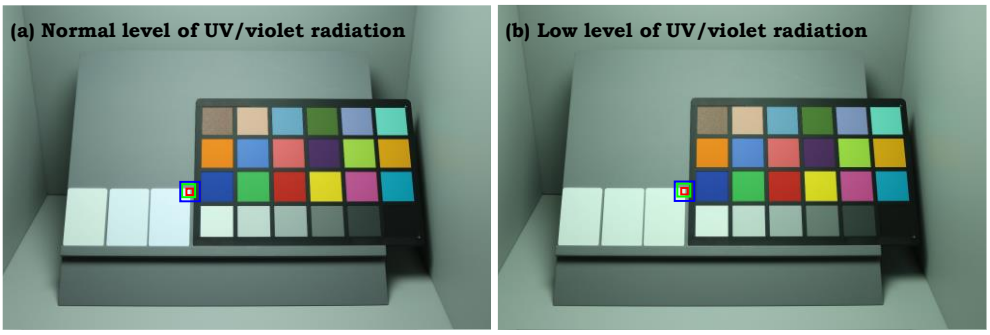

Fig. 4.7. Position of the pixels with the maximal RGB values, located at the centre of the squares, under the two illuminants. (a) Normal level of UV/violet radiation; (b) Low level of UV/violet radiation.

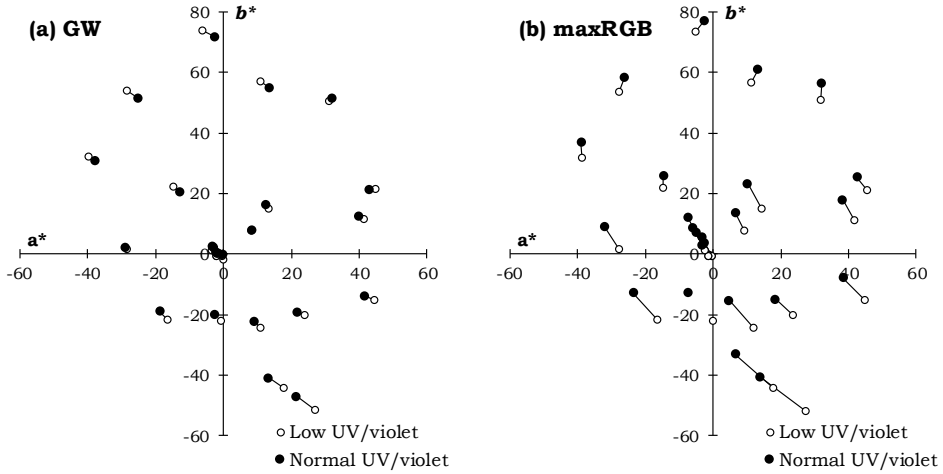

Fig. 4.8. Chromaticity shifts of the 24 patches on the ColourChecker caused by the low UV/violet radiation level in the *a-*b** plane of the CIELAB colour space. (a) The images balanced using the GW algorithm; (b) The images balanced using the maxRGB algorithm.**

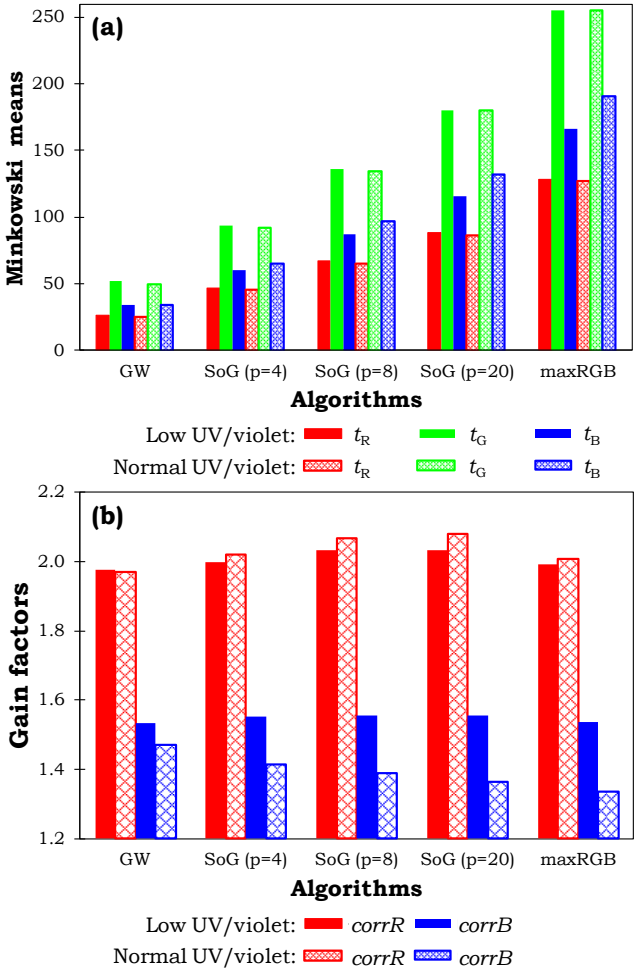

Fig. 4.9. Calculated Minkowski means and gain factors when using the GW, SoG, and maxRGB algorithms for the images captured under the two illuminants. (a) The Minkowski means; (b) The gain factors.

The low UV/violet radiation level generally had a similar impact on the images that were balanced using the MGW and Auto Level algorithms, in comparison to the GW and maxRGB algorithms respectively. Larger differences, however, were introduced to the images balanced with the SDWGW algorithm, though it was also developed based on the Grey World assumption. As shown in Fig. 4.10, the low UV/violet radiation level reduced the variations of B values in the blocks around $W_{138.9}$, making these blocks having lower weights in deriving the gain factors. Though the GWR algorithm was developed to combine the GW and maxRGB algorithms, the colour differences were more similar to those using the GW algorithm. As listed in Table 4.5, the image captured under the illuminant with a low UV/violet radiation level but balanced using the GW and the maxRGB algorithms had almost identical gain factors, which made the image balanced using the GWR algorithm also have similar gain factors. The balanced R and B values of the image that was captured under the illuminant with a normal UV/violet radiation and balanced using the GWR algorithm, however, were more similar to that balanced using the GW algorithm, as shown in Fig. 4.11, which was caused by the quadratic transformation used in the GWR algorithm.

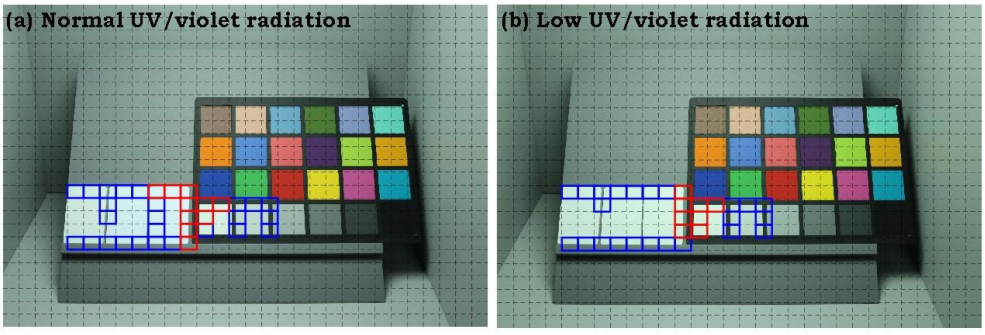

Fig. 4.10. Illustration of the blocks that had a standard deviation of B values—*std B*—larger than a certain value for the images captured under the two illuminants. (a) Normal UV/violet radiation; (b) Low UV/violet radiation. (Note: the blocks with a *std B* > 70 are labelled in red and the blocks with a *std B* > 40 are labelled in blue.)

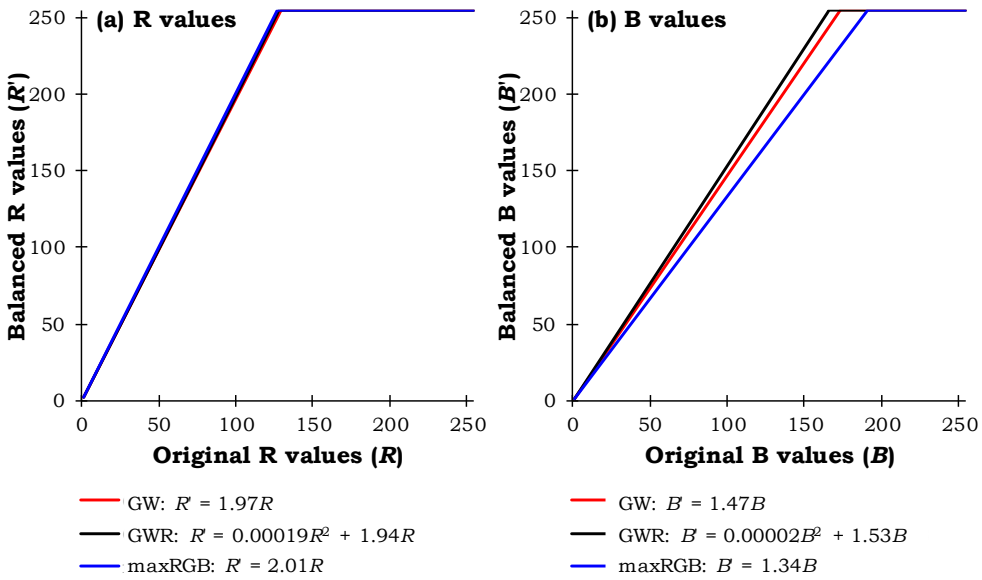

Fig. 4.11. Relationship between the balanced and the original R and B values using the three algorithms for the image captured under the illuminant with a normal UV/violet radiation. (a) R value; (b) B value.

Though the low UV/violet radiation level introduced a similar average colour shift to the three whiteness samples in the image that were balanced using the GW and maxRGB algorithms, the colour shifts of the individual samples were not similar. Specifically, it introduced a larger shift to a whiteness sample with fewer FWAs for the images balanced using the GW algorithm, but to a whiteness sample with more FWAs for the images balanced using the maxRGB algorithm. As shown in Fig. 4.12, the low UV/violet radiation level generally shifted the chromaticities of the whiteness samples towards the origin of the a^*-b^* plane, making them appear neutral. Such an effect also made the three whiteness samples appear similar in a balanced image regardless of the algorithms, though they contained different amounts of FWAs. As shown in Fig. 4.13, the shift of the chromaticities of the three whiteness samples towards the negative direction of b^* happened under the illuminant with a normal UV/violet radiation level, but not under the one with a low UV/violet radiation level.

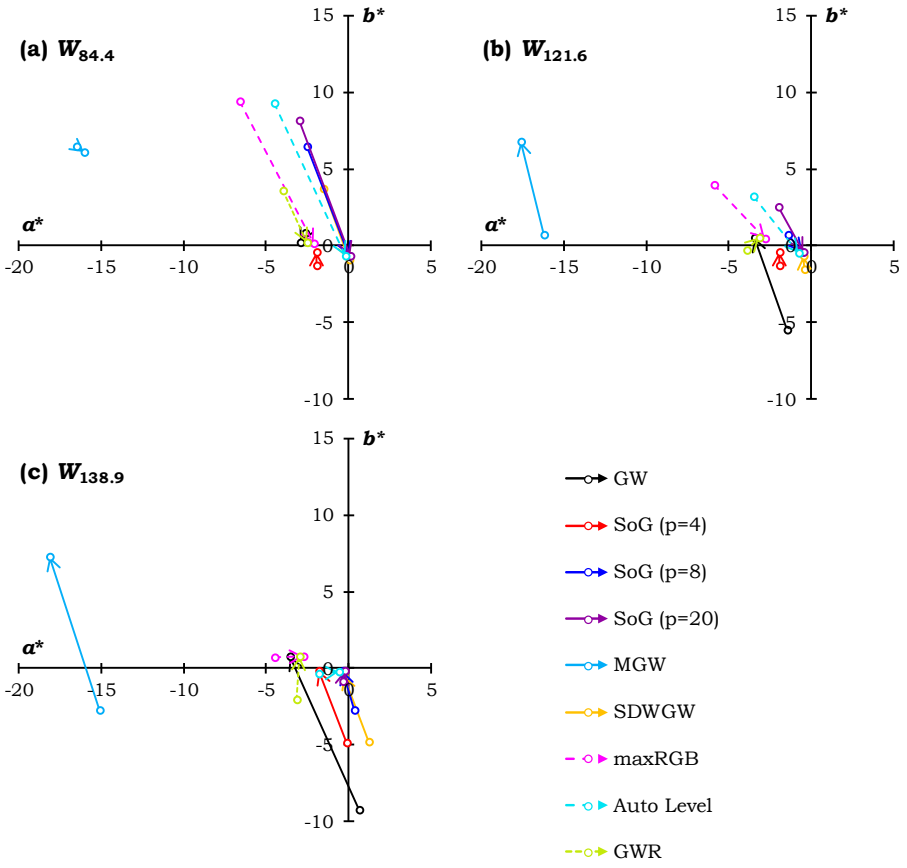

Fig. 4.12. Chromaticity shifts of the three whiteness samples caused by the low UV/violet radiation level, when using different white balance algorithms. (a) $W_{84.4}$; (b) $W_{121.6}$; (c) $W_{138.9}$.

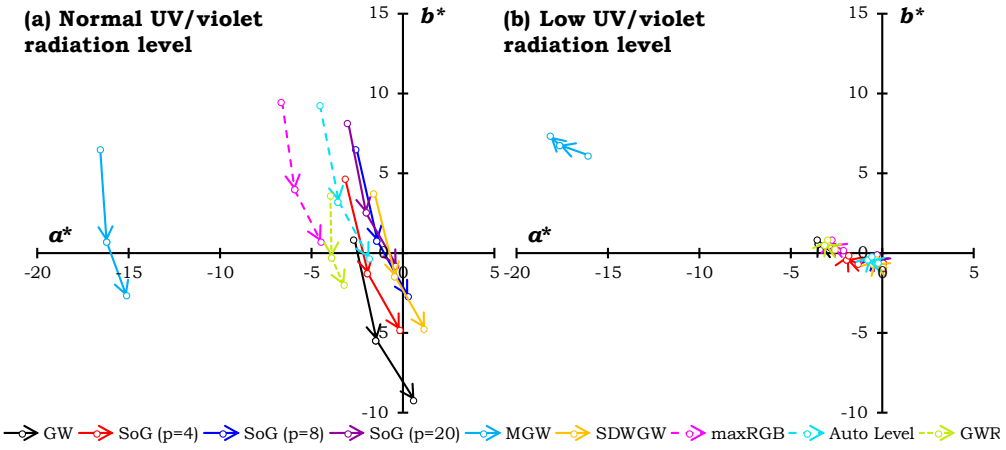

Fig. 4.13. Chromaticity shifts from $W_{84.4}$ to $W_{121.6}$ and $W_{138.9}$ in the a^*-b^* plane of the CIELAB colour space in the white-balanced images captured under the two illuminants using different algorithms. (a) Normal UV/violet radiation; (b) Low UV/violet radiation.

4.5 Summary

The effect of white appearance of surface colours in images on image colour reproduction was investigated. Three whiteness samples containing different

amounts of FWAs and a ColourChecker were captured using a digital still camera under two 6500 K illuminants and were white balanced using nine different statistical white balance algorithms. The two illuminants, with one containing a normal level of UV/violet radiation to simulate the CIE standard D65 and the other containing a low level of UV/violet radiation to simulate typical blue-pumped white LEDs, produced small colour differences to the ColourChecker both physically and in the unbalanced images. The lack of UV/violet radiation, however, significantly affected the appearance of the whiteness samples in the white balanced images, regardless of the white balance algorithms. The low UV/violet radiation shifted the chromaticities of the whiteness samples towards the origin in the a^*–b^* plane of the CIE LAB colour space, making them appear more similar to each other. The changes of the appearance of the white samples through the white balance algorithms also caused colour shifts to the colour samples on the ColourChecker. On average, such an effect was more significant when using the algorithms based on the Retinex theory (e.g., the maxRGB and Auto Level algorithms) than those based on the Grey World Assumption (e.g., the GW and MGW algorithms). In short, the white appearance of surface colours in images were affected by the illumination and had a significant impact on image colour reproduction.

Chapter 5 Investigation of Chromatic Adaptation Based on White Appearance

5.1 Motivation

Though white appearance is important to both surface colours and self-luminous colours (e.g., display and illuminant), past studies have revealed significant differences. For surface colours, white stimuli need to have chromaticities around the adapting chromaticities [Wei et al. 2017a; Wei et al. 2017b; Zhai and Luo 2018]; for self-luminous stimuli, white stimuli need to have chromaticities around the blackbody locus and have high CCT levels (e.g., above 6500 K) [Huang et al. 2018; Zhai and Luo 2018; Hunt and Winter 1975; Breneman 1987; Fairchild 1991; Berns and Gorzynski 1991; Choi and Suk 2016; High et al. 2017]. Such differences were commonly attributed to the different degrees of chromatic adaptation caused by the viewing media, with a lower degree of chromatic adaptation for viewing self-luminous stimuli [Fairchild 1991; Zhai and Luo 2018]. However, viewing medium and viewing mode were always confounded in these studies. Viewing medium refers to how stimuli are produced, with surface colours generally reflective and self-luminous stimuli generally emissive. Viewing mode refers to how stimuli are perceived and interpreted, which is related to the stimulus and background configurations. It was revealed that an identical colour stimulus could appear in different viewing modes due to the change of the luminance contrasts between the stimulus and the background [Evans 1974; Yamauchi and Uchikawa 2000; Uchikawa et al. 2001]. A self-luminous stimulus can be

viewed in the surface mode and a surface colour can be viewed in the self-luminous mode (e.g., fluorescence samples). Therefore, the difference in chromaticities for producing white appearance for surface colours and self-luminous stimulus may be caused by the viewing mode instead of the viewing medium.

The study in this chapter aimed to investigate whether the difference in chromaticities to produce white stimuli was caused by the different degrees of chromatic adaptation due to the viewing media (i.e., surface colours versus self-luminous stimulus). A psychophysical experiment was conducted. Observers were asked to adjust the colour appearance of a stimulus at different luminance level produced by an iPad display to the whitest under different adapting conditions (i.e., adapting CCT and luminance). The luminance levels of the stimulus and the adapting condition were systematically varied to create different viewing modes (i..e, surface and self-luminous), while the viewing medium was always a self-luminous display.

5.2 Method

5.2.1 Apparatus, Adapting Conditions, and Stimulus

The experiment was conducted using a viewing booth, with dimensions of 60 cm (width) × 60 cm (depth) × 60 cm (height). The interiors of the booth were painted with Munsell N7 neutral grey paint. A 45° tilt viewing table was placed at the booth centre, with an iPad Air 2 being placed at the centre of the table. A Munsell N7 sheet, with a 3 cm × 3 cm opening cut at the centre of the sheet, was used to cover the entire iPad display, as shown in Fig. 5.1. Eight 3 cm × 3 cm NCS colour samples (i.e., S0530-Y90R, S1040-R80B, S0580-Y90R, S0550-Y50R, S0550-Y10R, S4040-Y30R, S1030-G, S0540-

R30B) were attached around the opening to help the observers to adapt to the adapting conditions. During the experiment, the observers viewed the stimulus produced by the display through the opening with their chin resting on a chin rest mounted outside the viewing booth, so that the stimulus was viewed perpendicularly with an FOV around 4°.

Seventeen adapting conditions were produced for the experiment using spectrally tunable LED devices. Sixteen of the condition were organized as a 4 × 4 factorial design, comprising four levels of CCT (i.e., 2700, 3500, 5000, and 6500 K) and four levels of adapting luminance (i.e., $L_w \approx 115$, 300, 600, and 900 cd/m^2). An additional condition was created to have an L_w of 900 cd/m^2 and a CCT of 8000 K. The four adapting conditions with the adapting luminance L_w of 115 cd/m^2 were produced using an 11-channel THOUSLITE LEDCube and the other conditions were produced by a four-channel ARRI Skypanel S60-C. All the adapting conditions were carefully designed by a genetic algorithm [Wei et al. 2017c; Wei and Chen 2018] that optimized the intensity of each channel for achieving a CIE General colour Rendering Index (CRI R_a) greater than 90 with constrained chromaticities. The adapting conditions were calibrated using a calibrated JETI Specbos 1411UV spectroradiometer and a calibrated Labsphere reflectance standard placed at the centre of the viewing table. The colourimetric characteristics of the 17 adapting conditions are summarized in Table 5.1.

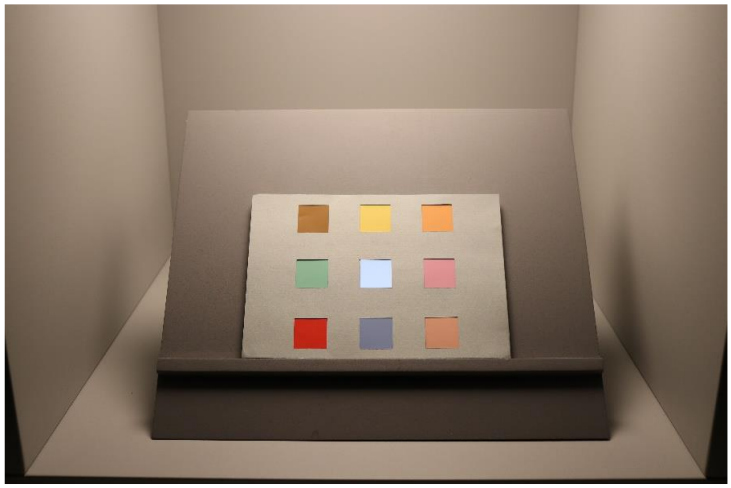

Fig. 5.1. Photograph of the experiment setup. The stimulus was produced by the iPad display behind the Munsell N7 sheet and was viewed through the opening at the centre of the sheet. The eight 3 × 3 cm NCS colour samples were placed around the stimulus to help chromatic adaptation.

Table 5.1. Colourimetric characteristics of the adapting conditions

Nominal L_w (cd/m^2)	Nominal CCT (K)	L_w (cd/m^2)	CIE 1976 (u'_{10},v'_{10})	CCT (K)	D_{uv}	CRI R_a	IES TM-30-15 R_f
115	2700	115.9	(0.267,0.525)	2704	-0.0012	97.3	93.7
	3500	116.1	(0.236,0.516)	3516	+0.0030	97.9	92.5
	5000	117.3	(0.208,0.493)	4997	+0.0080	96.8	96.4
	6500	116.7	(0.196,0.471)	6514	+0.0054	97.4	97.4
300	2700	300.0	(0.269,0.526)	2679	-0.0009	94.8	89.7
	3500	299.0	(0.240,0.508)	3498	-0.0030	88.4	88.9
	5000	302.0	(0.215,0.484)	4993	-0.0020	93.9	89.8
	6500	301.0	(0.204,0.466)	6482	-0.0016	94.2	88.2
600	2700	599.5	(0.268,0.526)	2693	-0.0004	94.6	89.7
	3500	604.0	(0.240,0.511)	3477	-0.0004	90.0	89.5
	5000	610.0	(0.216,0.482)	4994	-0.0028	94.2	89.8
	6500	609.5	(0.202,0.468)	6491	+0.0008	94.3	88.6
900	2700	900.1	(0.269,0.529)	2670	+0.0009	94.5	90.2
	3500	911.6	(0.240,0.511)	3485	-0.0008	90.1	89.7
	5000	907.7	(0.215,0.482)	5042	-0.0024	93.6	89.8
	6500	908.0	(0.204,0.466)	6501	-0.0015	94.2	88.0
	8000	910.3	(0.197,0.453)	8018	-0.0018	94.1	87.2

The iPad, with a default white point having a CCT of 6850 K and a D_{uv} of +0.0050, was calibrated using a gamma-offset-gain display (GOG) model

[Berns 1996] with the CIE 1964 10° CMFs. A customized program was developed based on the GOG model. It allowed the observers to use four arrow keys on a Bluetooth keyboard to adjust the chromaticities of the display along the u'_{10} and v'_{10} axes with a step of 0.001 unit in the CIE 1976 $u'_{10}v'_{10}$ chromaticity diagram at a constant luminance level. The display was calibrated to produce six luminance levels (i.e., 100, 150, 200, 250, 300, and 350 cd/m^2). The colour gamut of the display at each luminance level is shown in Fig. 5.2. The gamuts generally enclosed the chromaticities on the blackbody locus between 2700 and 8000 K, which was the range of the adapting CCT levels.

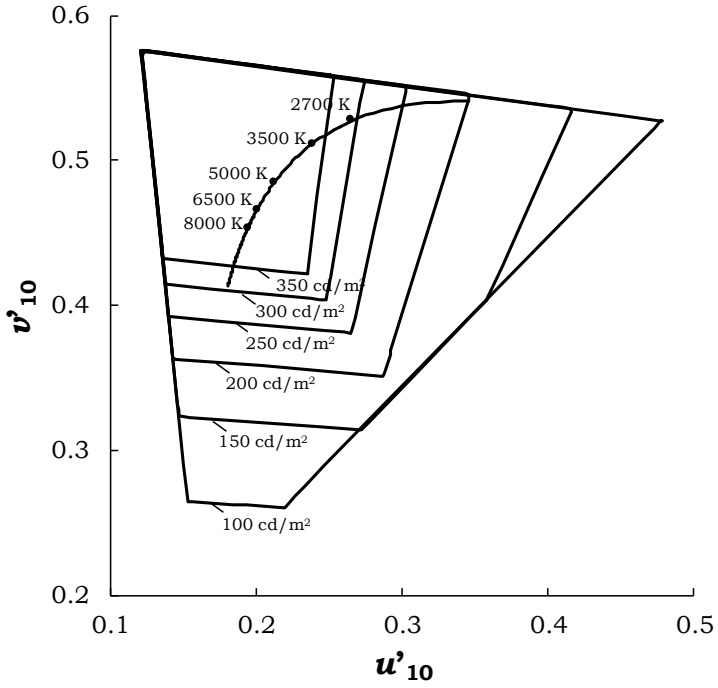

Fig. 5.2. Colour gamut of the display in the CIE 1976 $u'_{10}v'_{10}$ chromaticity diagram at each luminance level.

5.2.2 Observers

Eight observers (seven males and one female) between 22 and 28 years of age (mean = 24.3, std. dev. = 2.3) participated in the experiment. All the observers completed the Ishihara Colour Vision Test and had a normal colour vision.

5.2.3 Experimental Procedure

Upon arrival, the observer completed a general information survey and the Ishihara Colour Vision Test. The experimenter explained the task to the observer and guided them to the viewing booth. Under each adapting condition, the observer was asked to look into the booth for two minutes for chromatic adaptation. Then the experimenter set the luminance level of the iPad to one of the six levels and placed the iPad on the viewing table. Note that before the experiment, the iPad was switched on for at least 30 minutes for stabilization. The observer adjusted the colour appearance of the stimulus using the four arrow keys on the Bluetooth keyboard until the stimulus appeared the whitest to him or her. The experimenter helped the observer to verify his/her decision by showing them neighbouring colour stimuli with one-unit increase or decrease of u_{10}' or v_{10}'. The orders of the six display luminance and the adapting conditions at each adapting luminance were randomized.

5.3 Result

After the experiment, the SPDs of the stimuli adjusted by the observers were measured by the JETI spectroradiometer at the observer's eye position under the corresponding adapting conditions, which considered both the light produced by the display and the light reflected by the display. The chromaticities and luminance value of each adjusted stimulus were then calculated using the CIE 1964 10° CMFs. The measured luminance levels of the adjusted stimuli were 5.8% to 1.6% lower than the designed levels calibrated by the GOG model. The chromaticities of the adjustments were not close to the colour gamut at the corresponding display luminance level.

5.3.1 Inter-observer Variations

The inter-observer variation was characterized using the mean colour difference from the mean (MCDM) [Billmeyer and Alessi 1981] based on the chromaticities of the stimuli in the CIE 1976 $u'_{10}v'_{10}$ chromaticity diagram adjusted by each observer and an average observer under each adapting condition, as summarized in Table 5.2. In addition, the 95% confidence error ellipses of the adjusted stimuli under each adapting condition are shown in Fig. 5.3. The MCDM values and the sizes of the ellipses were generally comparable to those in several recent studies investigating white appearance [Smet et al. 2014; Smet et al. 2015; Huang et al. 2018; Zhai and Luo 2018] and memory colours [Ma et al. 2018a; Ma et al. 2018b]. As the inter-observer variation was small and the previous studies found that the memory colour matching experiments using achromatic colours were stable [Fairchild 1991; Speigle and Brainard 1991; Smet et al. 2017; Smet et al. 2017a; Smet et al. 2017b], the results derived from the eight observers were believed reliable.

Table 5.2.MCDM values calculated using the adjustments under each adapting condition

	L_w = 115 cd/m^2	L_w = 300 cd/m^2	L_w = 600 cd/m^2	L_w = 900 cd/m^2
2700K	0.0091	0.0196	0.0114	0.0102
3500K	0.0088	0.0115	0.0102	0.0080
5000K	0.0084	0.0088	0.0089	0.0063
6500K	0.0079	0.0083	0.0087	0.0056
8000K	-	-	-	0.0060

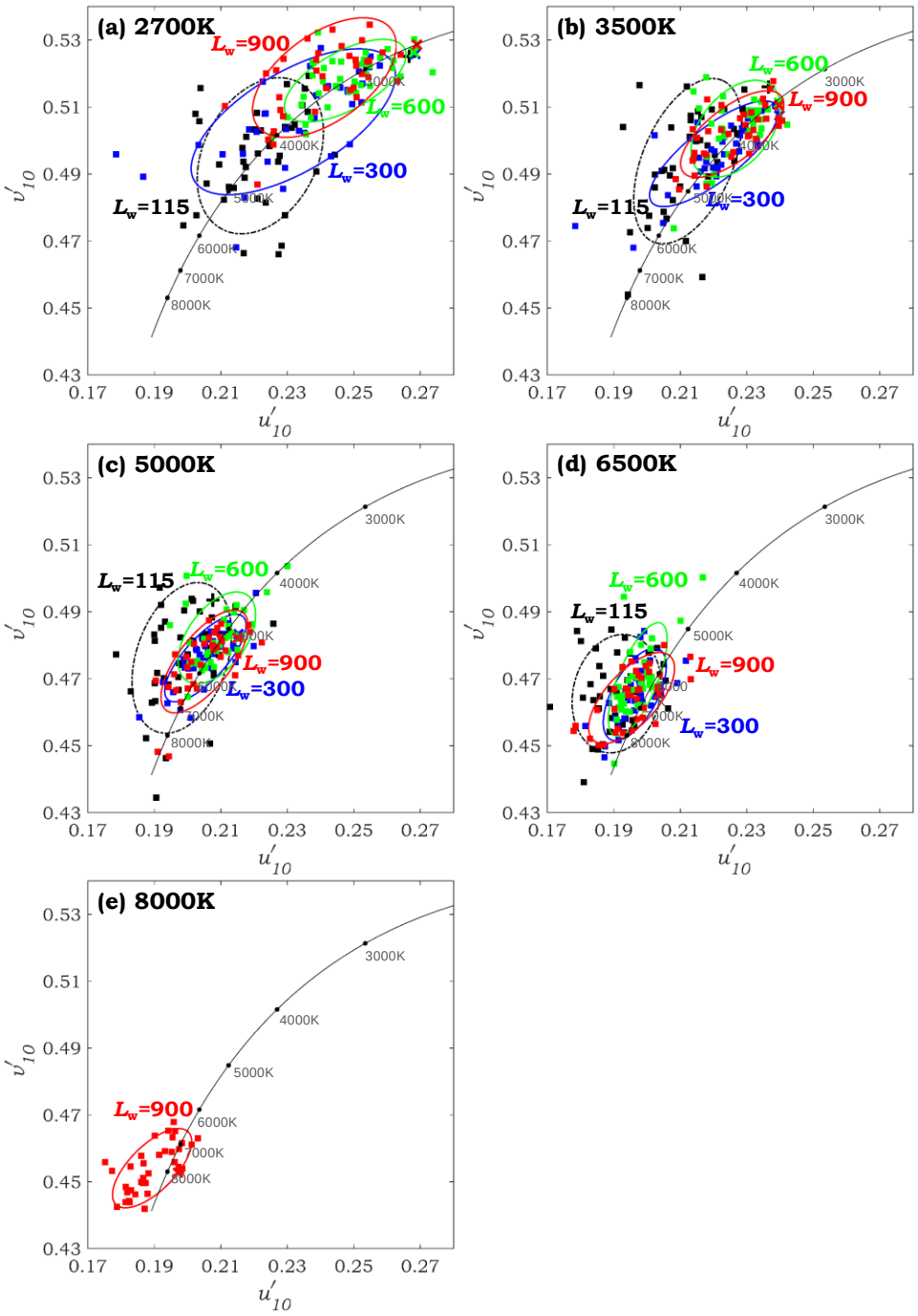

Fig. 5.3. Chromaticities of the adjusted stimuli, together with the 95% confidence error ellipses, made by the observers under each adapting luminance and CCT level in the CIE 1976 $u'_{10}v'_{10}$ chromaticity diagram. (a) 2700K; (b) 3500K; (c) 5000K; (d) 6500K; (e) 8000K.

5.3.2 Average Chromaticities of Adjusted Stimuli under Each Adapting Condition

The average chromaticities of the adjusted stimuli at each display luminance under each different adapting condition were calculated in the CIE 1976

$u'_{10}v'_{10}$ chromaticity diagram, as shown in Fig. 5.4. The average chromaticity differences between the adjusted stimuli and the adapting conditions, together with the 95% confidence interval, are shown in Fig. 5.5. Under the adapting conditions that had an L_w of 115 cd/m^2, the chromaticities of the adjusted stimuli generally shifted from the adapting chromaticities towards the direction of a higher CCT along the blackbody locus and they were above the blackbody locus. Under the adapting conditions that had an L_w higher than 115 cd/m^2, the chromaticities of the adjusted stimuli were around the blackbody locus. The chromaticities generally shifted towards the adapting chromaticities with the increase of L_w, which was more obvious when the adapting CCT was 2700 and 3500 K. The distance between the chromaticities of the adjusted stimuli and those of the adapting condition generally increased with the increase of the display luminance.

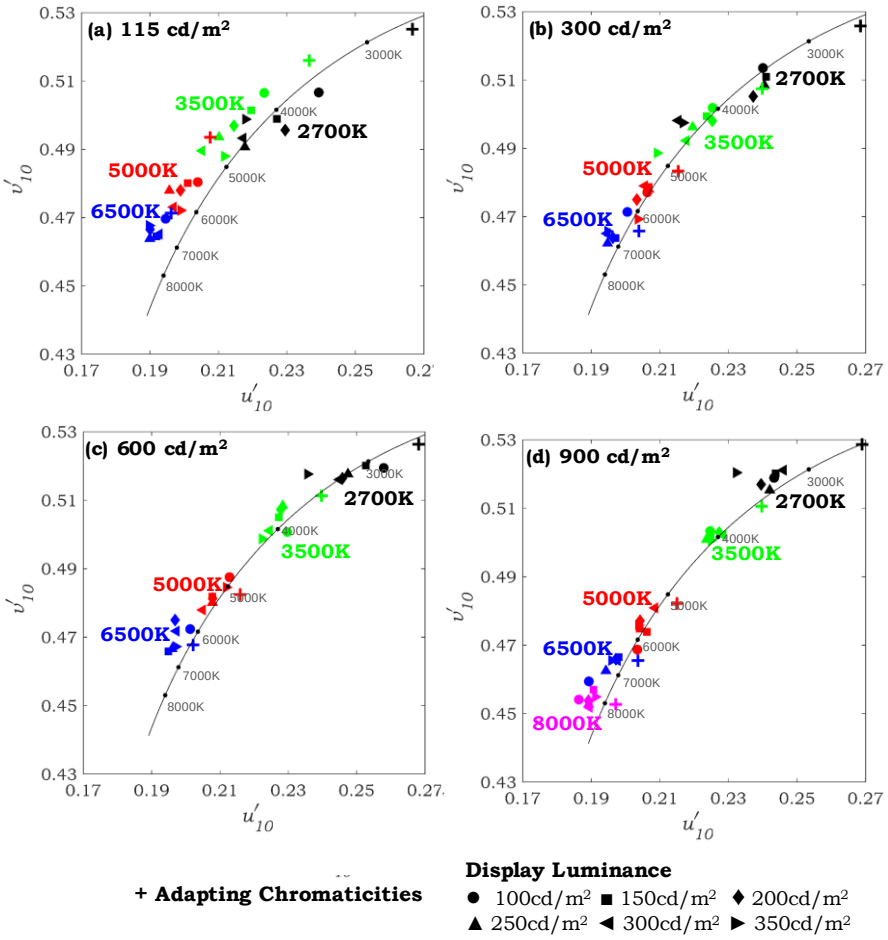

Fig. 5.4. Average chromaticities of the stimuli adjusted by the observers at each display luminance level under each adapting condition in the CIE 1976 $u'_{10}v'_{10}$ chromaticity diagram. (a) L_w = 115 cd/m²; (b) L_w = 300 cd/m²; (c) L_w = 600 cd/m²; (d) L_w = 900 cd/m².

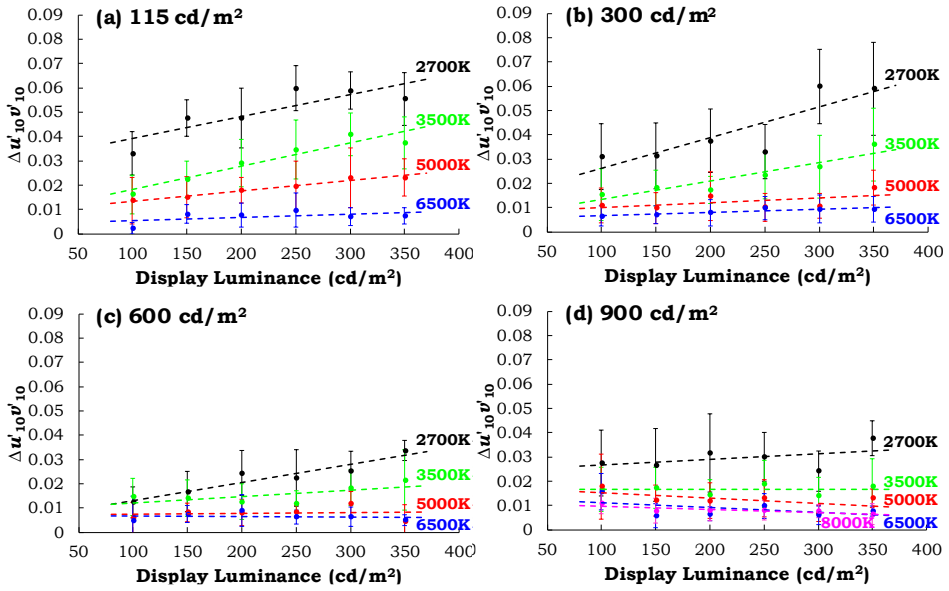

Fig. 5.5. Chromaticity differences, together with the 95% confidence interval, between the average chromaticities of the stimuli adjusted by the observers and the chromaticities of the adapting fields under each adapting condition in the CIE 1976 $u'_{10}v'_{10}$ chromaticity diagram. (a) L_w = 115 cd/m²; (b) L_w = 300 cd/m²; (c) L_w = 600 cd/m²; (d) L_w = 900 cd/m².

The average chromaticities of the adjusted stimuli were also calculated in CAM02-UCS, which embeds the chromatic adaptation transform CAT02, as shown in Fig. 5.6. The degree of chromatic adaptation factor *D* was set to 1. In CAM02-UCS, adapting chromaticities are converted to (0,0)—the origin in the a'_{10}-b'_{10} plane. The average chromaticity difference between the adjusted stimuli and the origin in the a'_{10}-b'_{10} plane of CAM02-UCS, together with the 95% confidence interval, are shown in Fig. 5.7. When the adapting luminance was lower than the display luminance, the adjusted stimulus had a lightness (i.e., *J*') greater than 100 and the stimulus was likely to appear self-luminous. The chromaticities were generally far away from the origin in the a'_{10}-b'_{10} plane. When the adapting luminance was higher than the display luminance, the adjusted stimulus had a *J*' lower than 100, which made the stimulus appear as a surface colour instead of a self-luminous stimulus. The chromaticities of the stimulus having a *J*' lower than 100 were shifted towards the origin in the a'_{10}-b'_{10} plane and the magnitude of the chromaticity shift was larger when the adapting CCT was 2700 and 3500 K.

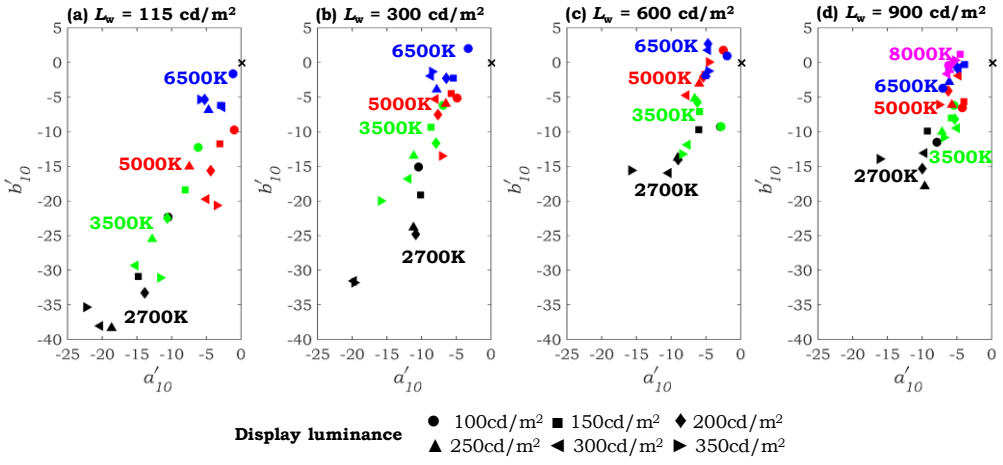

Fig. 5.6. Average chromaticities of the stimuli adjusted using the chromatic background under each adapting condition in the a'_{10}-b'_{10} plane of CAM02-UCS. (a) L_w = 115 cd/m²; (b) L_w = 300 cd/m²; (c) L_w = 600 cd/m²; (d) L_w = 900 cd/m².

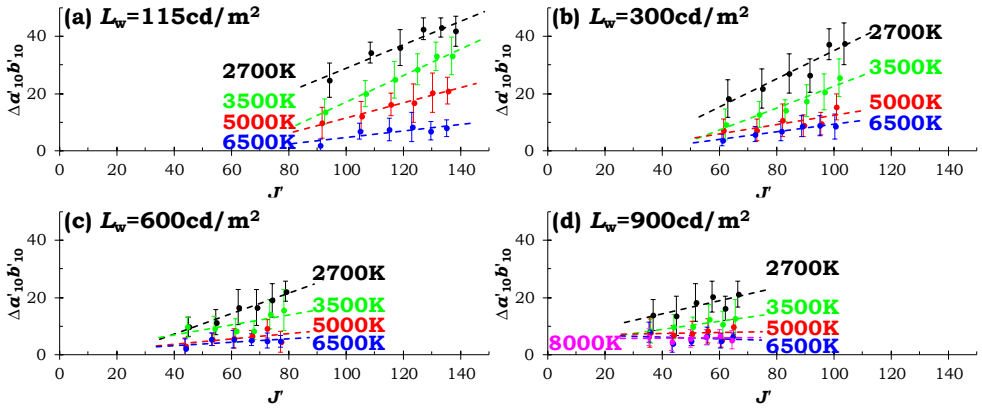

Fig. 5.7. Average chromaticity difference, together with the 95% confidence interval, between the stimuli adjusted using the chromatic background and the origin in the a'_{10}-b'_{10} plane of CAM02-UCS. (a) L_w = 115 cd/m²; (b) L_w = 300 cd/m²; (c) L_w = 600 cd/m²; (d) L_w = 900 cd/m².

5.4 Discussion

5.4.1 Effect of Adapting and Stimulus Luminance on Viewing Mode

Though only one viewing medium (i.e., a self-luminous display) was used in the experiment and all the observers were aware of the fact that the stimulus was produced by a display, it can be observed that the results produced under the adapting conditions that had L_w of 115 and 900 cd/m² were similar to those in the past studies using two different viewing media. Specifically, the results produced under the adapting conditions with an L_w of 115 cd/m², as shown in Fig. 5.4, were similar to those in the past studies using self-luminous displays [Hunt and Winter 1975; Breneman 1987; Fairchild 1991; Berns and Gorzynski 1991; Choi and Suk 2016; High et al. 2017; Huang et al. 2018; Zhai and Luo 2018, Zhu et al. 2018], while the results under the adapting conditions with an L_w of 900 cd/m² were similar to those in the past studies using reflective surface colour samples (e.g., Munsell samples or NCS samples) [Wei et al. 2017a; Wei et al. 2017b; Zhai and Luo 2018]. This result revealed that the chromaticities for producing white appearance using surface

colours and self-luminous displays, as found in many past studies, should not be attributed to the different viewing media, but to the viewing mode.

It should be noted that the chromaticity differences between the whitest stimulus and the adapting field at 2700 and 3500 K in this study were larger than those in [Zhai and Luo 2018], where the NCS colour samples were used as the colour stimuli. This was possibly due to the fact the colour gamut or chromaticity range that can be achieved using the surface colour samples were limited. For example, three of the four stimuli that were adjusted at the display luminance level of 100 cd/m^2 under the L_w of 115 cd/m^2 were outside the boundaries formed by the NCS samples with a similar *J*' level (i.e., around 90) and could not be produced by the NCS samples, as shown in Fig. 5.8.

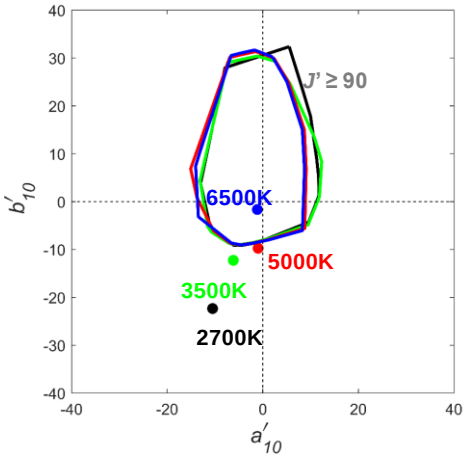

Fig. 5.8. Chromaticities of the 100 cd/m^2 stimuli adjusted by the observers under the adapting conditions that had an L_w of 115 cd/m^2 in the a'_{10}-b'_{10} plane of the CAM02-UCS and the boundary formed by the NCS samples under the same adapting conditions with a similar *J*' above 90. The stimuli with chromaticities outside the boundary cannot be produced by typical surface colour samples.

Under the different adapting luminance levels, the stimuli at a certain display luminance level had different lightness levels. Under the adapting conditions that had an L_w of 115 cd/m^2, the stimuli adjusted with the display luminance being set between 150 and 350 cd/m^2 had *J*' values greater than 100, as shown in Fig. 5.9, as the stimuli luminance values were higher than L_w (i.e., the luminance of a perfect reflector under the same adapting condition). Under

these conditions, the self-luminous stimuli were likely to be viewed in the self-luminous mode. When the adapting conditions had an L_w of 900 cd/m^2, the stimuli had J' values between 30 and 70, which may make the self-luminous stimuli appear reflective as surface colour samples. Thus, the findings in the past studies that self-luminous stimuli and surface colour samples need different chromaticities for producing white appearance were likely due to the different viewing modes (i.e., self-luminous mode versus surface mode) instead of the different viewing media (i.e., self-luminous displays versus reflective surface colour samples). Such an effect of viewing mode can also be observed by comparing the inter-observer variations, which was much smaller under the adapting conditions with an L_w of 900 cd/m^2 than for those under the conditions with an L_w of 115 cd/m^2, as shown in Fig. 5.3. Under the adapting conditions that had an L_w of 300 cd/m^2, all the adjusted stimuli had a J' around or below 100 and the stimuli were expected to appear in the surface mode. However, the chromaticities adjusted at the display luminance level of 300 and 350 cd/m^2 under 2700 K were significantly different from others, as shown in Figs. 5.6 and 5.7, which showed that these two stimuli may appear self-luminous. This was consistent to the findings that luminance was not the only factor to determine the transition of viewing modes (i.e., from reflective surface colours to self-luminous stimuli) for stimuli with different chromaticities [Yamauchi and Uchikawa 2000; Uchikawa et al. 2001].

It is worthwhile to note that the iPad display used in the experiment had a reflectance of 4 to 5% under a normal illumination and the reflected light may partially contribute to the change of viewing mode and the effect of adapting CCT under different adapting conditions. Further studies can be carried out

using self-luminous displays with an anti-reflective coating or electronic ink (E ink) displays to investigate the effects of adapting luminance on viewing modes without the influence of the reflectance.

5.4.2 Effect of Adapting Luminance and CCT on Degree of Chromatic Adaptation

When the adapting conditions had an L_w of 900 cd/m^2 and the stimuli were likely to be perceived as surface colours, the chromatic adaptation seemed to be almost complete when the adapting CCTs were 5000, 6500, and 8000 K since the chromaticities of the adjusted stimuli and the adapting conditions were close to each other. For the other adapting conditions, it can be observed that the degree of chromatic adaptation generally decreased with lower adapting luminance and CCT levels, as shown in Fig. 5.7, since the chromaticity differences between the adjusted stimuli and the adapting conditions became larger.

The degree of chromatic adaptation factors *D*, if calculated using Eq. 2.4 with a relative luminance value (i.e., Y_b) being set to 40, was equal to 0.893, 0.952, 0.966, and 0.987 under an L_w of 115, 300, 600, and 900 cd/m^2 respectively. In order to investigate the effect of adapting CCTs on chromatic adaptation, CAT16, with the *D* factor set to 1, was used to transform the tristimulus values of the adjusted stimuli under each adapting condition to those under the 6500 K adapting condition with the same L_w level. The chromaticity differences between the transformed stimuli and the stimuli under the 6500 K condition in the CIE 1976 $u'_{10}v'_{10}$ chromaticity diagram are shown in Fig. 5.9, with a larger chromaticity difference indicating a larger decrease of the degree of chromatic adaptation caused by the lower adapting CCT in comparison to 6500 K with the same L_w level. It can be observed that with

the same adapting luminance, the degree of chromatic adaptation was always lowest when the adapting CCT was 3000 K, followed by the adapting CCT of 3500 K. The degree of chromatic adaptation under 5000 and 6500 K were similar. The effect of adapting CCT became less obvious with the increase of adapting luminance. It merits further investigations whether a higher adapting luminance can achieve a complete degree of chromatic adaptation even the adapting CCT is relatively low (e.g., 3000 K). Moreover, when the stimuli were viewed in the self-luminous mode under the adapting conditions with an L_w of 115 cd/m^2, though it was obvious that the adapting CCT affected the colour appearance of the stimuli and the stimuli were still viewed as related colours, the effect of adapting CCT was smaller and the degrees of chromatic adaptation were much lower. It would be interesting to further investigate the effect of adapting CCT with an even lower adapting luminance and a possible threshold of adapting luminance to make stimuli appear as unrelated colours.

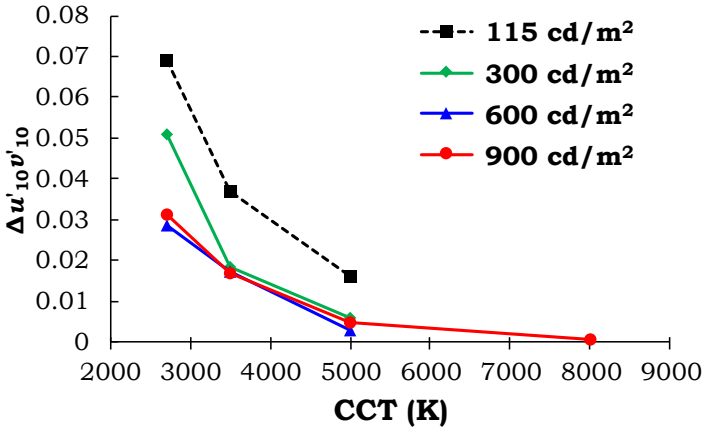

Fig. 5.9. Chromaticity differences between the average adjusted chromaticities under the 6500K adapting condition and those under the other adapting CCTs, which were all transformed to their corresponding chromaticities under the 6500 K adapting condition using CAT16 with the degree of chromatic adaptation factor *D* set to 1, at each adapting luminance level in the CIE 1976 $u'_{10}v'_{10}$ chromaticity diagram.

5.5 Summary

In this chapter, a study that investigated the effects of adapting luminance and CCT on the degree of chromatic adaptation was introduced through the

investigation of white appearance of a stimulus. The observers were asked to adjust the colour appearance of a stimulus, with a luminance level from 50 to 350 cd/m^2, produced by a self-luminous display until it appeared the whitest under 17 adapting conditions at different adapting luminance (i.e., L_w = 115, 300, 600, and 900 cd/m^2) and CCT levels (i.e., 2700, 3500, 5000, 6500, and 8000 K). The larger the chromaticity difference between the adjusted stimuli and the adapting conditions, the lower the degree of chromatic adaptation.

A joint effect of adapting CCT and luminance on the degree of chromatic adaptation was found. A higher adapting CCT was able to introduce a higher degree of chromatic adaptation. When the adapting CCT was above 5000 K, the degree of chromatic adaptation was generally high regardless of the adapting luminance levels. When the adapting CCT was below 5000 K, the effect of adapting luminance was more obvious, with a higher adapting luminance introducing a higher degree of chromatic adaptation.

Furthermore, though the viewing medium was kept unchanged, the chromaticities of the stimuli that were adjusted under the lowest and highest adapting luminance (i.e., L_w = 115 and 900 cd/m^2 respectively) were significantly different. Under the adapting conditions with an L_w of 115 cd/m^2, the chromaticities of the adjusted stimuli were generally shifted from the adapting chromaticities towards the direction of a higher CCT level, which was similar to the findings in the past studies using self-luminous displays as the viewing medium. In contrast, when the adapting luminance was high, the adjusted chromaticities were much closer to the adapting chromaticities, which was similar to the findings in the past studies using reflective surface colour samples as the viewing medium. Thus, it is likely that the different chromaticities for producing a white appearance using surface colour samples

and self-luminous displays, as reported in the past studies, was due to the different viewing modes (i.e., self-luminous mode versus surface mode) that were affected by the relationship between the adapting luminance and stimulus luminance, instead of the different viewing media (i.e., self-luminous displays versus surface colour samples). The degree of chromatic adaptation was generally lower when viewing stimuli in the self-luminous mode.

Chapter 6 White Appearance of Virtual Stimuli Produced by Augmented Reality

6.1 Motivation

With the development of reality technologies, including virtual reality (VR), augmented reality (AR), and mixed reality (MR), the human visual system is experiencing new challenges. When viewing AR stimuli, virtual stimuli are produced and overlaid on the real-world environment, which was a new viewing condition to humans. AR technologies can be categorized into two groups: optical see-through and video see-through. With an optical see-through device, virtual stimuli are directly overlaid on the real-world environment. Such devices typically use an optical combiner that is partially transparent and reflective, so that the user can view both the real-world environment through the device and the virtual stimuli projected by an embedded display. In contrast, a video see-through device captures the real-world environment by a camera in real time and renders the captured scene on a display. Virtual stimuli are rendered with the scene. When using AR technologies, users simultaneously view the virtual stimuli and the real-world environment, so that the colour appearance of the virtual stimuli cannot be simply characterized using the existing models. Such an issue needs to be investigated to improve the quality of colour reproduction in the AR applications. Few studies, however, investigated how the colour appearance of virtual stimuli is affected by different real-world and virtual environments.

In a previous study [Hassai 2019], two adapting conditions of 2800 and 4300 K were used in a colour matching experiment with an optical see-through AR setup and it was found that the adapting condition did not have a significant effect on the colour appearance of the stimuli produced by AR. However, this may due to the fact that the virtual stimuli in the study always had a much higher luminance than the adapting condition and the background colours, making the stimulus always appeared as self-luminous colours. Furthermore, the colour perception in the two different types of AR may also be much different. For example, the video see-through AR processes the captured scenes through white balance and tone mapping; while the optical see-through AR may only slightly change the colour of the scenes due to the transmittance of the lens.

In this study, psychophysical experiments were conducted to investigate the colour appearance of virtual stimuli produced by optical see-through and video see-through AR setups. The observers were asked to adjust the colour appearance of the virtual stimulus until it appeared the whitest.

6.2 Method

6.2.1 Experiment 1: White Appearance of Virtual Stimulus Produced by Optical See-through AR

6.2.1.1 Apparatus, Setup, and Adapting Conditions

In Experiment 1, an optical see-through AR setup was simulated as shown in Fig. 6.1. The viewing booth had dimensions of 60 cm (width) × 60 cm (depth) × 60 cm (height) and the interiors were painted with Munsell N7 neutral grey paint. A spectrally tunable LED device was placed above the viewing booth to produce a uniform illumination to the booth floor. A beam splitter and an

iPad Air 2 were mounted on a tripod in front of the viewing booth. The iPad, covered by a Munsell N7 sheet with a 3 cm × 3 cm opening in the centre, was placed horizontally. The beam splitter was tilted 45° so that a virtual image can be produced by projecting the square on the iPad display to the booth with the same size (i.e., 3 cm × 3 cm) of the display stimulus. The observer was seated 40 cm from the tripod, with his/her chin fixed on a chin-rest, so that he or she could view the virtual stimulus perpendicularly with an FOV around 4°. Figure 6.2 shows the condition viewed by an observer.

The iPad display was calibrated using the GOG display model [Berns 1996] and the CIE 1964 CMFs. Based on the GOG model, a customized program was developed and a Bluetooth keyboard was used to remotely adjust the nominal chromaticities of the display along the u'_{10} and v'_{10} axes in the CIE 1976 $u'_{10}v'_{10}$ chromaticity diagram with a step of 0.001 unit. The luminance level of the iPad display was fixed at 250 cd/m^2. The colour gamut of the iPad display in the CIE 1976 $u'_{10}v'_{10}$ chromaticity diagram at the luminance level of 250 cd/m^2 is shown in Fig. 6.3. The transmittance factor of the beam splitter was around 65% across the visible spectrum, with Fig. 6.4 showing the spectral transmittance distribution.

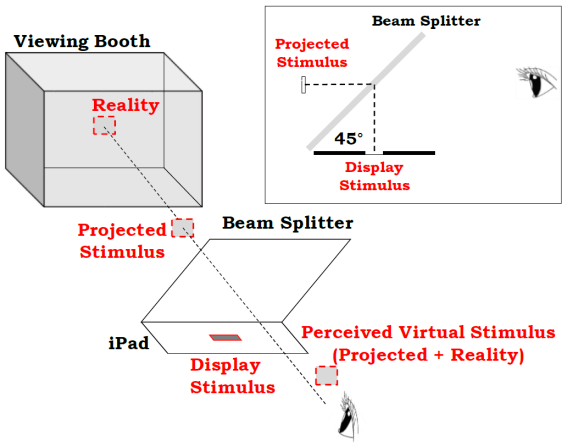

Fig. 6.1. Schematic of the experiment setup. The virtual stimulus was projected by the display colour through the beam splitter. The colour perceived by the observers was a mixture of the virtual colour and the booth colour.

Fig. 6.2. Photograph of the experiment setup, showing the condition viewed by an observer. The stimulus was projected from the iPad display through the beam splitter and was viewed by the observers perpendicularly with an FOV around 4°.

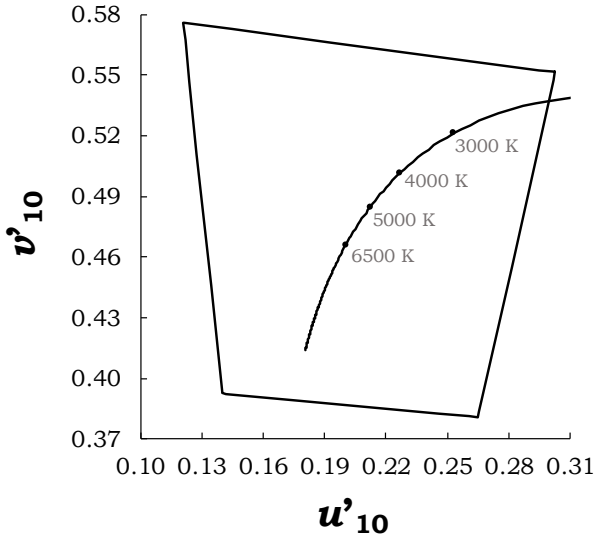

Fig. 6.3. Colour gamut of the iPad display in the CIE 1976 $u'_{10}v'_{10}$ chromaticity diagram at the luminance level of 250 cd/m^2.

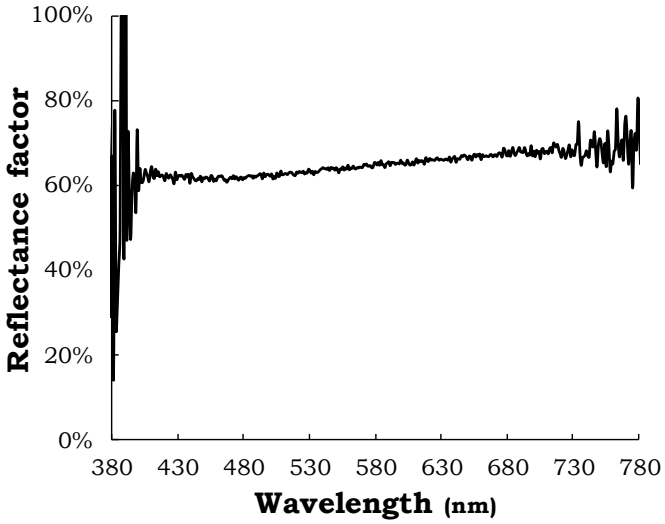

Fig. 6.4. Spectral transmittance distribution of the beam splitter.

Nine adapting conditions were used, with one being a dark condition and the other eight being produced by the spectrally tunable LED device. The eight adapting conditions comprised two levels of adapting luminance with an L_w of 110 and 550 cd/m^2 respectively and four CCT levels of 2700, 3500, 5000, and 6500 K, which were calibrated using a calibrated JETI Specbos 1411UV spectroradiometer and a calibrated Labsphere reflectance standard being placed at the place where the virtual stimulus appeared in the back wall of the viewing booth. The SPDs of the eight adapting conditions were measured from the observer's eye position with and without the beam splitter, with the former being considered as the real-world environment (i.e., reality) and the latter being considered as the virtual environment viewed by the observers. The colourimetric characteristics are summarized in Table 6.1 and the chromaticities are shown in Fig. 6.5.

Table 6.1. Colourimetric characteristics of the real-world environments and the virtual environments viewed by the observers

(a) Reality (real-world environment in the booth)					
Adapting luminance	**Nominal CCT (K)**	**L_w (cd/m^2)**	**CIE 1976 (u'_{10},v'_{10})**	**CCT (K)**	**D_{uv}**
Low	2700	107.8	(0.266,0.526)	2639	-0.002
	3500	115.7	(0.236,0.512)	3476	0
	5000	113.4	(0.210,0.486)	5043	+0.002
	6500	108.2	(0.197,0.469)	6536	+0.004
High	2700	536.0	(0.267,0.528)	2606	-0.001
	3500	547.5	(0.235,0.514)	3485	+0.002
	5000	574.5	(0.208,0.489)	5029	+0.004
	6500	559.0	(0.196,0.468)	6607	+0.005
(b) Virtual (virtual environment with the beam splitter)					
Adapting luminance	**Nominal CCT (K)**	**L_w (cd/m^2)**	**CIE 1976 (u'_{10},v'_{10})**	**CCT (K)**	**D_{uv}**
Low	2700	68.8	(0.269,0.528)	2569	-0.002
	3500	73.6	(0.340,0.514)	3362	0
	5000	71.8	(0.213,0.488)	4847	0
	6500	68.4	(0.200,0.471)	6221	+0.002
High	2700	342.0	(0.270,0.529)	2542	-0.001
	3500	347.9	(0.235,0.514)	3369	+0.001
	5000	363.6	(0.208,0.489)	4817	+0.003
	6500	352.7	(0.196,0.468)	6284	+0.003

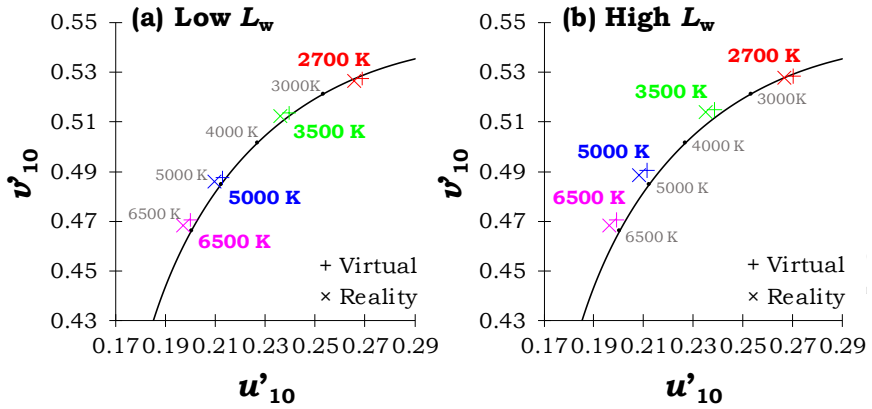

Fig. 6.5. Chromaticities of the adapting conditions in the real-world environments and the virtual environments in Experiment 1. (a) Low L_w; (b) High L_w.

6.2.1.2 Observers and Experimental Procedure

Nineteen observers (15 males and 4 female) between 20 and 29 years (mean = 22.6, std. dev. = 2.28) took part in the experiment. Two observers had an abnormal colour vision, as tested by the Ishihara Colour Vision Test, and their data were discarded in the following analyses. Upon arrival, the experimenter explained the procedures and tasks to the observer and guided them to the viewing booth. Under each adapting condition, the observer fixed his or her chin on the chin-rest and looked at the viewing booth through the beam splitter for two minutes for chromatic adaptation, with the iPad being covered by a black sheet. After the adaptation period, the experimenter removed the black sheet and adjusted the chromaticities of the display stimulus randomly as a starting point. Note that prior to the experiment, the iPad display was switched on for at least 30 minutes for stabilization. The observer then adjusted the colour appearance of the virtual stimulus, which was the image projected from the beam splitter by the iPad display, in the viewing booth along the u'_{10} and v'_{10} axes using the Bluetooth keyboard until the colour appearance of the virtual stimulus appeared the whitest to him or her. The experimenters helped the observer to verify his/her decision by showing him

or her the neighbouring colour stimulus with one-unit increase or decrease along the u'_{10} or v'_{10} axis. After the observer confirmed his/her decision, the experimenter recorded the nominal (u'_{10}, v'_{10}) adjusted by the observer. The experiment started with the dark condition, which helped the observers to reduce the time needed for the dark adaptation. The order of the four CCT levels and two levels of adapting luminance were randomized. The adjustments under the two 2700 K adapting conditions were repeated to evaluate the intra-observer variation.

6.2.2 Experiment 2: White Appearance of Virtual Stimulus Produced by Video See-through AR

6.2.2.1 Apparatus, Setup, and Adapting Conditions

In Experiment 2, a video see-through AR setup was built as shown in Fig. 6.6. A black Huawei P20 Pro was used to capture the real-world environment using the rear camera. A customized application was developed using Unity to render the captured scene on the camera display. At the same time, a 3D cube of 3 cm × 3 cm × 3 cm was rendered at the centre of the rendered scene as a virtual stimulus. The mobile phone was mounted on a tripod placed at the centre of the viewing booth. During the experiment, the observer was seated in front of the booth and fixed his/her chin on a chin-rest, so that he or she could view the virtual stimulus perpendicularly with an FOV around 3°.

Fig. 6.6. Photograph of the experiment setup. The stimulus was a 3-D cube produced by a customized Unity application and was viewed by the observers perpendicularly with an FOV around 3°.

The Huawei P20Pro mobile phone display was calibrated using the GOG display model [Berns 1996] and the CIE 1964 CMFs. Using the Bluetooth keyboard, the chromaticities of the virtual stimulus (i.e., the 3D cube) could be adjusted along the u'_{10} and v'_{10} axes with a step of 0.001 unit. The luminance level of the virtual stimulus was fixed at 200 cd/m^2 so that the lightness of the virtual stimulus was comparable to that of the virtual stimulus under the high L_w in Experiment 1. The colour gamut of the display at the luminance levels of 200 cd/m^2 in the CIE 1976 $u'_{10}v'_{10}$ chromaticity diagram is shown in Fig. 6.7.

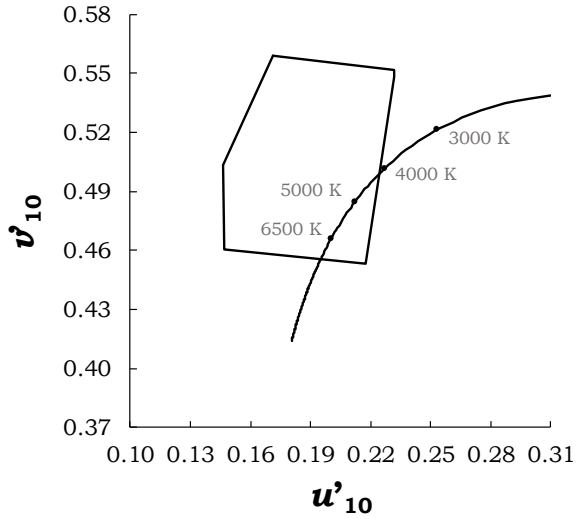

Fig. 6.7. Colour gamut of the mobile phone display at the luminance level of 200 cd/m^2 in the CIE 1976 $u'_{10}v'_{10}$ chromaticity diagram.

The experiment included eight adapting conditions, which had similar adapting luminance and CCT levels as those in Experiment 1. The eight adapting conditions comprised two levels of adapting luminance (i.e., low and high with an L_w = 115 and 560 cd/m^2 respectively) and four CCT levels (i.e., 2700, 3500, 5000, and 6500 K) that were calibrated using a calibrated JETI Specbos 1411UV spectroradiometer and a reflectance standard being placed at the centre of the viewing booth. The SPDs of the real-world and virtual environments (i.e., the background of the rendered scenes on the display) were measured from the observer's eye position. The colourimetric characteristics are summarized in Table 6.2 and the chromaticities are shown in Fig. 6.8. The virtual environments were much different to those in Experiment 1, since the mobile phone implemented automatic white balance to the captured scenes. As shown in Table 6.2, the white-balanced virtual environments under each adapting condition generally had similar luminance and CCT levels, except the condition with a CCT of 2700 K and the high L_w.

Table 6.2. Colourimetric characteristics of the real-world environments and the virtual environments

(a) Reality (real-world environment in the booth)					
Adapting luminance	**Nominal CCT (K)**	**L_w (cd/m^2)**	**CIE 1976 (u'_{10},v'_{10})**	**CCT (K)**	**D_{uv}**
Low	2700	118.6	(0.267,0.525)	2730	-0.001
	3500	115.7	(0.240,0.503)	3559	-0.005
	5000	118.4	(0.216,0.480)	4989	-0.005
	6500	117.8	(0.207,0.462)	6446	-0.006
High	2700	565.5	(0.264,0.519)	2758	-0.005
	3500	569.3	(0.238,0.500)	3573	-0.008
	5000	556.9	(0.216,0.479)	5013	-0.006
	6500	559.4	(0.201,0.466)	6583	0
(b) Virtual (virtual environment produced by the phone display)					
Adapting luminance	**Nominal CCT (K)**	**L_w (cd/m^2)**	**CIE 1976 (u'_{10},v'_{10})**	**CCT (K)**	**D_{uv}**
Low	2700	136.4	(0.219,0.489)	4566	-0.004
	3500	154.8	(0.210,0.480)	5288	-0.002
	5000	155.2	(0.208,0.480)	5396	0
	6500	150.0	(0.205,0.476)	5771	0
High	2700	87.7	(0.254,0.520)	2968	-0.002
	3500	159.4	(0.211,0.481)	5189	-0.002
	5000	160.1	(0.208,0.480)	5436	-0.001
	6500	158.9	(0.205,0.476)	5774	0

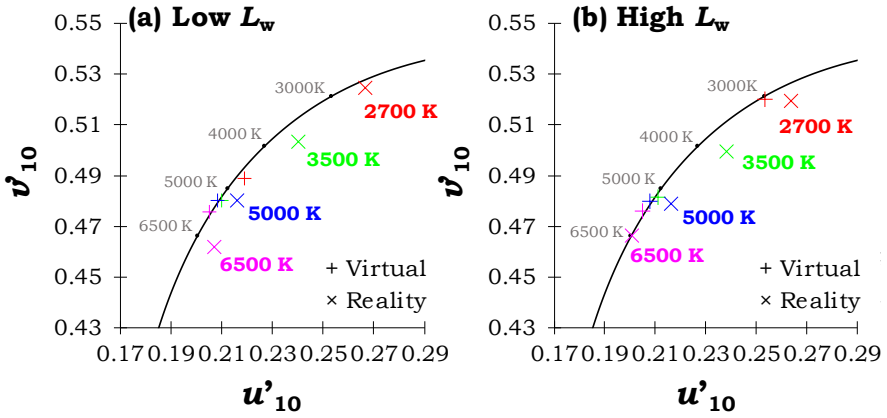

Fig. 6.8. Chromaticities of the adapting conditions in the real-world environments and the virtual environments in Experiment 2. (a) Low L_w; (b) High L_w.

6.2.2.2 Observers and Experimental Procedure

Eight observers (five males and three female) between 23 and 29 years (mean = 25.0, std. dev. = 2.00) completed the experiment. All the eight observers had a normal colour vision, as tested by the Ishihara Colour Vision Test.

The experiment procedure was similar to that of Experiment 1. Under each adapting condition, the observer fixed his or her chin on the chin-rest and looked into the viewing booth for two minutes for chromatic adaptation. During the adaptation period, the mobile phone display was switched off. The experimenter then turned on the phone and set the chromaticities of the 3D cube to a starting point. The observer was instructed to adjust the colour appearance of the 3D cube along the u'_{10} and v'_{10} axes in the CIE 1976 u'_{10}-v'_{10} chromaticity diagram using the Bluetooth keyboard until it appeared as the whitest. After the observer completed the adjustment, the nominal (u'_{10}, v'_{10}) of the 3D cube was recorded by the experimenter. The order of the adapting conditions was randomized. The adjustments under the two 2700 K adapting conditions were repeated for evaluating the intra-observer variation.

6.3 Result

The chromaticities of the adjusted stimuli in the CIE 1976 u'_{10}-v'_{10} under each adapting condition are shown in Fig. 6.9. These chromaticities were those recorded by the experimenter in the experiment. The chromaticities adjusted in the optical see-through AR setup were generally not close to the gamut boundary of the iPad display, except several chromaticities under the 2700 and 3500 K adapting conditions. In the video see-through AR, however, many chromaticities were on or close to the gamut boundary of the mobile phone display, especially under the 2700 K adapting conditions, due to the limited gamut area.

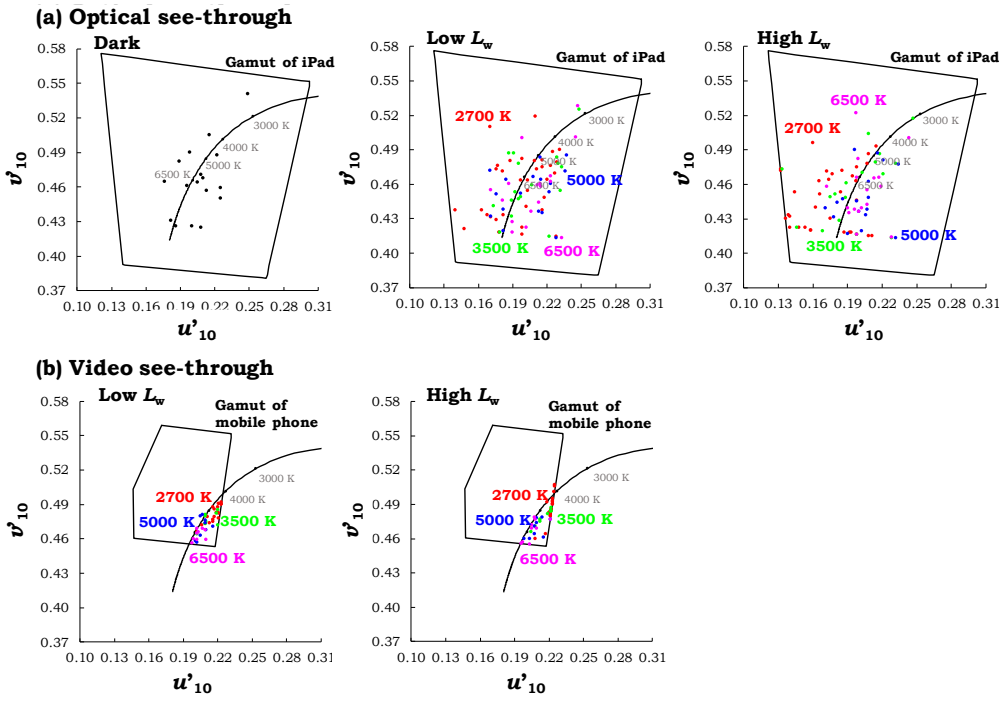

Fig. 6.9. Chromaticities of the stimuli adjusted by the observers under each adapting condition in the CIE 1976 $u'_{10}v'_{10}$ chromaticity diagram. (a) In the optical see-through AR setups; (b) In the video see-through AR setups.

After the completion of the experiments, the SPD of each virtual stimulus adjusted by the observers was measured under the corresponding adapting condition using the JETI specbos 1411UV spectroradiometer. In the optical see-through AR setup, the measured SPDs considered both the virtual stimulus and the light transmitting through the beam splitter. In the video see-through AR setup, the measured SPDs considered both the virtual stimulus and the light reflected by the mobile phone display. The chromaticities in the CIE 1976 $u'_{10}v'_{10}$ chromaticity diagram were calculated based on the measured SPDs.

6.3.1 Intra- and Inter-observer Variations

The intra-observer variations for each experiment were characterized using the MCDM values based on the average colour difference in the CIE 1976 $u'_{10}v'_{10}$ chromaticity diagram ($\Delta u'_{10}v'_{10}$) between the repeated adjustments made by each observer. For the optical see-through AR setup, the average

$\Delta u'_{10}v'_{10}$ ranged between 0.0001 and 0.043, with an average of 0.015; for the video see-through AR setup, the average $\Delta u'_{10}v'_{10}$ ranged between 0.006 and 0.014, with an average of 0.010. Figure 6.10 shows the 95% confidence error ellipses for the repeated adjustments in the two AR setups.

The inter-observer variations were characterized by the MCDM values based on the adjustments made by each observer and the average adjustments made by the observers (i.e., an average observer) under each adapting condition in the CIE 1976 u_{10}'-v'_{10} chromaticity diagram. Table 6.3 summarizes the MCDM value under each adapting condition of the two AR setups. The adjustments made by the observers and the 95% confidence error ellipse under each adapting condition are shown in Fig. 6.11. The MCDM values and the sizes of the ellipses of the optical see-through AR setups were comparable to those in previous studies investigating white appearance and memory colours [Huang et al. 2018; Zhai and Luo 2018; Zhu et al. 2018; Ma et al 2018a; Ma et al 2018b]. In comparison, the ellipses of the video see-through AR setups were much smaller. This may partly due to the fact that the gamut area of the mobile phone display was limited and the chromaticities of the many adjusted stimuli, as shown in Fig. 6.9, were on the boundary of the gamuts.

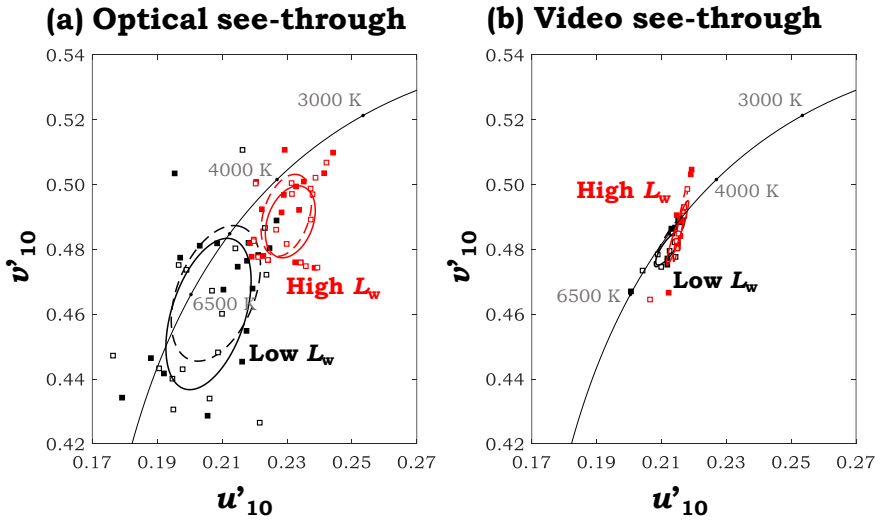

Fig. 6.10. Chromaticities and the one standard-error ellipses of the repeated adjustments made by the observers under the two adapting conditions at 2700 K. (a) In the optical see-through AR; (b) In the video see-through AR.

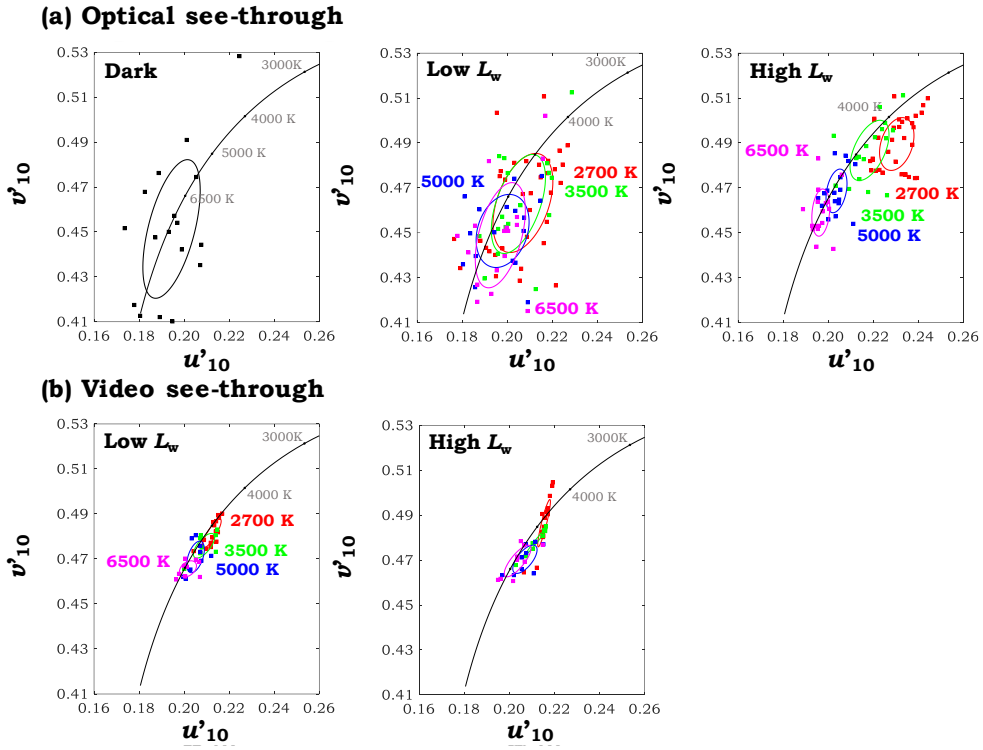

Fig. 6.11. Chromaticities and the 95% confidence error ellipses of the adjusted stimuli under each adapting condition in the CIE 1976 $u'_{10}v'_{10}$ chromaticity diagram. (a) In the optical see-through AR setups; (b) In the video see-through AR setups.

Table 6.3. Inter-observer variations in terms of the MCDM values in the CIE 1976 $u'_{10}v'_{10}$ chromaticity diagram under each adapting condition

Nominal CCT (K)	Adapting luminance	MCDM	
		Optical see-through	Video see-through
Dark		0.0259	/
2700 K	Low	0.0231	0.0063
	High	0.0130	0.0082
3500 K	Low	0.0210	0.0059
	High	0.0138	0.0063
5000 K	Low	0.0178	0.0071
	High	0.0091	0.0071
6500 K	Low	0.0206	0.0045
	High	0.0091	0.0075

6.3.2 Chromaticities of the Adjusted Stimuli under Each Adapting Condition

The average chromaticities of the adjusted stimuli in the CIE 1976 u_{10}'-v'_{10} chromaticity diagram under each adapting condition are shown in Fig. 6.12. For both AR setups, the adjusted chromaticities were generally below the blackbody locus, which was different from the results of the experiments using surface colours and self-luminous stimuli in the previous chapter. For the optical see-through AR setups, the average chromaticities of the adjusted stimuli under the dark condition were around 8000 K. When the adapting luminance was low, the average adjusted chromaticities under the 5000 and 6500 K adapting conditions were also around 8000 K and those under the 2700 and 3500 K adapting conditions were around 6500 K. When the adapting luminance was high, the average adjusted chromaticities shifted towards the direction of a lower CCT, being closer to the chromaticities of the virtual and real-world environments. For the video see-through AR, the average adjusted chromaticities under the low adapting luminance were

located around 5000 to 6500 K. Under the high adapting luminance, the chromaticities shifted slightly towards the direction of a lower CCT. It should be noted that under 2700 K, such a chromaticity shift could be larger if the gamut area of the mobile phone display was larger.

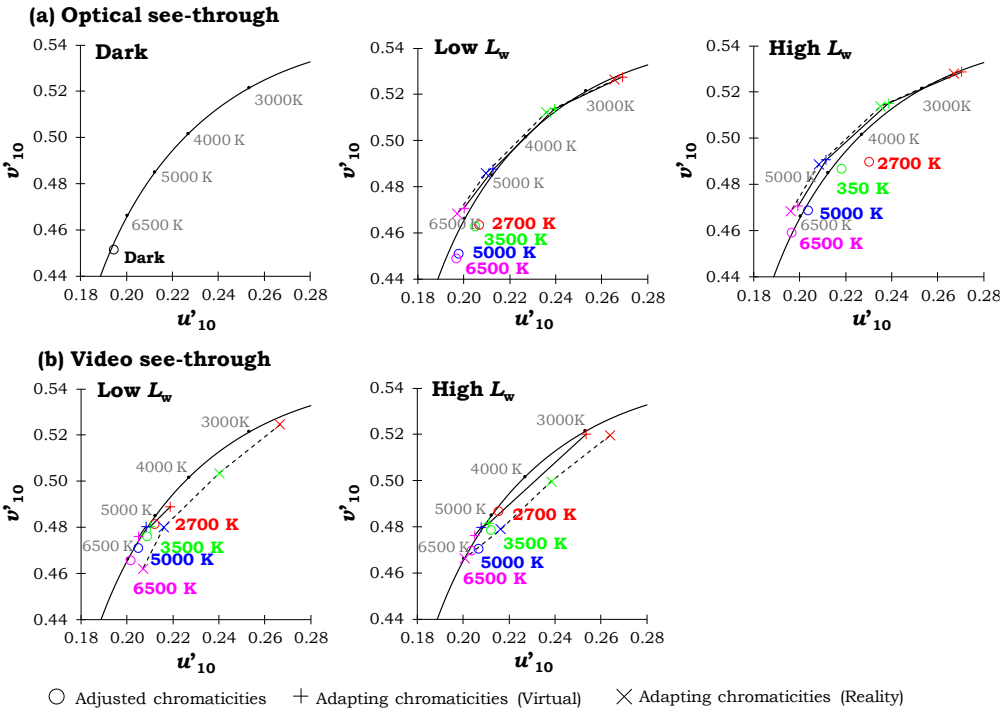

Fig. 6.12. Average chromaticities of the adjusted stimuli under each adapting condition in the CIE 1976 $u'_{10}v'_{10}$ chromaticity diagram under each CCT level. (a) In the optical see-through AR setups; (b) In the video see-through AR setups.

To consider the possible effect of the adapting chromaticities, the chromaticities of the adjustments were also calculated in the CAM02-UCS with the degree of chromatic adaptation factor *D* being set to 1, as shown in Fig. 6.13. For both setups, since the virtual environments (i.e., the environment viewed through the beam splitter in the optical see-through AR setups and the rendered scene in the video see-through AR setups) were around the virtual stimulus, they should be considered as the adapting fields according to the definitions of colour appearance models [Fairchild 2013]. Figure 6.14 shows the chromaticity difference between the average chromaticities of the adjustments and the origin of the a'_{10}-b'_{10} plane in the

CAM02-UCS, which represents the chromaticities of the adapting field, versus the lightness of the virtual stimulus. It can be observed from Figs. 6.13 and 6.14 that for the optical see-through AR setups, the chromaticities shifted towards the origin with an increase of the adapting CCT. For the video see-through AR setups, the chromaticities were generally close to the origin except those under the 2700 K adapting condition at the high L_w. It should be noted that the virtual environment under the 2700 K adapting condition at the high L_w was much different from those under the other adapting conditions, as shown in Table 6.2, due to the white balance implemented by the mobile phone. The average chromaticities of the adjusted stimuli under the 2700 K adapting condition at the high L_w were much further to the origin, as shown in Figs. 6.13 and 6.14. This was likely due to the high lightness value of the virtual stimulus caused by the low adapting luminance of the virtual environment.

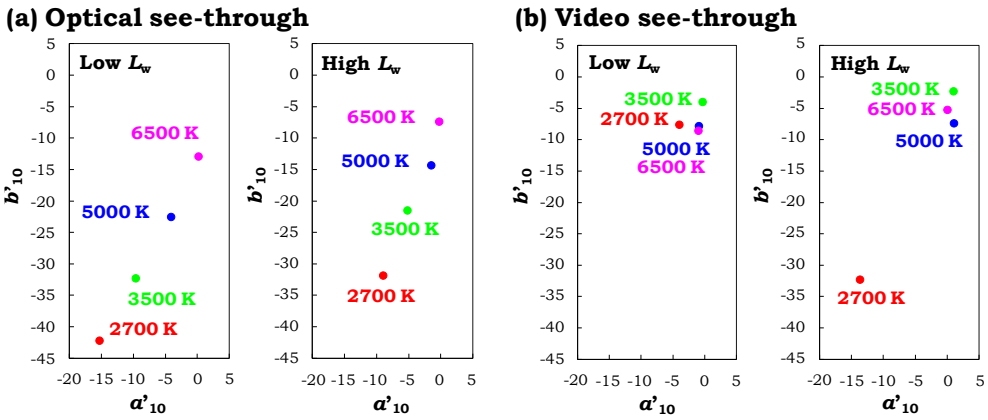

Fig. 6.13. Average chromaticities of the adjusted stimuli under each adapting condition in CAM02-UCS under each CCT level. (a) In the optical see-through AR; (b) In the video see-through AR.

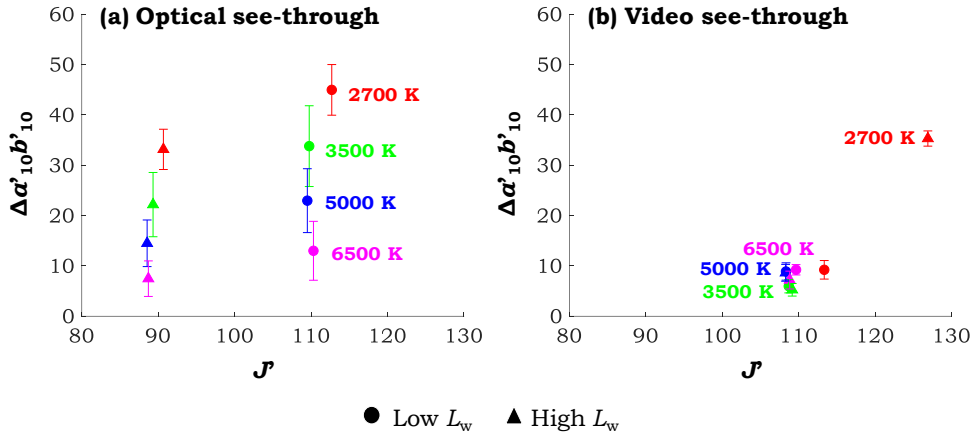

Fig. 6.14. Chromaticity differences, together with the 95% confidence intervals, between the average chromaticities of the adjusted stimuli and the origin in the a'_{10}-b'_{10} plane of the CAM02-UCS. (a) In the optical see-through AR setups; (b) In the video see-through AR setups.

6.4 Discussion

6.4.1 White Appearance of Stimuli Produced by AR

The study revealed the white appearance of the virtual stimulus perceived in optical and video see-through AR setups. The adjusted chromaticities of the white appearance, as shown in Fig. 6.11, were different between the two types of AR setups and varied with different adapting conditions. The intra- and inter-observer variations in the video see-through AR was smaller than those in the optical see-through AR, with the adjusted chromaticities being located in a small area below the blackbody locus, as shown in Fig. 6.11. This suggested that the colour perception in a video see-through AR environment was more consistent than that in the optical see-through AR environment. It should be noted, however, that the colour gamut of the video see-through device (i.e., the mobile phone display) was limited and the chromaticities adjusted by the observers were close to the gamut boundaries, especially under the 2700 K adapting conditions(as shown in Fig. 6.9).

6.4.2 Adaptation to Real-world or Virtual Environments

The effect of the real-world environments needs to be considered. Though the virtual environment was around the virtual stimuli and should be regarded as the adapting field by definition, the observers could also view the adapting condition in reality and may adapt to the real-world environments in both experiments. Therefore, the chromaticities in the CAM02UCS and the distance from the origin of the a'_{10}-b'_{10} plane were also calculated using the real-world environments as the adapting fields, as shown in Figs. 6.15 and 6.16. Since a number of chromaticities adjusted under the 2700 K adapting conditions in the video see-through AR setups were on or close to the gamut boundary, as shown in Fig. 6.9, the adjusted stimuli would have lower CCT values and the chromaticities would be closer to the origin of the a'_{10}-b'_{10} plane if the colour gamut was larger. It can be observed that for the optical see-through AR setups, the lightness levels (i.e., J') of the virtual stimuli were lower when using the real-world environments as the adapting fields, and the chromaticity differences between the average adjusted chromaticities and origin (i.e, $\Delta a'_{10}b'_{10}$) were smaller. For the video see-through AR setups, there was a large difference between the results calculated using the virtual and real-world environments as the adapting fields. Using the virtual environments as the adapting fields, the lightness levels of the stimuli were always greater than 100 since the virtual stimuli were brighter than the virtual environments produced by the mobile phone display. The distances between the chromaticities and the origin were generally small (except when the adapting condition was 2700 K and the L_w was high), which may due to the fact that the chromaticities of the virtual environments produced by the phone display shifted away from the chromaticities of real-world environments towards a higher CCT level. In comparison, it can be observed that the results

calculated using the real-world environments as the adapting fields were comparable to those of the optical see-through AR setups, with similar lightness and $\Delta a'_{10}b'_{10}$ values under each adapting condition.

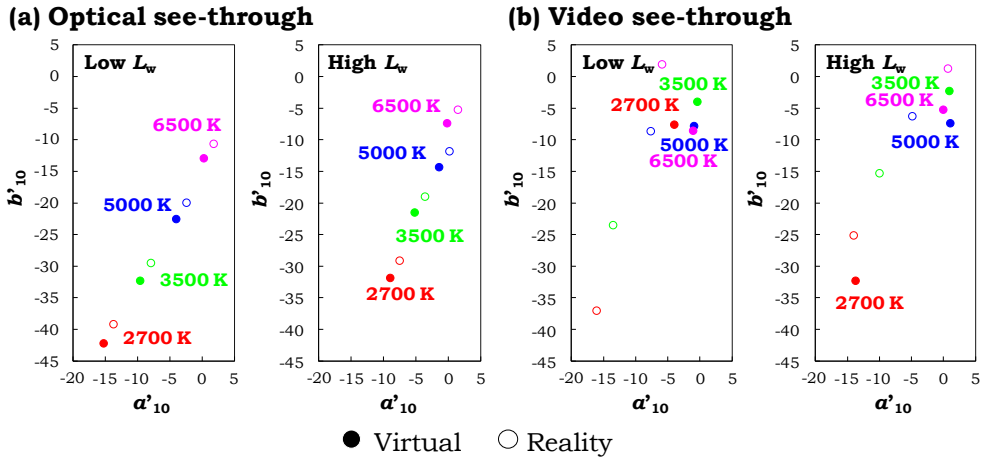

Fig. 6.15. Average chromaticities of the adjusted stimuli under each adapting condition in the CAM02-UCS under each CCT level. The chromaticities were calculated using the virtual and real-world environments as the adapting fields. (a) In the optical see-through AR setups; (b) In the video see-through AR setups.

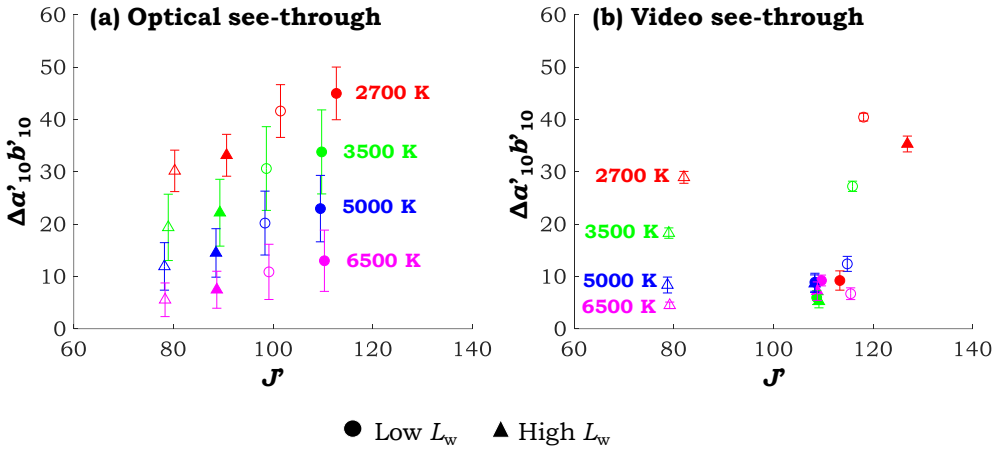

Fig. 6.16. Chromaticity differences, together with the 95% confidence intervals, between the average chromaticities of the adjusted stimuli and the origin in the a'_{10}-b'_{10} plane of the CAM02-UCS. The chromaticities were calculated using the virtual and real-world environments as the adapting fields. The solid symbols represent the chromaticities calculated using the virtual setups as the adapting fields; the open symbols represent the chromaticities calculated using the real-world environments as the adapting fields. (a) In the optical see-through AR setups; (b) In the video see-through AR setups.

Whether the observers were adapted to the virtual or real-world environments merits a further discussion. It was revealed that using the real-world environments as the adapting fields can lead to similar results for both the optical see-through and video see-through AR setups in the CAM02-UCS, as

shown in Figs. 6.15 and 6.16. This suggested that considering the effect of the real-world environments, together with the effect of the virtual environments, may help to better characterize the colour appearance of AR stimuli. It is possible that the observers were adapted to a mixed condition between the virtual and real-world environments instead of a single environment. By replacing the CAT02 with a mixed CAT model recommended by CIE [CIE 2010], the chromaticities under each adapting condition in each AR setup were calculated in the CAM02-UCS, as shown in Fig. 6.17. The adaptation ratio to the virtual environments was set to 0.6, which was typically used for the adapting field around the stimulus [CIE 2010; Xiao et al. 2013], and the degree of chromatic adaptation factor *D* was set to 1. Table 6.4 lists the colourimetric characteristics of the mixed conditions of the real-world and virtual conditions in the two AR setups. It can be observed that the colourimetric characteristics of the mixed conditions were between those of the virtual and real-world conditions, and the chromaticities calculated using the mixed chromatic adaptation were generally between the chromaticities calculated using the virtual and real-world conditions individually. Figure 6.18 shows the distance between the chromaticities calculated using the mixed chromatic adaptation and the origin of the a'_{10}-b'_{10} plane. (Note: The CCT levels of the mixed conditions in the video see-through AR environment are labelled in the figure to allow direct comparisons between the adjusted stimuli under the similar mixed adapting conditions in the two AR setups.) For the optical see-through AR setups, the chromaticities of the stimuli with a higher lightness level *J*' had larger distances from the origin, which may due to the fact the stimuli with higher *J*' appeared self-luminous and the adaptation to the mixed condition was less

complete. For the video see-through AR setups, it can be observed that with a similar lightness level of about 110, the $\Delta a'_{10}b'_{10}$ values were generally smaller than that in the optical see-through AR setups, suggesting a higher degree of chromatic adaptation to the mixed conditions.

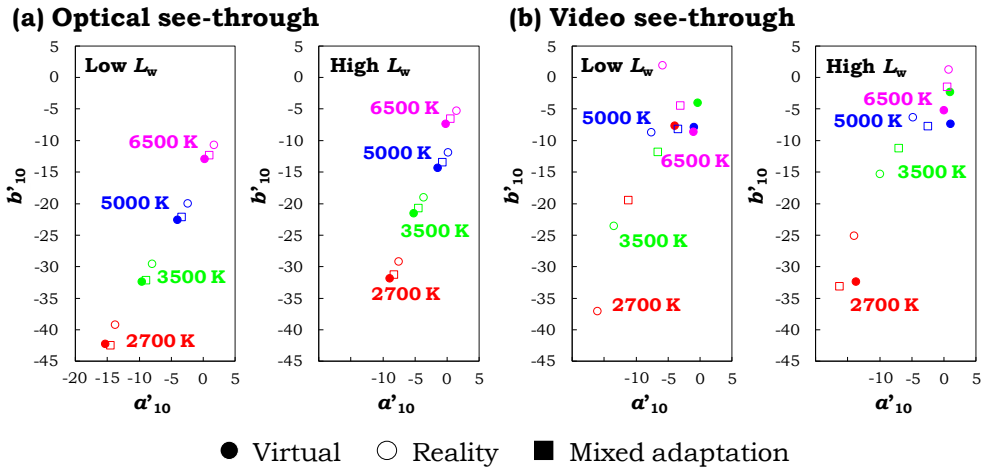

Fig. 6.17. Average chromaticities of the adjusted stimuli under each adapting condition in CAM02-UCS under each CCT level. In addition to the virtual and real-world environments, the mixed conditions of the virtual and real-world environments were used as the adapting fields. (a) In the optical see-through AR setups; (b) In the video see-through AR setups.

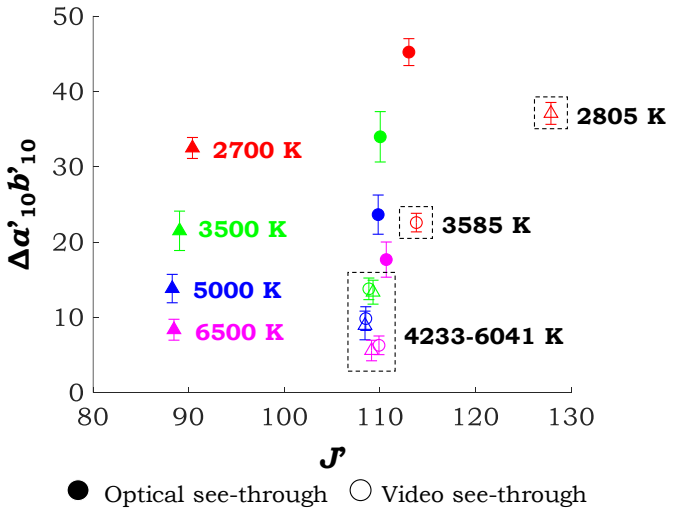

Fig. 6.18. Chromaticity differences, together with the 95% confidence intervals, between the average chromaticities of the adjusted stimuli and the origin in the a'_{10}-b'_{10} plane of the CAM02-UCS. The chromaticities were calculated using the mixed conditions the as adapting fields. The circle symbols represent the conditions at the ow L_w and the triangle symbols represent the conditions at the high L_w. The values in black are the CCT levels of the mixed conditions for the video see-through AR setups.

Table 6.4. Colourimetric characteristics of the mixed conditions of the real-world and virtual conditions in the two AR setups

		Optical see-through			Video see-through		
Nominal CCT (K)	Adapting luminance	Luminance (cd/m^2)	CCT (K)	D_{uv}	Luminance (cd/m^2)	CCT (K)	D_{uv}
2700 K	Low	83.0	2599	-0.002	129.1	3585	-0.006
	High	412.7	2570	-0.001	213.1	2805	-0.004
3500 K	Low	88.9	3408	0.000	138.2	4428	-0.004
	High	420.5	3420	+0.001	283.4	4233	-0.006
5000 K	Low	86.9	4929	+0.001	139.7	5151	-0.002
	High	440.3	4908	+0.003	280.8	5140	-0.003
6500 K	Low	82.8	6356	+0.003	136.5	5877	-0.002
	High	427.7	6423	+0.004	280.5	6041	0.000

6.4.3 Degree of Chromatic Adaptation when Viewing Virtual Stimuli Produced by AR

Assuming that the visual system adapts to a mixture of the virtual and real-world environments when viewing virtual stimuli produced by AR, the degree of chromatic adaptation factor *D* under each adapting condition was analysed. Figure 6.19 shows the scatter plot of the $\Delta a'_{10}b'_{10}$ values versus the CCT levels of the mixed conditions for the average virtual stimuli that had a lightness level *J*' around 110 (i.e., all the average stimuli except those adjusted under the high L_w in the optical see-through environment and the one adjusted under the 2700 K condition with the high L_w in the video see-through environment). It can be observed that for the stimuli with similar lightness levels, $\Delta a'_{10}b'_{10}$ values decreased with the increase of CCT level of the mixed conditions, indicating a higher degree of chromatic adaptation. In addition, it can be observed from the average stimuli under the 3500, 5000, and 6500 K adapting conditions of the video see-through setups that the luminance of the real-world environments (or the adapting luminance of the mixed conditions) did not have a significant effect on the degree of chromatic adaptation. This may suggest that at the lightness levels above 100, the virtual

stimuli appeared self-luminous and the chromatic adaptation was not significantly affected by the adapting luminance.

The degree of chromatic adaptation when viewing virtual stimuli was different from that when viewing physical stimuli, which can be observed by comparing the $\Delta a'_{10}b'_{10}$ values in this study and those reported in Chapter 5, as shown in Fig. 6.20. It was found that under the adapting conditions with low CCT levels (i.e., 2700 and 3500 K adapting conditions for viewing physical stimuli and mixed conditions with similar CCT levels for viewing virtual stimuli), the $\Delta a'_{10}b'_{10}$ values were always larger when viewing the virtual stimuli. This suggested that the degree of chromatic adaptation was lower when viewing the virtual stimuli, which may due to the fact that the virtual stimuli appeared self-luminous and were less affected by the CCT and luminance levels of the adapting conditions.

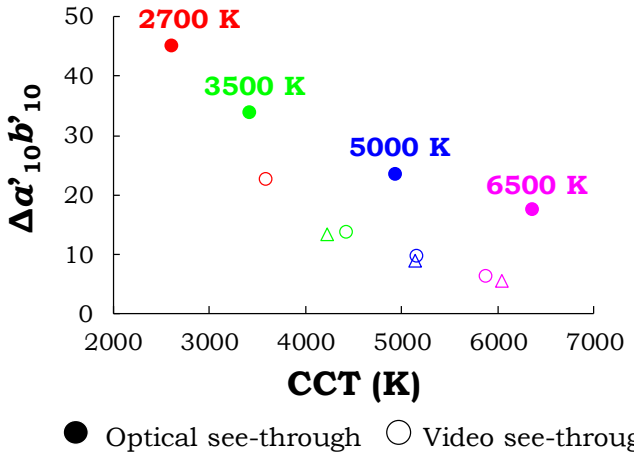

Fig. 6.19. Chromaticity differences between the average chromaticities of the adjusted stimuli and the origin in the a'_{10}-b'_{10} plane versus the CCT levels of the mixed conditions for the average stimuli with a lightness level J' around 110. The circle symbols represent those under the adapting conditions at the low L_w and the triangle symbols represent those under the adapting conditions at the high L_w.

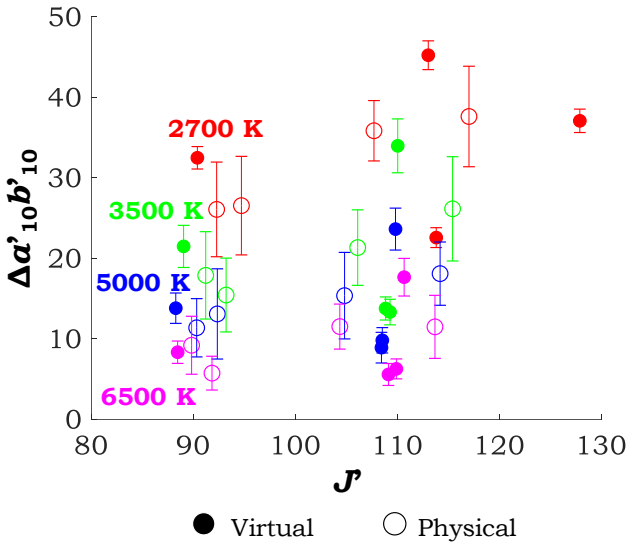

Fig. 6.20. Chromaticity differences, together with the 95% confidence intervals, between the average chromaticities of the adjusted stimuli and the origin in the a'_{10}-b'_{10} plane of CAM02-UCS. The solid markers represent the virtual stimuli in this study and the open markers represent the physical stimuli in Chapter 5.

6.5 A Follow-up Experiment using Another Optical See-through AR Setup

To confirm the effect of adapting CCT on the colour appearance of the virtual stimulus produced by AR, a follow-up experiment was conducted using an optical see-through AR setup in a past study [Hassani 2019]. This experiment also aimed to investigate the possible effects of the position (i.e., whether the virtual stimulus appears as if being overlaid on a real-world object or floating in the air) and visual complexity of the virtual stimulus on its colour appearance. It was hypothesized that a higher level of visual complexity and being overlaid on a real-world object may lead to a higher degree of chromatic adaptation when viewing a virtual stimulus.

6.5.1 Method

6.5.1.1 Apparatus, Adapting Conditions, and Stimuli

The experiment was carried out using a viewing booth, as shown in Fig. 6.21. The viewing booth had dimensions of 85 cm (width) × 59 cm (depth) × 50

cm (height) and the interiors were painted with Munsell N7 neutral grey paint. The front side of the booth had an opening to allow the observers to look into the viewing booth. Two Philip Hue White light bulbs were placed above the booth to provide a uniform illumination to the booth. A 50° beam splitter that had a transmittance around 70% was placed in front of the booth. The beam splitter was large enough to cover the entire front opening of the viewing booth, so that the observers did not view the real environment at all. A Dell P2715Q LCD display was placed horizontally below the booth. In the booth, two black sheets were mounted side-by-side at the centre of the viewing booth, and they had different distances from the beam splitter. A Munsell N7 neutral grey sheet was attached on each black sheet. The position of the left sheet was carefully adjusted, so that the virtual stimulus appeared to be overlaid on the surface. The right sheet was about 3 cm behind the left sheet, so that the virtual stimulus appeared to float in the air. The virtual stimulus was produced by the LCD display and projected by the beam splitter into the booth. The colour appearance of the virtual stimulus was perceived as a mixture of the colour projected by the beam splitter and the colour of the grey sheet. A graphical user interface (GUI) was designed in MATLAB and a keyboard was used to allow observers to adjust the colour appearance of the stimulus by adjusting the chromaticities of the pixels along the u'_{10} and v'_{10} axes in the CIE 1976 $u'_{10}v'_{10}$ chromaticity diagram with a step of 0.001 unit using four arrow keys. The pixels having a sum of R, G, and B values lower than 50 were considered as shadows and their RGB colour values were fixed during the adjustment.

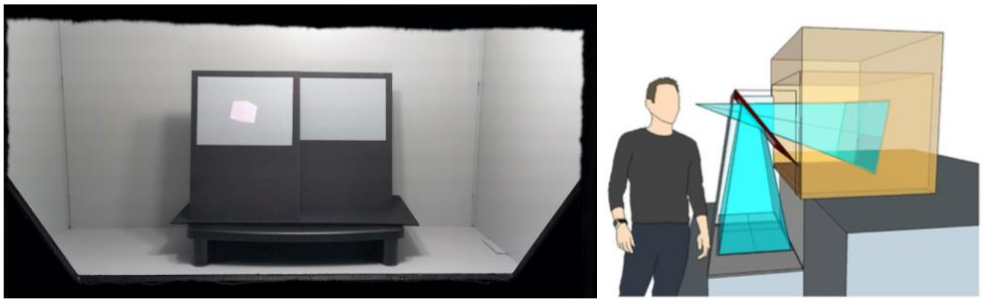

Fig. 6.21. Photograph of the experiment setup and the schematic of the setup.

The light bulbs were calibrated using a PR-655 spectroradiomter to produce two adapting conditions with the CCT levels of 6500 and 3000 K and an adapting luminance level L_A (i.e., the luminance measured at the grey sheet) around 32 cd/m^2. The measurements were taken through the beam splitter, with the colourimetric characteristics being summarized in Table 6.5.

Table 6.5. Colourimetric characteristics of the two adapting conditions

Nominal CCT (K)	L_A (cd/m^2)	CIE 1976 (u'_{10},v'_{10})	CCT (K)	D_{uv}
3000	32.7	(0.253,0.521)	3108	+0.0034
6500	31.8	(0.201,0.466)	6670	+0.0014

Another independent variable was the visual complexity of the virtual stimulus. Three levels of visual complexity were used, including a simple 2D patch (Level 1), a 3D cube (Level 2), and a spiky object (Level 3), as shown in Fig. 6.22. The pixels of the stimulus in each image had the same chromaticities. The luminance of the brightest pixel in each image was fixed at 23 cd/m^2.

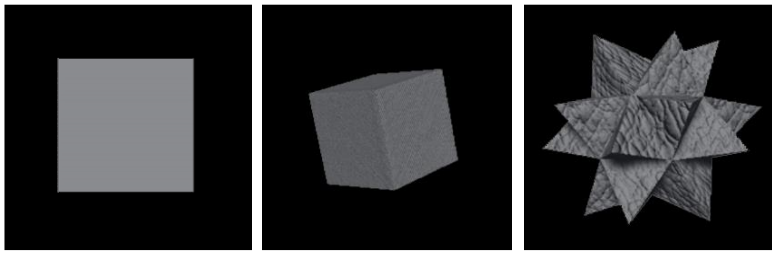

Fig. 6.22. Three stimuli at different levels of visual complexity used in the experiment. (a) A simple 2D patch (Level 1); (b) A 3D cube (Level 2); (c) A spiky object (Level 3).

6.5.1.2 Observers

Six observers (4 males and 2 female) between 26 and 38 years (mean = 28.33, std. dev. = 4.76) took part in the experiment. The observers all had a normal colour vision as tested using the Ishihara Colour Vision Test.

6.5.1.3 Experimental Procedures

Upon arrival, the observer reported his or her general information and was seated in front of the viewing booth. The head of the observer was not fixed and he or she could adjust his or her head position freely during the experiment. Under each adapting condition, the observer adapted to the adapting condition for two minutes. After the adaptation period, a stimulus was projected onto the left or right neutral sheet. The chromaticities of the pixels were set randomly as a starting point and the observer was asked to adjust the colour appearance of the stimulus using four arrow keys on the keyboard until it appeared the whitest. The adjustments were repeated four times for each stimulus under each viewing condition. The orders of the two sides (i.e., left and right) and the three levels of visual complexity were randomized. The order of the adapting condition was counterbalanced between the observers. In total, 288 adjustments were made by the observers (i.e., 6 observers × 2 adapting conditions × 3 visual complexity × 2 sides × 4 repeats).

6.5.2 Results

After the completion of the experiment, the chromaticities of adjustments were used to produce a 2D patch on the corresponding side of the neutral sheet and the SPDs were measured under the corresponding adapting condition at a similar position of the observers' eyes.

6.5.2.1 Intra- and Inter-observer Variations

The intra- and inter-observer variations were characterized using the MCDM values in $u'_{10}v'_{10}$ units. The intra-observer variation was characterized using the four repeated adjustments made by each observer. The MCDM values were between 0.0027 and 0.0055, with an average of 0.0035. The inter-observer variations were calculated based on the average chromaticities of the four repeated adjustments made by each observer and the average chromaticities of the adjustments made by all the observers (i.e., an average observer), as shown in Table 6.6. The intra- and inter-variations in this follow-up experiment were smaller than those in Experiment 1 and previous studies investigating white appearance [Smet et al. 2014; Smet et al. 2015; Huang et al. 2018; Zhai and Luo 2018].

Table 6.6. Inter-observer variations in terms of MCDM under each viewing condition

Adpating CCT (K)	Overlaied or floating	Visual complexity	MCDM
3000	Overlaid	Level 1	0.0061
	Overlaid	Level 2	0.0052
	Overlaid	Level 3	0.0058
	Floating	Level 1	0.0072
	Floating	Level 2	0.0069
	Floating	Level 3	0.0037
6500	Overlaid	Level 1	0.0035
	Overlaid	Level 2	0.0034
	Overlaid	Level 3	0.0050
	Floating	Level 1	0.0034
	Floating	Level 2	0.0035
	Floating	Level 3	0.0031

6.5.2.2 Chromaticities of Adjusted Stimuli

The chromaticities of the stimulus adjusted under each adapting illuminant and each location were shown in Fig. 6.23 and the 95% confidence error ellipses were as shown in Fig. 6.24. It can be observed that when the adapting

CCT was 6500 K, the chromaticities of the adjusted stimuli were generally between 6500 and 8000 K, which were similar to the adapting CCT. In contrast, when the adapting CCT was 3000 K, the adjusted stimuli had CCTs between 4000 and 5000 K, which were generally greater than the adapting CCT. The chromaticities of the adjusted stimuli were generally below the blackbody locus. The sizes and shapes of the ellipses of the chromaticities of those of the stimuli being overlaid on the background and those for the stimuli floating in the air were similar. Figure 6.25 shows the 95% confidence error ellipses for the stimuli of each level of visual complexity under the two adapting conditions. The different levels of visual complexity did not cause a significant difference to the sizes and shapes of the ellipses.

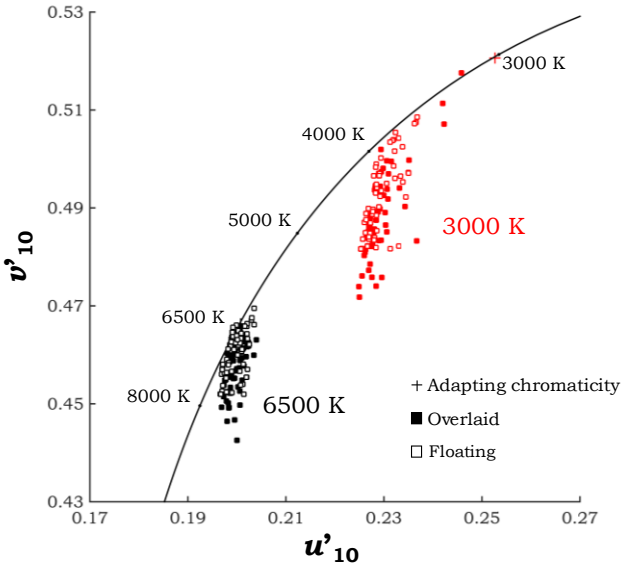

Fig. 6.23. Chromaticities of the adjusted stimuli by the observers under each adapting condition at different locations.

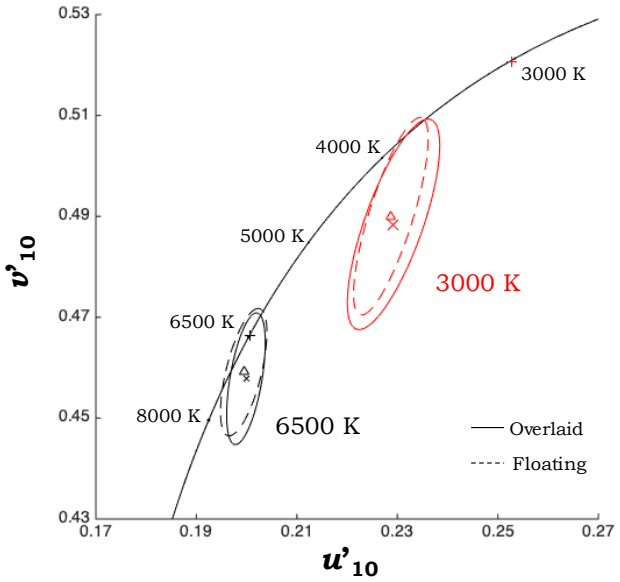

Fig. 6.24. Average chromaticities, together with the 95% confidence error ellipses, of the adjusted stimuli at different locations under each adapting condition.

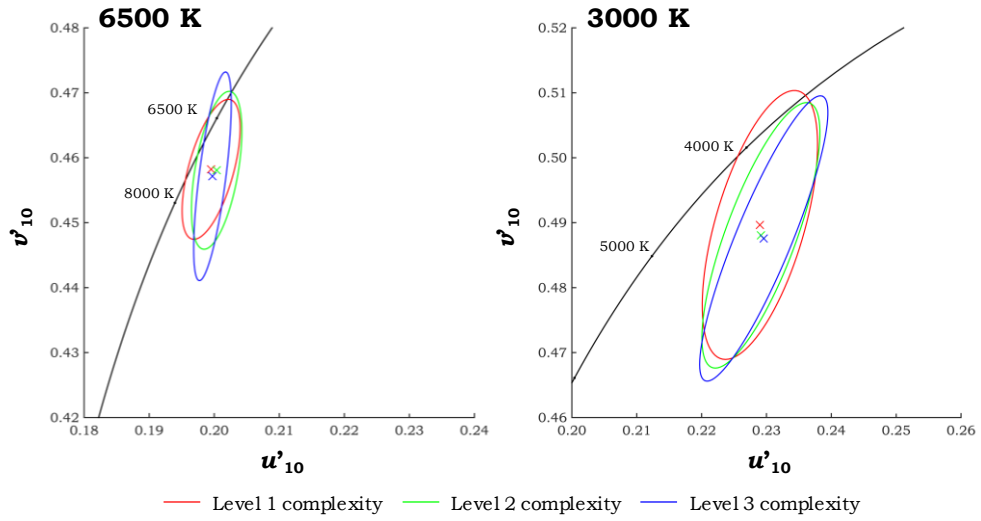

Fig. 6.25. Average chromaticities, together with the 95% confidence error ellipses, of the stimuli at different levels of visual complexity under each adapting condition.

6.5.3 Discussion

The effect of adapting CCT on the degree of chromatic adaptation collaborated the findings in the previous two experiments. The location and visual complexity of the virtual stimulus, however, did not significantly affect the degree of chromatic adaptation. It was possible that the shadows were not rendered according to the illumination in the booth, so that the changes of complexity and position did not appear realistic.

6.5 Summary

In this study, a series of psychophysical experiments were carried out to investigate the white appearance of virtual stimuli and degree of chromatic adaptation when using AR. Two types of AR setups (i.e., optical see-through and video see-through AR setups) were investigated. Different adapting conditions with different levels of CCT and adapting luminance were considered. In a follow-up experiment, the AR setup developed in a previous study [Hassani 2019] was used to further investigate how the location and visual complexity of a virtual stimulus affected the degree of chromatic adaptation.

By comparing the results of the optical and video see-through AR setups, it was found that both the virtual and real-world environments affected the colour appearance of the virtual stimuli and the observers may adapt to a mixed condition of the virtual and real-world environments. Therefore, a simultaneous consideration of the virtual and real-world environments may better characterize the colour appearance of virtual stimuli produced by AR. Similar to physical stimuli, the colour appearance of virtual stimuli was found to be significantly affected by the adapting conditions, as the degree of chromatic adaptation generally decreased with the decrease of CCT and adapting luminance levels. In addition, the degree of chromatic adaptation for viewing virtual stimuli was found to be lower than that for viewing physical stimuli at similar lightness levels, which suggested that the virtual stimuli in AR appeared self-luminous and were less affected by the adapting conditions. The follow-up experiment further confirmed the effect of the adapting CCT on the white appearance of virtual stimuli produced by optical see-through

AR setups. The location and visual complexity of a virtual stimulus did not seem to significantly affect its colour appearance. Further investigation is needed to comprehensively investigate the degree of chromatic adaptation and colour appearance for virtual stimuli produced by AR, which would be critically important to the quality of AR technologies and devices.

Chapter 7 Conclusion

This dissertation comprehensively investigated the white appearance of colour stimuli produced by surface colours, self-luminous displays, and different types of AR setups, which was used to better understand the chromatic adaptation mechanism of the human visual system.

It starts with the investigation of whiteness appearance of surface colours under the illumination at different CCT levels to address the weaknesses of the existing CIE whiteness formula. The observers evaluated the whiteness appearance of a series of whiteness samples under a haploscopic viewing condition, with one eye viewing four reference whiteness samples under a reference illuminant (i.e., a high quality CIE D65 simulator) and the other eye viewing eight whiteness samples containing different amounts of FWAs under six illuminants organized as a 3 × 2 factorial design, including three levels of CCT and two levels of UV/violet radiation. The whiteness values calculated using the existing CIE whiteness formula were found to well correlate to the perceived whiteness of the samples under each individual CCT level, but they failed to characterize the perceived whiteness under the illuminants across different CCT levels. Specifically, a sample under an illuminant with a lower CCT was evaluated to be less white than that having a similar magnitude of chromaticity shift from the illuminant chromaticities under an illuminant with a higher CCT, which was considered to be caused by a lower degree of chromatic adaptation. An optimization was performed on the degree of chromatic adaptation factor *D* in CAT02, which significantly improved the performance of the CIE whiteness formula. At the same time, the whiteness appearance of surface colours was also investigated from a

perspective of image quality. A scene, including three whiteness samples containing different amounts of FWAs and a Macbeth ColourChecker, was captured using a digital still camera under two 6500 K illuminants, with one simulating a high quality D65 illuminant and the other containing a similar amount of UV/violet radiation as a typical blue-pumped white LED. Nine white balance algorithms were used to process the RAW images. It was found that the lack of UV/violet radiation in the illumination significantly affected the appearance of the whiteness samples in the images, regardless of the white balance algorithms. It also simultaneously affected the appearance of the various colours on the ColourChecker. Such an effect was more obvious for the algorithms based on the Retinex theory (e.g., the maxRGB and Auto Level algorithms) than those based on the Grey World Assumption (e.g., the GW and MGW algorithms).

The white appearance was further investigated using a self-luminous display to produce stimuli under various adapting conditions, in terms of adapting CCT and luminance levels. Under each adapting condition, the observers adjusted the colour appearance of the stimulus to the whitest. The stimulus was designed to have six luminance levels by changing the display luminance. In total, there were 17 adapting conditions with different levels of adapting CCT and luminance. The larger the chromaticity difference between the adjusted white and the adapting condition, the lower the degree of chromatic adaptation. It was found that when the adapting luminance was high enough, the stimulus appeared reflective and was viewed in the surface mode. The adapting luminance and adapting CCT jointly affected the degree of chromatic adaptation. A higher adapting CCT was able to introduce a higher degree of chromatic adaptation. When the adapting CCT was above 5000 K,

the degree of chromatic adaptation was generally high regardless of the adapting luminance levels; when the adapting CCT was below 5000 K, a higher adapting luminance introduced a higher degree of chromatic adaptation. In contrast, when the adapting luminance was low, the stimulus appeared self-luminous and was viewed in the self-luminous mode. Under such a viewing mode, the degree of chromatic adaptation was generally low. Therefore, the experiment results did not support the conclusions in the past studies that surface colours and self-luminous displays needed different chromaticities to produce a white appearance due to the lower degree of chromatic adaptation when viewing the self-luminous displays. The viewing mode (surface mode versus self-luminous mode), instead of the viewing medium (i.e., surface colours versus self-luminous display), caused the different degrees of chromatic adaptation, with a lower degree of chromatic adaptation for the self-luminous mode. And the viewing mode depends on the relationship between the luminance of a stimulus and its adapting field.

Finally, the white appearance of virtual stimuli produced by AR was investigated. Psychophysical experiments were carried out using the apparatus simulating optical see-through and video see-through AR setups. Similar to the previous experiments, the observers adjusted the colour appearance of virtual stimuli to the whitest under various adapting conditions, in terms of adapting CCT and luminance levels. The degree of chromatic adaptation for viewing a virtual stimulus produced by AR was found to be affected by both the virtual and real-world environments and the observers were likely to adapt to a mixed condition of the virtual and real-world environments. In comparison to the results of the experiments using surface colours and displays to produce stimuli, a lower degree of chromatic

adaptation was found when viewing virtual stimuli produced by the AR setups.

In short, a series of experiments were carried out to investigate the white appearance of colour stimuli produced by different technologies under different adapting conditions, which was used to better understand the chromatic adaptation mechanism in the human visual system. The degrees of chromatic adaptation when viewing stimuli produced by different viewing media under different viewing conditions were thoroughly investigated. The findings are beneficial to various communities related to colour reproduction and imaging systems. Further work is needed to collect more data for the stimuli produced by different technologies under different viewing conditions and to develop a new formula to calculate the degrees of chromatic adaptation. The performance of chromatic adaptation transforms would be enhanced by characterizing the degrees of chromatic adaptation more accurately and better colour appearance models can be developed to characterize the colour appearance of stimuli produced by different technologies under different viewing conditions more accurately.

Publication Arising from Dissertation

Journal articles:

- Chen S, Wei M. 2018. LED illumination and color appearance of white-balanced images. LEUKOS. 16(3):203-215.
- Chen S, Wei M. 2019. Chromaticities for producing white stimuli depend on viewing mode rather than viewing medium: A pilot study. LEUKOS. 16(4):255-265.
- Wei M, Chen S. 2019. Effects of adapting luminance and CCT on appearance of white and degree of chromatic adaptation. Optics Express. 27(6):9276-9286.
- Wei M, Chen S, Huang HP, Luo MR. 2018. Development of a whiteness formula for surface colors under an arbitrary light source. Optics Express. 26(14):18171-18181.

Conference articles:

- Chen S, Wei M. 2018. White balance under white-light LED illumination. 26th Color and Imaging Conference. Nov. 12-16, 2018. Vancouver, Canada. 140-144.
- Chen S, Wei M. 2019. Real-world environment affects the color appearance of virtual stimuli produced by augmented reality. Oct. 21-25, 2019. Paris, France. 19-22.
- Wei M, Chen S, Luo MR. 2018. Effect of stimulus luminance and adapting luminance on viewing mode and display white appearance. 26th Color and Imaging Conference. Nov. 12-16, 2018. Vancouver, Canada. 308-312.

References

[CIE] 1986. Colorimetry. CIE Publication No. 15.2. Vienna, Austria.

[CIE] 2004. Colorimetry 3rd edition. CIE Publication No. 15.3. Vienna, Austria.

[CIE] 2010. Chromatic adaptation under mixed illumination condition when comparing softcopy and hardcopy images. CIE Publication No. 162. Vienna, Austria.

Barnard K, Cardei V, Funt B. 2002. A comparison of computational color constancy algorithms I: Methodology and experiments with synthesized data. IEEE Transactions on Image Processing. 11(9):972-983.

Berns R. 1996. Methods for characterizing CRT displays. Displays. 16(4):173-182.

Berns R, Gorzynski M. 1991. Simulating surface colors on CRT displays: The importance of cognitive clues. AIC Conference: Colour and Light. Jun 25-28, 1991. Sydney(NSW), Australia.

Billmeyer FW, Alessi PJ. 1981. Assessment of colour-measuring instruments. Color Research and Application. 6(4):195-202.

Breneman E. 1987. Corresponding chromaticities for different states of adaptation to complex visual fields. Journal of the Optical Society of America A. 4(6):1115–1129.

Buchsbaum G. 1980. A spatial processor model for object colour perception. Journal of the Franklin Institute. 310(1):1-26.

Cheng D, Prasad DK, Brown MS. 2014. Illuminant estimation for color constancy: Why spatial-domain methods work and the role of the color distribution. Journal of the Optical Society of America A. 31(5):1049-1058.

Chikane V, Fuh CS 2006. Automatic white balance for digital still cameras. Journal of Information Science and Engineering. 22:497-509.

Choi K, Suk HJ. 2016. Assessment of white for displays under dark- and chromatic-adapted conditions. Optics Express. 24(25):28945-28957.

Ciurea F, Funt B. 2003. A large image database for color constancy research. 11th Color and Imaging Conference. Nov 4-7, 2003. Scottsdale(AZ), USA. 160-164.

Dain SJ. 2004. Clinical colour vision tests. Clinical and Experimental Optometry. 87(4-5):276–293.

David A, Krames MR, Houser KW. 2013. Whiteness metric for light sources of arbitrary color temperatures: proposal and application to light-emitting-diodes. Optics Express. 21(14):16702–16715.

DOLBY. 2016. White paper. Link: https://professional.dolby.com/siteassets/pdfs/ictcp_dolbywhitepaper_v071.pdf

Evans RM. 1974. The Perception of Color. John Wiley & Sons. New York(NY), USA.

Fairchild MD. 1991. Formulation and testing of an incomplete-chromatic-adaptation model. Color Research and Application. 16(4):243-250.

Fairchild MD. 1993. Chromatic adaptation in hard-copy/soft-copy comparisons. Proceedings of the Society of Photo-Optical Instrumentation Engineers: Color hard copy and graphic arts II. Jan 31-Feb 5, 1993. San Jose(CA), USA. 1912:47-61.

Fairchild MD. 2013. Color Appearance Models. 3rd edition. John Wiley & Sons. Hoboken(NJ), USA.

Finlayson GD, Trezzi E. 2004. Shades of gray and colour constancy. 12th Color and Imaging Conference. Nov 9-12, 2004. Scottsdale(AZ), USA. 37-41.

Gabbard J, Swan J, Zedlitz J, Winchester W. 2010. More than meets the eye: An engineering study to empirically examine the blending of real and virtual color spaces. 2010 IEEE Virtual Reality Conference. Mar 20-24, 2010. Waltham(MA), USA. 79–86.

García PA, Huertas R, Melgosa M, Cui G. 2007. Measurement of the relationship between perceived and computed color differences. Journal of the Optical Society of America A. 24(7):1823–1829.

Gehler PV, Rother C, Blake A, Minka T, Sharp T. 2008. Bayesian color constancy revisited. IEEE Conference on Computer Vision and Pattern Recognition (CVPR). Jun 23-28, 2008. Anchorage(AK), USA. 1-8.

Hassani N. 2019. Modelling color appearance in Augmented Reality. PhD thesis. Rochester Institute of Technology.

Helson H, Michel W. 1948. The effect of chromatic adaptation on achromaticity. Journal of the Optical Society of America. 38(12):1025-1032.

Hering E. 1964. Outlines of A Theory of the Light Sense. Harvard University Press. Cambridge(MA), USA.

High G, Green P, Nussbaum P. 2017. Content-dependent adaptation in a soft proof matching experiment. Proceedings of IS&T International Symposium on Electronic Imaging. Jan 29-Feb 2, 2017. Burlingame(CA), USA. 67-75.

Houser KW, Wei M, David A, Krames MR. 2014. Whiteness perception under LED illumination. LEUKOS. 10(3):165-180.

Huang HP, Wei M, Ou LC. 2018. White appearance of a tablet display under different ambient lighting conditions. Optics Express. 26(4):5018-5030.

Huang M, Liu Y, Wu B, Liu H. 2011. Evaluation of adaptation and additivity failures using printed and monitor samples. 4th International Congress on Image and Signal Processing. Oct 15-17, 2011. Shanghai, China.

Hunt RWG, Pointer MR. 2011. Measuring Color. John Wiley & Sons. New York (NY), USA.

Hunt RWG, Winter L. 1975. Colour adaptation in picture-viewing situations. The Journal of Photographic Science. 23(3):112-116.

Huo J, Chang Y, Wang J, Wei X. 2006. Robust automatic white balance algorithm using gray color points in images. IEEE Transactions on Consumer Electronics. 52(2):541-546.

Hurvich L, Jameson D. 1951. A psychophysical study of white. I. Neutral adaptation. Journal of the Optical Society of America. 41(8):521-527.

Judd DB, Wyszecki G. 1975. Colour in Business Science and Industry. Wiley. New York (NY), USA.

Kuo W, Luo M, Bez H. 1995. Various chromatic-adaptation transformations tested using new colour appearance data in textiles. Color Research and Application. 20(5):313-327.

Lam EY. 2005. Combining gray world and Retinex theory for automatic white balance in digital photography. 9th International Symposium on Consumer Electronics. Jun 14-16, 2005. Macau, China. 134-139.

Lam HK, Au OS, Wong CW. 2004. Automatic white balancing using standard deviation of RGB components. 2004 International Symposium on Circuits and Systems. May 23-26, 2004. Vancouver(BC), Canada. 921-924.

Land EH, McCann JJ. 1971. Lightness and retinex theory. Journal of the Optical Society of America. 61(1):1–11.

Limare N, Lisani J, Morel J, Petro A, Sbert C. 2011. Simplest color balance. Image Processing on Line. 1:297-315.

Liu Y, Chan W, Chen Y. 1995. Automatic white balance for digital still camera. IEEE Transactions on Consumer Electronics. 41(3):460-466.

Livingston M, Barrow J, Sibley C. 2009. Quantification of contrast sensitivity and color perception using head-worn Augmented Reality displays. 2009 IEEE Virtual Reality Conference. Mar 14-18, 2009. Lafayette(LA), USA. 115–122.

Lukac R. 2008. Single-sensor Imaging: Methods and Applications for Digital Cameras. CPC Press. Boca Raton(FL), USA.

Luo MR. 1995. A review of chromatic adaptation transforms. Coloration Technology. 30:77-92.

Ma S, Hanselaer P, Teunissen C, Smet K. 2018a. The impact of the starting point chromaticity on memory color matching accuracy. CIE Expert Tutorial and Workshop on Research Methods for Human Factors in Lighting. Aug 13-14, 2018. Copenhagen, Denmark.

Ma S, Hanselaer P, Teunissen K, Smet K. 2018b. The influence of adapting field size and degree of chromatic adaptation. CIE 2018 Smart Lighting Conference. Apr.24-28, 2018. Taipei(Taiwan), China.

Ma S, Wei M, Liang J, Wang B, Chen Y, Pointer M, Luo MR. 2016. Evaluation of whiteness metrics. Lighting Research and Technology. 50(3):429-445.

MacAdam D. 1956. Chromatic adaptation. Journal of the Optical Society of America. 46(7):500-513.

Malvar HS, He L, Cutler R. 2004. High quality linear interpolation for demosaicing of Bayer-patterned color images. 2004 IEEE International Conference on Acoustics, Speech, and Signal Processing. May 17-21, 2004. Montreal(QC), Canada. 3:485-488.

McCann J, McKee S, Taylor T. 1976. Quantitative studies in retinex theory - comparison between theoretical predictions and observer responses to color Mondrian experiments. Vision Research. 16(5):445-458.

Menk C, Koch R. 2013. Truthful color reproduction in spatial augmented reality applications. IEEE Transactions on Visualization and Computer Graphics. 19(2):236–248.

Merenda C, Smith M, Gabba J, Burnett G, Large D. 2016. Effects of real-world backgrounds on user interface color naming and matching in automotive AR HUDs. IEEE VR 2016 Workshop on Perceptual and Cognitive Issues in AR. Mar 19-23, 2016. Greenville(SC), USA. 1–6.

Oicherman B, Luo MR, Rigg B, Robertson A. 2008. Adaptation and colour matching of display and surface colours. Color Research and Application. 34(3):182-193.

Osborne N. 1917. Scientific Papers of the Bureau of Standards. Government Printing Office. Washington DC, USA.

Safdar M, Cui G, Kim Y, Luo MR. 2017. Perceptually uniform color space for image signals including high dynamic range and wide gamut. Optics Express. 25(13):15131-15151.

Shamey R, Cárdenas L, Hinks D, Woodard R. 2010. Comparison of naive and expert subjects in the assessment of small color differences. Journal of the Optical Society of America A. 27(6):1482–1489.

Sharma G, Bala R. 2002. Digital Color Imaging Handbook. CRC Press. Boca Raton(FL), USA.

Sharma G, Wang S. 2001. Spectrum recovery from colorimetric data for color reproductions. Proceedings of the Society of Photo-Optical Instrumentation Engineers 4663: Color Imaging: Device-Independent Color, Color Hardcopy, and Applications VII. Dec 28, 2001. San Diego(CA), USA. 8-14.

Smet K, Deconinck G, Hanselaer P. 2014. Chromaticity of unique white in object mode. Optics Express. 22(21):25830-25841.

Smet K, Deconinck G, Hanselaer P. 2015. Chromaticity of unique white in illumination mode. Optics Express. 23(10):12488-12495.

Smet K, Zhai Q, Luo MR, Hanselaer P. 2017a. Study of chromatic adaptation using memory color matches, Part I: neutral illuminants. Optics Express. 25(7):7732-7748.

Smet K, Zhai Q, Luo MR, Hanselaer P. 2017b. Study of chromatic adaptation using memory color matches, Part II: coloured illuminants. Optics Express. 25(7):8350-8365.

Speigle JM, Brainard DH. 1999. Predicting color from gray: the relationship between achromatic adjustment and asymmetric matching. Journal of the Optical Society of America A. 16(10):2370-2376.

Sridharan S, Hincapié-Ramos J, Flatla D, Irani P. 2013. Color correction for optical see-through displays using display color profiles. Proceedings of the 19th ACM Symposium on Virtual Reality Software and Technology. Oct 6-8, 2013. New York (NY), USA. 231–240.

Sumner R. Processing RAW images in MATLAB. https://users.soe.ucsc.edu/~rcsumner/rawguide/RAWguide.pdf. [accessed May 11, 2018].

Tran SH, Wilson CG, Seib FP. 2018. A review of the emerging role of silk for the treatment of the eye. Pharmaceutical Research. 35(12):248.

Uchida H. 1998. A new whiteness formula. Color Research and Application. 23(4): 202–209.

Uchida H, Fukuda T. 1987. Estimation of whiteness of fluorescent whitened objects. Journal of the Color Science Association of Japan. 11:113-120.

Uchikawa K, Koida K, Meguro T, Yamauchi Y, Kuriki I. 2001. Brightness, not luminance, determines transition from the surface-color to the aperture-color mode for colored lights. Journal of the Optical Society of America A. 18(4):737-746.

Valberg A. 1971. A method for the precise determination of achromatic colors including white. Vision Research. 11(2):157-160.

van Krevelen DWF, Poelman R. 2015. A survey of augmented reality technologies, applications and limitations. International Journal of Virtual Reality. 9(2):1-20.

Wei M, Chen S. 2018. Impact of spectral power distribution of daylight simulators on whiteness specification for surface colors. Color Research and Application. 43(1):27-33.

Wei M, Houser KW. 2012. Status of solid-state lighting based on entries to the 2010 US DOE Next Generation Luminaire Competition. LEUKOS. 8(4):237-259.

Wei M, Houser KW, David A, Krames MR. 2014. Blue-pumped white LEDs fail to render whiteness. Proceedings of CIE 2014 Lighting and Energy Efficiency. Apr 23-26, 2014. Kuala Lumpur, Malaysia. 150-159.

Wei M, Ma S, Wang Y, Luo MR. 2017a. Evaluation of whiteness formulas for FWA and non-FWA whites. Journal of the Optical Society of America A. 34(4):640-647.

Wei M, Wang Y, Ma S, Luo MR. 2017b. Chromaticity and characterization of whiteness for surface colors. Optics Express. 25(23):27981-27994.

Wei M, Yang B, Lin Y. 2017c. Optimization of a spectrally tunable LED daylight simulator. Color Research and Application. 42(4):419-423.

Weiland C, Braun A, Heiden W. 2009. Colorimetric and photometric compensation for optical see-through displays. International Conference on Universal Access in Human-Computer Interaction. San Diego(CA), USA. 603–612.

Xiao K, Fu C, Mylonas D, Karatzas D, Wuerger S. 2013. Unique hue data for colour appearance models. Part II: Chromatic adaptation transform. Color Research and Application. 38(1):22-29.

Xu W, Wei M, Smet K, Lin Y. 2016. The prediction of perceived color differences by color fidelity metrics. Lighting Research and Technology. 49(7):805-817.

Yamauchi Y, Uchikawa K. 2000. Upper-limit luminance for the surface-color mode appearance. Journal of the Optical Society of America A. 17(11):1933–1941.

Zapryanov G, Ivanova D, Nikolova I. 2012. Automatic white balance algorithms for digital still cameras - a comparative study. Information Technology and Control. 1:16-22.

Zhai Q, Luo MR. 2018. Study of chromatic adaptation via neutral white matches on different viewing media. Optics Express. 26(6):7724-7739.

Zhai Q, Luo MR, Hanselaer P, Smet K. 2016. Modeling incomplete chromatic adaptation and color contrast using memory color. 24th Color and Imaging Conference. Nov 7-11, 2016. San Diego(CA), USA. 82–86.

Zhu Y, Zhai Q, Luo M. 2018. Investigating chromatic adaptation via memory colour matching method on a display. 26th Color and Imaging Conference. Nov. 12-16, 2018. Vancouver(BC), Canada. 313-331.